

I N F L U E N C E O F M E D I A L E N T O R H I N A L C O R T E X O N
C A 1 P O P U L A T I O N B U R S T S

ALIREZA CHENANI



Dissertation
zur Erlangung des Grades eines Doktors der Naturwissenschaften
an der Fakultät der Biologie
der Ludwig-Maximilians-Universität München

2018

Alireza Chenani: *Influence of Medial Entorhinal Cortex on CA1 Population Bursts*

Supervisor: Prof. Dr. Christian Leibold

2nd reviewer: Prof. Dr. Andreas VM Herz

Tag der Abgabe: 28.02.2018

Tag der mündlichen Prüfung: 25.10.2018

Contents

	<i>List of Abbreviations</i>	13
	<i>Summary</i>	15
1	<i>Introduction</i>	19
	1.1 <i>Anatomy and Evolution of Hippocampal Formation</i>	20
	1.1.1 <i>Evolution</i>	21
	1.1.2 <i>Anatomical Overview</i>	21
	1.2 <i>Role of Hippocampal Formation in Navigation</i>	23
	1.2.1 <i>Hippocampal place cells</i>	24
	1.2.2 <i>Other spatially modulated neurons</i>	24
	1.3 <i>Oscillatory Modes in Hippocampal Networks</i>	25
	1.3.1 <i>The Theta Rhythm</i>	25
	1.3.2 <i>The Gamma Rhythm</i>	26
	1.3.3 <i>Sharp-Wave Ripples</i>	28
	1.4 <i>Memory Episodes and Hippocampal Formation</i>	30
	1.4.1 <i>Associative Network, an Essential Part of Memory Systems</i>	30
	1.4.2 <i>Pattern Separation and Memory Formation</i>	31
	1.5 <i>Memory Replay in the Hippocampus</i>	32
	1.6 <i>Scientific Goals of this Thesis</i>	34
	1.7 <i>Animal Experimental Methods</i>	36
	1.7.1 <i>Animal model</i>	36
	1.7.2 <i>Surgeries & Implantation</i>	36
	1.7.3 <i>Behavior</i>	38
	1.7.4 <i>Histology</i>	40

2	<i>Materials and Methods</i>	43
2.1	<i>Data Analysis</i>	43
2.1.1	<i>Rest Periods</i>	43
2.1.2	<i>Spike Sorting</i>	44
2.1.3	<i>Place Cell Identification</i>	46
2.1.4	<i>Population rate & population bursts</i>	47
2.1.5	<i>Pattern activation analysis</i>	48
2.1.6	<i>Sequence Analysis</i>	50
2.1.7	<i>Local field potential (LFP) analysis</i>	52
3	<i>Results</i>	57
3.1	<i>Co-activation Patterns in Hippocampal Network with MEC Lesion</i>	57
3.2	<i>Are place cell sequences replayed in MEC-lesioned animals?</i>	59
3.3	<i>Diversity in Spike Content of Population Bursts</i>	65
3.4	<i>Individual Contribution of Place Cells in Population Bursts</i>	67
3.5	<i>Distinct Types of High Frequency Events in Hippocampal LFP</i>	69
3.6	<i>HFE classes are not exclusive to Rats</i>	76
4	<i>Discussion</i>	83
4.1	<i>MEC-lesioned Rats Exhibit Coordinated Activity Among their CA1 Neurons</i>	83
4.2	<i>MEC Lesions Disturb the Activity of CA1 Network</i>	84
4.3	<i>Reduction in Hippocampal Replay</i>	85
4.4	<i>Replay Quality in Absence of MEC Input</i>	85
4.5	<i>Specific Decrease in Relative Rate of Sharp Wave Ripples</i>	86
4.6	<i>Decline in Plasticity Over the Course of Reconsolidation</i>	89
	<i>Bibliography</i>	95

List of Figures

- 1.1 Comparison of shape of hippocampal formation in rodents (left) and primates (right). Note the expansion (both in volume and surface area) of neocortex compared to hippocampus in primates. Modified with permission from (Strange et al., 2014). 20
- 1.2 Schematics of the main subdivisions of the embryonic vertebrate brain. Earlier stages are depicted on the left side. Source: Wikipedia.org/wiki/Cerebrum 21
- 1.4 Mammalian hippocampus, top: sagittal view, bottom Nissl stain of the tissue and its structure in mirror diagram in a coronal section. 22
- 1.5 Trisynaptic loop in hippocampus. Connections from DG to CA3 and CA1 and finally back to entorhinal cortex are depicted in blue arrows. 22
- 1.6 Parallel streams along MEC and LEC. 23
- 1.7 Schematics of firing activity of a typical place cells in hippocampus. The black trace depicts the trajectory of the animal in a box. Red dots represent the locations where this particular cell spiked. 24
- 1.8 Firing activity of a typical grid cell. Black trace shows the trajectory of the animal, while red dots indicate the locations of spikes. High activity locations are arranged on a triangular lattice which partially depicted by the blue hexagon on the bottom left corner of the box. 24
- 1.9 Theta sequence in hippocampus during navigation. As an animal traverses through the environment, spikes from consecutive place cells appear on consecutive phases of the theta rhythm. Adapted with permission from (Colgin, 2016). 26
- 1.10 Slow and fast gamma oscillations. Slow and fast gamma frequencies seem to stem from different origins. Adapted with permission from (Colgin, 2016). 27

- 1.11 Neurons in the CA₃ (N₁ to N₄) usually receive input from perforant path (PP) neurons (N_a to N_c) as well as other CA₃ pyramidal cells. The flow of activity during encoding of a particular activity pattern (**top**) and its retrieval from a degraded input pattern is indicated with red arrows (**bottom**). **Top:** PP-cells representing a particular input pattern (N_b,N_c) activate a subset of CA₃ neurons (N₂,N₄) and the coactivation of these neurons results in the strengthening of their synapses (orange circles). The coactivation of CA₃ neurons, in turn, results in additional strengthening of the collateral synapses between them (yellow circles). As a result of such process, a characteristic output pattern is then conveyed to hippocampal area CA₁. **Bottom:** After establishment of the connectivity matrix, the encoded pattern could be fully retrieved even with degraded input. Activation of N_c alone results in the direct activation of CA₃ pyramidal cell N₄ (not N₂). N₂ is then activated via its collateral synapse with N₄ yielding the complete output pattern. Adapted with permission from (Rolls, 2016) 30
- 1.12 Granule cell layer in DG work as pattern separator network. Cells that represent an individual firing pattern are either magenta or purple, and cells that represent both patterns are bi-colored. The connectivity of each cell in the input layer can be traced by following the colored lines. In this simplified schematic, each output cell needs to accumulate at least 1.5 inputs of one kind to reach firing threshold. 31
- 1.13 Schematics of connections between DG, CA₃, CA₁ sub-networks of hippocampus. 31
- 1.14 Experience dependent replay of hippocampal activity. Modified from (Wilson and Mcnaughton, 1994) 32
- 1.15 Replay of waking neuronal spike sequences during sleep as reported by Lee & Wilson, Modified with permission from (Lee and Wilson, 2002) 33
- 1.16 The Long-Evans rat is an outbred rat developed by Drs. Long and Evans in 1915 by crossing several Wistar females with a wild gray male. 37
- 1.17 Scheme of behavioral paradigm. Rats running on a linear track for rewards at the end points (RUN). 1 hour rest sessions are recorded in a familiar environment prior (PRE) and post (POST) linear track session 39
- 1.18 MEC lesions were nearly complete. 41
- 2.1 Spike waveform and sampling. The electric potential was sampled with 32 KHz, providing 32 sampling point per typical spike time of 1 ms. 44
- 2.2 Tetrode and its usage in recording pyramidal layer of CA₁. The right plots depict difference in shape of waveforms of red and blue neurons as seen by different channels on the tetrode. Source: [Wikipedia.org/wiki/Tetrode](https://en.wikipedia.org/wiki/Tetrode) 44

2.3	Spike Clusters Identification	45	
2.4	Recorded Trajectory of a Rat	46	
2.5	Activity of Two Representative uni and bi-directional Place Cells on a linear track maze.	47	
2.6	Place Cell Templates	47	
2.7	Detection of Population Bursts	48	
2.8	Rank-Order distribution of Random Sequences	51	
2.9	Detection of High Frequency Events (HFE)	52	
2.10	Clustering result of HFE's across all animals	53	
3.1	Epoch wide Correlation Matrices	58	
3.2	co-activation patterns persisted across epochs.	58	
3.3	Average Reactivation of RUN patterns	59	
3.4	Average Reactivation of RUN patterns (Regression Slopes)	60	
3.5	Place Cell Templates	61	
3.6	LFP and spiking activity during RUN	61	
3.7	Sequence Rasters	62	
3.8	Spatial Similarity Index (SSI)	62	
3.9	Comparison of significant sequence replays	63	
3.11	MEC lesions induce a delay in hippocampal replay.	64	
3.13	Burst rate and sequence replays	65	
3.14	Motif similarity indices.	66	
3.16	Reoccurring sequences.	67	
3.18	Spatial sequences recur more frequently.	68	
3.19	Place cell participation in spatial sequences.	70	
3.20	Participation indices correlate with place field properties.	71	
3.21	LFP high frequency events	71	
3.22	Clustering of high frequency events	72	
3.23	Overall contribution of SWRs and FGBs in LFP high frequency events	72	
3.24	Neuronal activity during HFEs	73	
3.25	Population burst during HFEs	74	
3.26	Spatial sequences during HFEs	74	
3.28	Spatial sequences during HFEs	75	
3.30	co-activation patterns during HFEs	76	
3.31	Sharp wave ripple examples observed in Mongolian gerbils.	77	
3.32	Fast gamma burst examples observed in Mongolian gerbils.	77	
3.33	HFE's cluster in two distinct classes in Mongolian gerbils.	78	
3.34	Inter-event intervals and duration of HFEs in Mongolian gerbils.	78	
3.35	Inter-event intervals and duration of HFEs in Mongolian gerbils.	79	
3.36	CA1 population activity during HFE's in Mongolian gerbils.	79	

List of Tables

- 1.1 Quantification of lesion extent in different individuals in MEC lesioned group. 38

List of Abbreviations

CA	Cornu Ammonis
DG	Dentate Gyrus
EC	Entorhinal Cortex
EEG	Electroencephalogram
FGB	Fast Gamma Burst
FFT	Fast Fourier Transform
HF	Hippocampal textbfFormation
LEC	Lateral Entorhinal Cortex
LFP	Local Field Potentials
LIA	Large Irregular Activity
LTD	Long-Term-Depression
LTP	Long-Term-Potentiation
MEC	Materal Entorhinal Cortex
NMDA	N-Methyl-D-Aspartate
PaS	Parasubiculum
PER	Perirhinal cortex
POR	Postrhinal cortex
PrS	Presubiculum
REM	Rapid Eye Movement
SPW	Sharp Wave
SWR	Sharp Wave-Ripple
STDP	Spike-Timing-Dependent Plasticity
Sub	Subiculum
SWS	Slow Wave Sleep

Summary

The hippocampal formation is believed to play an irreplaceable role in the processes of formation and retrieval of episodic memories. Located at the end of the pallial areas in the mammalian brain, it receives streams of pre-processed sensory information as well as higher order cognitive signals. The hippocampus is an essential brain structure responsible for preserving and recalling episodic memories. Without it, we would have serious problems preserving the integrity of our actions in a meaningful way. One of the main tasks of the hippocampus is to help us with keeping track of the ordinality of events. It has been shown that the hippocampal place cells would preserve the order of their activity for a significant amount of time. They usually engage in coordinated bursts of activity lasting between 50 to 500 ms. During these bursts hippocampal neurons present rather stereotypical patterns of population activity. This is believed to reflect the replay of different episodes of recent experiences for long term consolidation. This phenomena has been extensively observed among place cells of the hippocampus, specially in the area CA1. Another brain structure with a high number of spatially modulated cell is the medial entorhinal cortex (MEC). Since entorhinal cortex is the main input/output gate of hippocampus, the interaction between these two structures must play an immense role in the dynamics and content of hippocampal population bursts and in term the quality of memory consolidation and memory recall. To investigate the effect of this interaction on hippocampal replays, I analysed resting activity in rats with bilateral MEC lesions. I found that during the course of awake immobility periods in a new spatial experience, sequence re-

play in MEC-lesioned rats was reduced compared to control animals. However, the reduction in replay is no longer detectable during rest sessions following behaviour. MEC inputs thereby seem to facilitate plasticity of population burst activity as quantified by co-activation analysis and the participation of place cells in sequence replay. Moreover, in both animal groups there is only a minor increase of pattern activation due to a novel spatial experience, indicative of a strong intrinsic network structure that is similar prior and subsequent to the behavioural session.

1

Introduction

Memory is one of (if not) the most important function of the nervous system. Our daily activities as well as long term developments of our psyche are entirely memory dependent. It has been shown that sequential activity of neurons in the mammalian brain works as effective strategy to store and retrieve information in different areas of the brain (Nádasdy et al., 1999; Lee and Wilson, 2002). Therefore, understanding the nature and characterizing the detail of such sequential activities among neuronal assemblies are gaining increasing attention in modern neuroscience.

The discovery of place cells by John O'Keefe (O'Keefe and Dostrovsky, 1971; O'Keefe, 1976) put the hippocampus in the spotlight as prime candidate for quantitative research on the formation and recall of spatial memory. About a decade earlier, Scoville and Milner (Scoville and Milner, 1957) reported the loss of the ability to form new declarative memories after bilateral medial temporal lobectomy (large volume in the brain including both hippocampi) on an epilepsy patient. This was the first hint on the recognition of the hippocampal formation as a memory-related brain area.

Years of research and active discussion had led the scientific community to the common belief that the hippocampus is acting as a part of a larger network receiving streams of preprocessed information. Using these streams of high level (sensory and cognitive) input, the hippocampus forms associations on different levels and influences memory driven thoughts which ultimately lead to our decisions and

actions. Sitting at the end of the cortical structure, the hippocampus interacts with the entire brain through an adjacent structure, namely the entorhinal cortex (EC). As a main gate of information to the hippocampus, entorhinal cortex has a vital role in both providing and retrieving highly processed information from the hippocampus to the cortex and vice versa.

Realization of the flow of time is an extremely important part in any conscious system. The discovery of place cell sequences in the hippocampus (Lee and Wilson, 2002) demonstrates a possible way that our brain deals with such problems. Hippocampal neurons preserve the order of activity among themselves regardless of the behavioral state. They even keep on repeating such ordered activities for certain time window possibly for consolidation in other parts of the brain for longer time periods. Maybe this mechanism is the foundation of how we put things in context and have a continuous experience of the outside world.

In this thesis, I will discuss the details of my doctoral studies on the effects of Medial Entorhinal Cortex (MEC) connections on the population behavior of neurons in a part of hippocampus namely CA1. I will discuss the effect of MEC-lesions on neuronal population activity using spike times of individual neurons and the hippocampal Local Field Potential (LFP).

In the first chapter I will introduce the anatomy, evolution and role of hippocampal formation in the mammalian brain, followed by a brief overview of different systems in the hippocampus and their part in the procedure of learning and memory formation. I will cover the methods used for performing the experiments and data analysis. The results of this study are presented in the third chapter followed by the final chapter on discussion of results in the context of other studies and evidences.

1.1 Anatomy and Evolution of Hippocampal Formation

Stemming from the medial and dorsomedial telecephalon of the vertebrate embryonic brain, the Hippocampal formation (HF, usually referred as medial pallium in non-mammalian vertebrates) takes over a crucial role in the memory representation of space and even episodes in mammals and birds (Bingman et al., 2009, 2017).

Hippocampal tissue in rodents reminds us of a pair of miniature bananas, joined at their stems. In primates, the hippocampus tends to get thinner as we follow the structure from the base of the temporal lobe to higher and more medial regions (Figure 1.1).

In each hemisphere, the dorsal portion of hippocampus lies next to the septal nuclei and it is connected to its mirror tissue via the

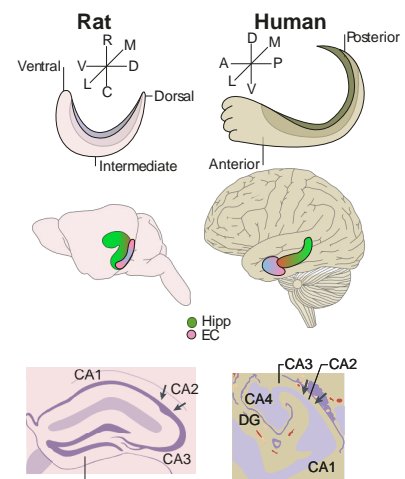


Figure 1.1: Comparison of shape of hippocampal formation in rodents (left) and primates (right). Note the expansion (both in volume and surface area) of neocortex compared to hippocampus in primates. Modified with permission from (Strange et al., 2014).

hippocampal commissure. The ventral section usually extends into the temporal lobe where it ends next to the amygdaloid complex.

The mammalian hippocampus is generally thought of as a three layered structure consisting of three major subsections (Figure 1.4): the dentate gyrus (DG), corna amonis (CA₁,CA₂,CA₃) and the subiculum (SB).

1.1.1 Evolution

During long evolutionary history, the hippocampus as a part of the cerebral cortex which develops from the medial edge of telencephalic pallium is present across all vertebrates (Figure 1.2). Along the evolutionary path, the hippocampal formation preserved some properties such as its connection to other brain areas and altered other important features such as cytoarchitectural organization among different vertebrate classes. These changes could be summarized in 3 categories (Bingman et al., 2009).

- Architectural transition towards lamination of cells.
- Weakening direct connection to thalamic sensory inputs and increase in preprocessed sensory inputs.
- Increase in complexity of internal network.

These changes (specially the last two) are still apparent across the mammalia class. Over the course of mammalian evolution, we observe a disproportional growth in volume of the neocortex. According to such a change, hippocampal inputs shifted from mainly sensory, spatial and motor components in rodents to higher order cortical areas in primates. The hippocampal formation can be thought of as a module, composed of several components (DG, CA₃, CA₂, CA₁). As it will be explained in the following sections, the large recurrent axon collateral system (located in CA₂-CA₃) has developed the ability to mix and segregate the input signals without any special consideration about the nature of its source. This is in essence the core functionality of hippocampus.

1.1.2 Anatomical Overview

Different regions in the hippocampal formation are identified based on their 3 layered structure. In the middle of each region we can observe a well arranged sheet of somata of principal cells sandwiched between two other layers containing somata of interneurons, dendrites of projecting neurons as well as afferent and efferent fibers

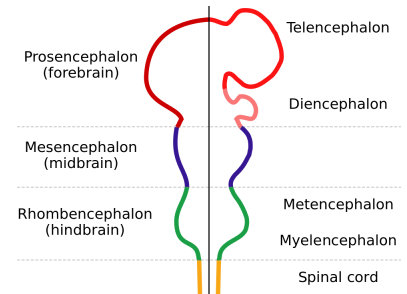


Figure 1.2: Schematics of the main subdivisions of the embryonic vertebrate brain. Earlier stages are depicted on the left side. Source: [Wikipedia.org/wiki/Cerebrum](https://en.wikipedia.org/wiki/Cerebrum)

(van Strien et al., 2009; Witter and Amaral, 2004). In this section I will give a short overview of hippocampal anatomy to support the discussion about the role of hippocampal formation in the organization of episodic memories. For a detailed description of hippocampal anatomy please consult (Witter and Amaral, 2004; Amaral and Lavenex, 2007). This overview covers 3 major organizational principles in the hippocampal formation.

- organization along the transverse axis
- organization along the longitudinal axis
- parallel streams along MEC and LEC

ORGANIZATION ALONG THE TRANSVERSE AXIS. The transverse axis is usually referred to as the cross-sectional plane of the hippocampus containing the trisynaptic loop, starting from DG to CA3 and CA1 (Figure 1.5). Despite the major emphasis on this feed forward loop, we are aware of parallel pathways and feedback loops along the transverse axis which presumably play an important role in the functionality of the whole network. Entorhinal cortex connects directly to all regions in the hippocampus. While EC layer III projects to CA1 and subiculum, layer II of the EC projects to DG and CA3. The granule cell layer in DG projects to CA3 while it receives feedback projections from CA3 via mossy cells. CA3 in turn sends feed forward projections to CA1 known as Schaffer collaterals as well as feedback connection to itself known as recurrent collaterals. Finally CA1 sends out projections to the subiculum as well as layers V and VI in EC known as the deep EC layers.

ORGANIZATION ALONG THE LONGITUDINAL AXIS. The longitudinal axis is also known as the septotemporal or dorsoventral axis of the hippocampus (Figure 1.1). There are clear signs of functional gradients along this axis. Place fields shrink in size going from ventral to dorsal hippocampus (Jung et al., 1994; Kjelstrup et al., 2008; Royer et al., 2010). Dorsal hippocampus is preferentially connected to retrosplenial cortex and the more precise grid cells of the dorsocaudal MEC whereas ventral hippocampus is connected to prefrontal cortex, amygdala and the ventral MEC. These findings suggest that dorsal hippocampus should be more involved in precise spatial localization tasks whereas ventral parts maybe more involved in processing contextual and emotional parts of experience (Moser and Moser, 1998; Ferbinteanu et al., 1999; de Hoz et al., 2003).

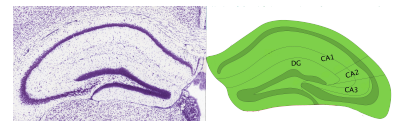
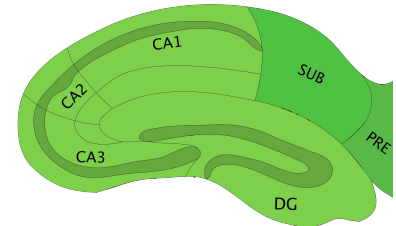


Figure 1.4: Mammalian hippocampus, top: sagittal view, bottom Nissl stain of the tissue and its structure in mirror diagram in a coronal section.

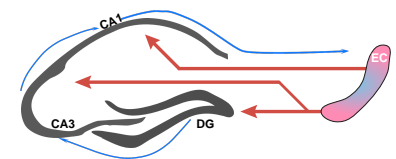


Figure 1.5: Trisynaptic loop in hippocampus. Connections from DG to CA3 and CA1 and finally back to entorhinal cortex are depicted in blue arrows.

PARALLEL STREAMS ALONG MEC AND LEC. The majority of inputs are delivered to the hippocampus through the entorhinal cortex. The medial and the lateral parts of entorhinal cortex are terminals for two distinct processing streams of information that are quite detached as far as the connectivity patterns are concerned. Despite this segregation, substantial cross talk is observed among two streams. Most of the input to the LEC is provided through perirhinal cortex, which is thought to be involved in processing of complex objects and receives its inputs mostly from sensory areas (Burrwell, 2006). In contrast, the input to the MEC is coming from postrhinal cortex which receives its inputs from visuospatial regions. The parahippocampal place area, as a part of the parahippocampal region in primates is observed to respond to visual scenery (Epstein and Kanwisher, 1998). MEC has strong connections with presubiculum (prS), parasubiculum (paS) and retrosplenial cortical regions. These areas contain a variety of spatially modulated cells including head-direction cells, grid cells, border cells and place cells.

This high degree of anatomical segregation has been the main source of evidence, leading scientists to believe that these well separated streams of processed information could be functionally related to variety of daily life dualities like what vs. where, content vs. context, self vs. other etc. (Manns and Eichenbaum, 2006; Knierim et al., 2006; Lisman, 2007; Lever et al., 2014).

1.2 Role of Hippocampal Formation in Navigation

When an animal explores an environment, one can think of the process of information as a set of organized spatial memories that could be retrieved in suitable moments. Spatial memory could be understood as memories formed on spatial information describing the layout and contextual structure of a non-egocentric environment (Tolman, 1948; Nakazawa et al., 2004). These memories are often thought to form the scaffold of what is called "cognitive map". Such a map benefits the animal with an allocentric understanding of the environment and provides the opportunity to take novel paths and make novel decisions in order to achieve a goal in a more efficient manner. Using extracellular electrophysiology techniques, scientists have observed neurons which tune their firing activity with respect to the animal's location (Skaggs et al., 1996; Mankin et al., 2015; Leutgeb et al., 2007). Although one can observe such neurons outside the hippocampal formation, the majority of these neurons live within hippocampus and form the spatial content of the cognitive map. The first and the most famous of such cells are hippocampal place cells

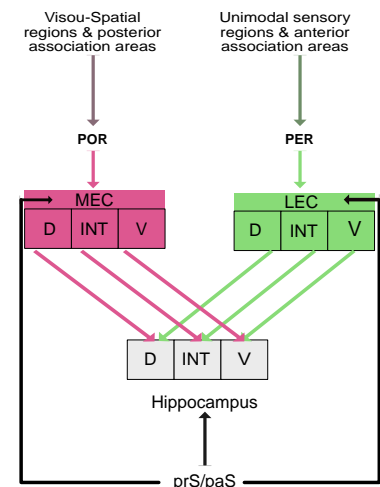


Figure 1.6: Parallel streams along MEC and LEC.

discovered by John O'Keefe in 1971 (O'Keefe and Dostrovsky, 1971).

1.2.1 Hippocampal place cells

Under a typical experimental conditions ($\sim 1\text{m}^2$ box), between 20 to 60 percent of pyramidal cells in area CA1 and CA3 become active around particular locations forming firing patterns called place fields (Figure 1.7). It has been reported that distribution of place field locations is established after few minutes of exploring a novel environment (Leutgeb et al., 2004; Frank et al., 2004). Place field locations are fairly stable during subsequent visits of the same environment, while during initial phases of map formation, place fields are more anchored to the location of landmarks. They will cover the whole environment and remain fairly stable even in total darkness once the spatial map is formed (Quirk et al., 1990; Wilson and McNaughton, 1993; Gothard et al., 1996). Place fields are driven by sensory information as well as self-motion information (Gothard et al., 1996; McNaughton et al., 2006; Haas, 2017; Evans et al., 2016). Place fields are observed in different species across the mammalian kingdom, in other rodents like mice (Mankin et al., 2012) and Mongolian gerbils (Mankin et al., 2019), in bats (Yartsev et al., 2011; Ulanovsky and Moss, 2007) and also primates including humans (Rolls, 1999; Rolls et al., 2005; Rolls and Stringer, 2005; Jacobs and Kahana, 2010; Miller et al., 2013).

1.2.2 Other spatially modulated neurons

Head direction (HD) cells (Taube et al., 1990a,b) are among other types of spatial neurons analyzing a part of the information crucial for forming the cognitive map. Each head direction cell responds to a narrow range of head orientation angles in an allocentric frame of reference. Collectively they provide the animal with heading direction in any instance (Taube et al., 1992; Taube, 1995; Sargolini et al., 2006; Acharya et al., 2016). Grid cells (Figure 1.8) are another type of neurons with spatial activity (Hafting et al., 2005). Their response field is not confined to a single location or angle, but rather arranged in a equilateral triangular mesh spanning the entire space. Although they are mainly present in MEC layer II, they have been observed in other MEC regions, prS and paS (Fyhn et al., 2004; Hafting et al., 2005; Sargolini et al., 2006; Boccara et al., 2010).

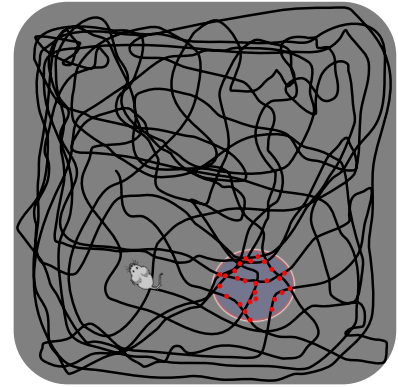


Figure 1.7: Schematics of firing activity of a typical place cells in hippocampus. The black trace depicts the trajectory of the animal in a box. Red dots represent the locations where this particular cell spiked.

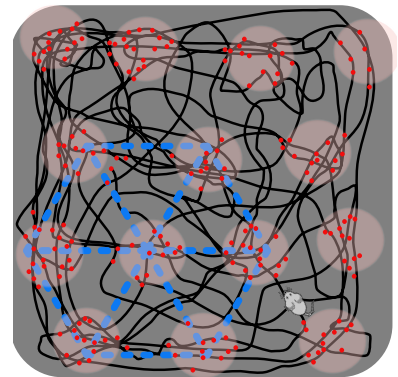


Figure 1.8: Firing activity of a typical grid cell. Black trace shows the trajectory of the animal, while red dots indicate the locations of spikes. High activity locations are arranged on a triangular lattice which partially depicted by the blue hexagon on the bottom left corner of the box.

1.3 Oscillatory Modes in Hippocampal Networks

One of the most fundamental challenges of any memory system is to sort the temporal organization of events. It is a common belief that such organization in hippocampus is done by accurate interplay of spike timing of different neurons with respect to the phase of different oscillations across hippocampal tissue. Such oscillations arise from synchronized activity of ensembles of neurons deflecting the electric field due to synchronous current flow during these activities (Colgin, 2016). These oscillations are best observable in the local field potential (LFP). Particularly in the hippocampus there are several well defined frequency bands with different functional and behavior correlates. These bands include delta (0 – 4Hz), theta (5 – 12Hz), gamma (20 – 150Hz) and ripples (150 – 250Hz). I will give a quick overview of characteristics and functionality of these bands in following subsections.

1.3.1 The Theta Rhythm

Theta rhythms are fairly regular oscillations in the range of 5 – 12Hz with a peak frequency around 8Hz. They are observable in all hippocampal regions during awake states and rapid eye movement (REM) sleep (Vanderwolf, 1969; Colgin, 2013). After their discovery in rabbits (Jung and Kornmüller, 1938), they have been consistently observed in rats, mice, gerbils, bats, monkeys and humans (Green and Arduini, 1954; Grastyán et al., 1959; Ekstrom et al., 2005; Ulanovsky and Moss, 2007; Jutras et al., 2013; Mankin et al., 2019). Theta is the most studied frequency band in the rodent hippocampus. Since a lesion study by Green & Arduin in 1954, people think of medial septum as a pacemaker for hippocampal theta. Interneurons in DG, CA3 and CA1 are targeted by neurons in septum. Rhythmic dis-inhibition of hippocampal pyramidal cells by septal interneurons promote theta rhythmic firing in the hippocampus.

A series of electroencephalography studies in 1970's showed that theta power is a reliable predictor of performance in learning and memory tasks (Landfield et al., 1972; Winson, 1978; Berry and Thompson, 1978). Since then several studies have confirmed the importance of theta in mnemonic tasks (Mizumori et al., 1990; Macrides et al., 1982; Orr et al., 2001; Hyman et al., 2003; Griffin et al., 2004; Siegle and Wilson, 2014; Belchior et al., 2014). Surprisingly, a recent study by Brandon and colleagues observed formation of new place fields (which currently is an accepted indicator for spatial learning) despite the absence of theta rhythm due to septal inactivation (Brandon et al., 2014). It is also known that place cells in bats show a very

weak if at all any correlation with theta in their firing patterns (Yartsev and Ulanovsky, 2013). Although surprising, these studies do not provide any direct evidence indicating the irrelevance of theta in the learning process. These observations report the formation of a group of place cells in hippocampus without the theta rhythm. According to current understanding of the memory system, different ensembles of neurons activating in harmony is required to represent different components of a memory.

Wang and colleagues, have examined this idea on rats (Wang et al., 2014). They have shown that theta blockage disrupts the organization of place cell activation in a specific order known as theta sequences (Figure 1.9) (Skaggs et al., 1996; Dragoi and Buzsáki, 2006; Foster and Wilson, 2007). It is worth to note that these sequences are not solely reflecting the wiring among neurons in different ensembles but also change dynamically according to behavioral intention of the animal (Wikenheiser and Redish, 2015).

There is also another line of evidence indicating a role of theta oscillations in multimodal sensory integration. We know that theta is strongly modulated by movement of an animal which in turn is correlated with the way sensory stimuli being sampled by the animal (Macrides et al., 1982; Komisaruk, 1970). This intrinsic fact makes theta a suitable tool for coordination of multi sensory inputs into hippocampal formation (Jutras et al., 2013; Kepecs et al., 2007; Berg et al., 2006). The multimodal coordination helps the hippocampus to organize different aspects of experience in a meaningful manner.

Finally, it is worthwhile to mention that coordinated activity of pyramidal cells in hippocampus could translate to different firing patterns in downstream networks. These induced firing activities could be useful in cases yet to be discovered, but Monsalve-Mercado & Leibold have build a model explaining the emergence of hexagonal firing patterns (the one of grid cells in MEC) from random initial state trough time correlated activity of hippocampal place cells (Monsalve-Mercado and Leibold, 2017). Looking at this neat example one could think of the influence of such theta coordinated activity in introducing firing patterns which provide the nervous system with metrics of the outside world. Developing an intrinsic metric for stimuli of different nature accelerates the rate of information processing (i.e. comparisons, additions etc.) without constant need of reference to past memories.

1.3.2 The Gamma Rhythm

Gamma rhythms are observed during a variety of behaviors in hippocampus (Buzsáki et al., 1983; Csicsvari et al., 2003). In compari-

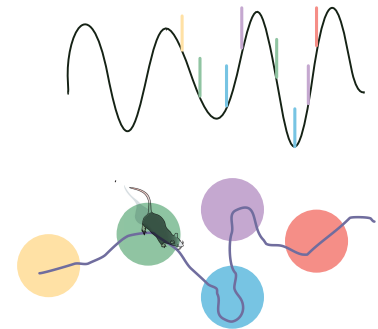


Figure 1.9: Theta sequence in hippocampus during navigation. As an animal traverses through the environment, spikes from consecutive place cells appear on consecutive phases of the theta rhythm. Adapted with permission from (Colgin, 2016).

son to other major oscillations in hippocampal formation, the broad frequency band (20 – 150Hz) of the gamma rhythm makes it a more complicated subject of systematic study.

In recent years, the community is converging towards the hypothesis that the gamma band (20 – 150Hz) consists of several functionally distinct oscillations. CA3 is the main drive in the low frequency (20 – 50Hz) regime, while MEC uses the mid frequency range (60 – 100Hz) as communication channel with CA1 (Figure 1.10) (Colgin et al., 2009; Belluscio et al., 2012; Kemere et al., 2013; Schomburg et al., 2014).

Perhaps the most certain fact about mechanisms generating the gamma rhythm is the involvement of interneurons. The connection between gamma periods and inhibitory events has been observed via intracellular recordings of pyramidal cells in the hippocampus and granule cells in DG (Soltesz and Deschênes, 1993; Buzsáki, 1996; Colgin and Moser, 2010; Bartos et al., 2007; Pernia-Andrade and Jonas, 2014). Consistently, interneuron spikes in these regions show phase locking to gamma oscillation (Buzsáki et al., 1983; Csicsvari et al., 2003; Tukker et al., 2007; Senior et al., 2008). Gamma phase locked firing is not restricted to a specific type of interneuron, it has been reported in axo-axonic cells, bistratified cells, parvalbumin positive basket cells and cholecystokinin expressing cells (Tukker et al., 2007). These findings suggest that synchronized spiking of interneurons could raise the observed gamma rhythms.

Researchers have recently started systematic investigation on the functionality of different gamma bands. Several scenarios have been put forward but it is yet far from a solid picture. Mid-range gamma which is believed to be triggered from MEC is thought to encode sensory components of memories and experiences in hippocampus (Newman et al., 2013; Bieri et al., 2014; Zheng et al., 2015, 2016), while MEC is responsible for processing of sensory input to the hippocampus. On the other hand slow gamma is believed to play a role in memory retrieval. As indicated in the next section, memories are stored and retrieved in the CA3 network and as mentioned before slow gamma activity is entrained by CA3 activity making slow gamma a viable candidate as a channel for the memory retrieval process (Colgin, 2016). In support of this idea, there are studies reporting lower performance in memory-based tasks in accordance to a decrease in theta-slow gamma coordination (Shirvalkar et al., 2010; Igarashi et al., 2014).

In the high frequency end of the gamma band, one can observe wave packets of roughly 50ms in duration usually referred to as fast gamma bursts (FGB) or epsilon bursts (Buzsáki, 2015). During theta states they are residing at troughs of theta waves and are modulated

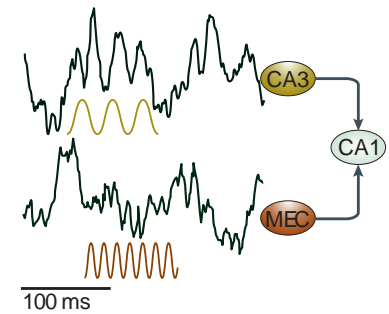


Figure 1.10: Slow and fast gamma oscillations. Slow and fast gamma frequencies seem to stem from different origins. Adapted with permission from (Colgin, 2016).

by MEC (Colgin et al., 2009). In absence of theta, they appear in coincidence with sharp waves making them the doppelganger of sharp-wave ripple (SWR) complexes. Despite the qualitative similarity there are clear quantitative distinctions between these events and SWRs both in physical characteristics and targeted sub-networks in hippocampus and cortex (Sullivan et al., 2011; Ramirez-Villegas et al., 2015).

Finally, it is very important to note that all these findings suggest different scenarios for origin, function and categorization of different sub-bands, and are matter of active research and therefore debate.

1.3.3 *Sharp-Wave Ripples*

Sharp wave-ripples are large amplitude, irregularly occurring LFP patterns that are observed in mammals during waking immobility and during slow wave sleep (SWS), as well as during consummatory behaviors (i.e. drinking, eating and grooming) (Buzsáki et al., 1983). Traces of SWRs could be spotted in studies as early as the 1960's, it has been called by various names such as hippocampal spindles, mini-spindles, mini population spikes and LIA spikes. In 1992, György Buzsáki has characterized the interplay between SWRs and the fast oscillatory population behavior among the CA1 pyramidal neurons (Buzsáki et al., 1992). Since then he started to use the term ripple in his publications in the honor of John O'Keefe who has coined the term in his early observations of hippocampal LFP (O'Keefe, 1976). This type of oscillation is specific to hippocampal formation with most of it occurring in hippocampus and some in entorhinal cortex (Buzsáki et al., 1987). It has been reported in virtually all mammalian species under hippocampal studies from bats to different types of rodents and several primates including humans (Jouvet and Michel, 1959; Vanderwolf, 1969; Freeman et al., 1969; Mankin et al., 2019; Ulanovsky and Moss, 2007). Based on consistent observation of SWRs in hippocampal slices (Kubota et al., 2003; Maier et al., 2003; Colgin et al., 2004; Papatheodoropoulos and Koniaris, 2011) it is widely accepted that SWRs originate in the hippocampus.

The coupled name of SWRs suggests that low frequency sharp waves and ripples could be part of the same phenomenon stemming from a common origin, but experimental evidences suggest a different scenario. While sharp-waves are excitatory events originating in CA3 and transmitting to CA1 (Buzsáki, 1986; Sullivan et al., 2011), ripples seem to be generated locally in the CA1 network (Ylinen and Buzsáki, 1995; Klausberger et al., 2006; Schlingloff et al., 2014; Maier et al., 2011). Furthermore, pyramidal cells in CA1 are phase locked to ripple frequency while such behavior is absent among CA3 neurons.

In addition, ripples in CA₃ and CA₁ are not coherent and indeed CA₃ ripples are usually observed at lower frequencies than in CA₁ (Csicsvari et al., 1999; Sullivan et al., 2011).

Despite these differences sharp-waves and ripples have a close relation. We think of sharp-wave ripple complexes as emergent phenomena. During such events coordinated activity of several neurons would lead to the most synchronous population event we know across the entire brain resulting in a transient excitability among neurons in the hippocampal formation (Buzsáki et al., 1983; Chrobak and Buzsáki, 1994; Csicsvari et al., 1999). This is so fine tuned that small alteration in recruitment of neurons during such an event can turn a physiological event into a pathological one (Suzuki and Smith, 1988; Buzsáki, 1989).

Finally, the most interesting observation about sharp-wave ripples is its spike content. Despite the extreme synchrony in spiking activity at the first glance, we know that pyramidal cells of the hippocampus (and to some extent in neighboring regions such as MEC) preserve a sort of activation order during SWRs (Wilson and McNaughton, 1994; Skaggs et al., 1996; Nádasdy et al., 1999; Lee and Wilson, 2002). This phenomenon which is mostly studied among hippocampal place cells is often referred as replay or reactivation. The order of these spikes match the sequential neuronal firing patterns in the waking animal compressed roughly by a factor of 10 (Lee and Wilson, 2002). These features of hippocampal sharp-wave ripples has made them the prime candidate for a hypothetical mechanism which through compressed spike sequences transfer information from the hippocampus to the neocortex when the brain is not actively processing the environmental stimuli. The basic idea behind this hypothesis suggests that during learning, the neocortex provides the necessary information in order to guide the transient synaptic reorganization demanded for a given cognitive task. Following the behavior, the modified hippocampal content would then be transferred back to the neocortical circuits (SWR state) (Buzsáki, 1989). These ideas are supported by several experimental studies indicating the necessity of SWRs for both encoding and retrieval of information during memory related tasks. In 2009, Girardeau and colleagues actively disrupted SWRs during sleep session right after a hippocampus dependent memory task. They have reported a 20% decrease in performance in a test group as compared to controls where the disruption stimulus was applied with a random time delay with respect to SWRs keeping them intact while controlling for other potential side effects of such interventions (Girardeau et al., 2009). This finding is supported in later studies using similar techniques to interfere with SWRs during rest (Ego-Stengel and Wilson, 2010) and behavior (Jadhav et al.,

2012) emphasizing the impact of SWRs on both formation and retrieval of memories. Considering the accumulating body of evidence, sharp-wave ripples have become the first definite biomarker for cognitive operations (Buzsaki, 2015) and that is one of the reasons I have characterized its dynamics in the absence of input from MEC in this thesis.

1.4 Memory Episodes and Hippocampal Formation

Over 30 years of careful observation of the hippocampal formation suggests that this particular part of the mammalian brain has the tools to collect, form and retrieve quite accurate maps of different episodes of animals experience.

1.4.1 Associative Network, an Essential Part of Memory Systems

David Marr in his pioneering work on the function of the mammalian archicortex (Marr, 1971), suggested that a high degree of recurrent connectivity accompanied by a set of very plastic synapses could facilitate the storage and retrieval of distinct memories. These memories stored as maps in a constellation of synapses in such a recurrent network could be reactivated even by partial stimulation; Process called pattern completion. Following his ideas, researchers have confirmed the existence of such a network in the CA3 sub-region of hippocampus (Treves and Rolls, 1994, 1992; McClelland et al., 1995). CA3, is mainly distinguishable from the neighboring regions DG and CA1 due to the existence of such recurrent collaterals with highly modifiable synapses (Colgin and Moser, 2010).

There are plenty of physiological studies hinting at the ability of hippocampus to recover complete memories from degraded input. O'Keefe and Speakman showed that place cells retain their firing pattern even if a subset of environmental cues are not present. In another study, Nakazawa and colleagues have shown that mice with knocked out NMDA genes in area CA3 cannot perform as control mice in retrieving the complete spatial map they have formed during previous exposure to an environment in case that some environmental cues have been missing (Nakazawa et al., 2002).

There are several studies providing evidence in favor of associative activity of hippocampal neurons. First, it has been shown that both primates and rodents with hippocampal damage, suffer a severe impairment in tasks involving place-object or odor-place associations (Burgess et al., 2002; Crane and Milner, 2005; Gaffan, 1994; Gaffan and Saunders, 1985; Parkinson et al., 1988; Smith and Milner, 1981;

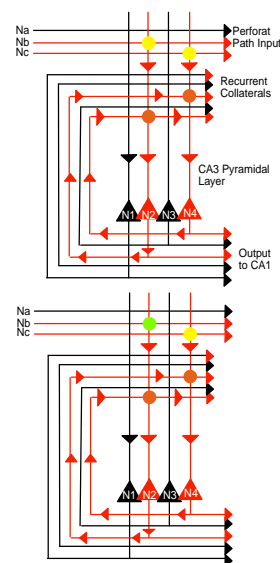


Figure 1.11: Neurons in the CA3 (N1 to N4) usually receive input from perforant path (PP) neurons (Na to Nc) as well as other CA3 pyramidal cells. The flow of activity during encoding of a particular activity pattern (top) and its retrieval from a degraded input pattern is indicated with red arrows (bottom). **Top:** PP-cells representing a particular input pattern (Nb,Nc) activate a subset of CA3 neurons (N2,N4) and the coactivation of these neurons results in the strengthening of their synapses (orange circles). The coactivation of CA3 neurons, in turn, results in additional strengthening of the collateral synapses between them (yellow circles). As a result of such process, a characteristic output pattern is then conveyed to hippocampal area CA1. **Bottom:** After establishment of the connectivity matrix, the encoded pattern could be fully retrieved even with degraded input. Activation of Nc alone results in the direct activation of CA3 pyramidal cell N4 (not N2). N2 is then activated via its collateral synapse with N4 yielding the complete output pattern. Adapted with permission from (Rolls, 2016)

Day et al., 2003; Langston and Wood, 2008; Kesner et al., 2008). Second, electrophysiology studies of ensembles of neurons during the period of forming associative memory between objects showed that a significant population of hippocampal neurons change their response from either of the individual objects to the association between them (Rolls et al., 1989; Miyashita et al., 1989; Cahusac et al., 1993; Wood et al., 1999; McKenzie et al., 2013; Gill et al., 2011).

1.4.2 Pattern Separation and Memory Formation

Any memory system without a strong pattern separator unit is doomed to fail. Consider such system in need of recalling important information from a set of stored memories with high degree of common components, like the content of different lectures in a course held in a same classroom. In this case recurrent connection recover the activity of very similar patterns. Theoretically, one can get around this problem by separating patterns into very distinct ones prior to the associative recurrent network. This is exactly what is supposed to happen in DG, an area upstream of CA3 and CA1. Modifying an old model for pattern separator network in cerebellum (Marr, 2008), O'Reilly and McClelland demonstrated how granule cells in DG, disambiguate the cortical input and guide them in separate patterns into the CA3 recurrent network.

DG granule layer cells are inter-connected through inhibitory synapses allowing them to act as a competitor network. It means any cell receiving enough input to fire and action potential will suppress such activity in other members (its "competitors") of the network. Considering the high input resistance and extremely low membrane potential measured in granule cells (Ewell and Jones, 2010; Piatti et al., 2013), odds are generally against them eliciting an action potential at anytime. As a result of these important features, the DG is capable of transforming the signal of plenty of highly active cortical neurons into sparse but very distinct patterns (Rapp and Gallaqher, 1996; Knierim and Neunuebel, 2016). It is noteworthy to mention that cells in the DG have strong feed forward connections to CA3.

In summary, sparse and distinct input from DG helps CA3 with forming different patterns of activity to encode different memories. Once the synaptic weights are stabilized even partial or weaker activity of cortical neuronal ensembles can evoke memories in hippocampus.

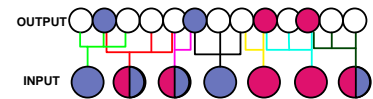


Figure 1.12: Granule cell layer in DG work as pattern separator network. Cells that represent an individual firing pattern are either magenta or purple, and cells that represent both patterns are bi-colored. The connectivity of each cell in the input layer can be traced by following the colored lines. In this simplified schematic, each output cell needs to accumulate at least 1.5 inputs of one kind to reach firing threshold.

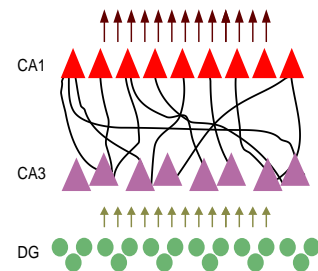


Figure 1.13: Schematics of connections between DG, CA3, CA1 sub-networks of hippocampus.

1.5 Memory Replay in the Hippocampus

As mentioned before, the hippocampal formation plays a crucial role in a declarative memory system that allows us to operate routinely by memorizing daily experiences and recall the most relevant information in different occasions (Squire and Zola-Morgan, 1991; Scoville and Milner, 1957; Squire, 1982). The study of place cells opened a new window towards understanding mechanisms of such consolidation and recall processes. The fact that it is pretty straightforward to map places to mathematical entities facilitates studying population activity of neuronal ensembles in association to what they are coding for in a quantitative manner. In 1989, Pavlides and Winson were the first to recognize that the firing rates and burst probabilities of the place cells with high coordination are more likely to be elevated during the subsequent sleep episode (Pavlides and Winson, 1989). This was the first direct observational hint about the effect of sleep on memory formation but since there were no recordings of neuronal activity in sleep preceding navigational behavior, one could not pin point whether this elevated activity is a result of some pre-existing correlations among neurons or it is indeed reflecting what has been experienced during navigation. In a distinguished study, Wilson and McNaughton were the first to show that pyramidal cells with overlapping place cells during exploratory behavior (RUN) are showing more correlated activity in subsequent sleep (POST) even if they were barely active during sleep before (PRE) behavior (Wilson and Mcnaughton, 1994).

They put forth a hypothesis that neuronal population in the hippocampus which encode some aspect of experience, play back their state to the neocortex. In this way, the hippocampus fits the contextual information for other elements of the experience and unifies different aspects in the neocortex as part of the memory consolidation process. Later on, Skaggs and McNaughton (Skaggs and McNaughton, 1996) showed that the temporal order of activity during RUN is preserved to a large extent in POST sleep. Despite interesting outcomes in these series of studies, there was still some room for improvement. One should note that increased co-activation in POST relative to PRE sleep may be a reflection of the elevated firing rate since correlation is proportional to the cells' firing rates (de la Rocha et al., 2007). Furthermore, the exact temporal structure of neuronal sequences could not be deduced from cross-correlograms, especially when considering higher order correlations to be necessary. In a simple "synfire" chain scenario (Abeles et al., 1993), sequence $\alpha \mapsto \beta \mapsto \gamma$ is present with no connection between α and γ . Now if unit β also participates in sequence $\delta \mapsto \beta \mapsto \eta$, activity of unit β would predict

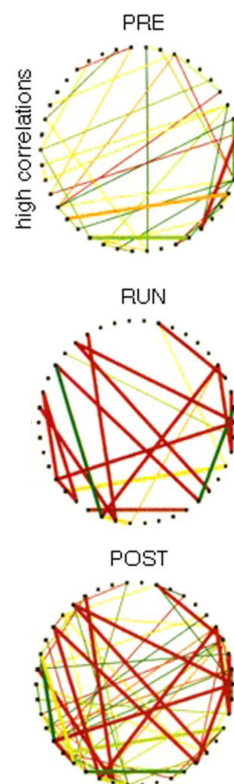


Figure 1.14: Experience dependent replay of hippocampal activity. Modified from (Wilson and Mcnaughton, 1994)

both γ and η (Nádasdy et al., 1999).

Using template-matching methods, Nádasdy and colleagues looked for repeating spike sequence in hippocampus. Reliably, they have reported reoccurring sequences of spikes in both awake and sleeping animals. Interestingly, the spike sequences observed in waking while the rat was exploring a novel environment were "replayed" on a much shorter timescale during SWRs of non-REM sleep. The incidence of RUN sequences was significantly more frequent during POST in comparison to PRE sleep. This was the first evidence showing neuronal activity patterns during SWRs as a consequence of firing patterns formed during exploration (Nádasdy et al., 1999). Lee and Wilson were the first to build a sequential template of CA1 place cells on a linear track during RUN. They used the position of the peak of smoothed firing fields to sort them and construct the template which they have recruited to analyze replays (Lee and Wilson, 2002).

They have observed sequential activation of neurons which preserved the spatial order of place fields (Figure 1.15). They coined the term hippocampal replays for such brief activities and proposed their role in memory consolidation. The time span of these sequences during POST sleep is about 100ms and they preferably occur in time windows dominated by SWRs which is in line with findings on causal role of SWRs in memory formation (Ego-Stengel and Wilson, 2010; Jadhav et al., 2012). This time scale is 10 to 20 times faster than in the behaviorally defined template sequence, i.e., the time elapsed between place field peaks, but in the same order of magnitude with theta sequences (Diba and Buzsáki, 2007). Follow-up studies revealed some aspects about the dynamics of these sequences. In general, sequences tend to incorporate cells which are part of assemblies for novel experiences (Cheng and Frank, 2008; Csicsvari et al., 2007). The probability of recruiting a cell in a sequence is related to its firing dynamics during awake behavior (O'Neill et al., 2008) as well as more emotional components such as coding for reward positions (Dupret et al., 2010).

If the hippocampal neuronal activity during SWRs is consistently enhancing consolidation of memories, it should have consistent observable effect on cortical target regions of hippocampus. There are several studies that recorded simultaneously the activity of different parts of cortex and hippocampus in association with a learning/memory task. It has been shown that population activity in sensory cortices could potentially trigger SWRs in the hippocampus (Ji and Wilson, 2007; Sirota et al., 2003). Peyrache and colleagues observed brief orchestrated packets of neuronal activity in prefrontal cortex (PFC) mainly during sleep after rats learning a new rule in

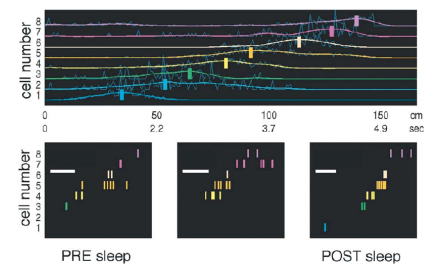


Figure 1.15: Replay of waking neuronal spike sequences during sleep as reported by Lee & Wilson, Modified with permission from (Lee and Wilson, 2002)

the behavioral experiment. They saw that virtually all of prefrontal population bursts are preceded by SWRs in hippocampus with average of 40ms, consistent with expected time for signal to traverse the mono-synaptic path between hippocampus and PFC (Peyrache et al., 2009). These results suggest that activity of sensory cortices triggers SWRs embodying replay of information (which is recently learned) to PFC for long term consolidation.

Ensembles of neuronal sequences observed during SWRs are much richer than a set of sequentially active neurons on linear tracks or open field environments. This is not surprising if one thinks of hippocampus regularly generating self organized sequences of neuronal activity to be recruited later on for encoding information about the outside world. This facilitates the process of forming neuronal engrams for new experiences by providing some sort of partially pre-configured engrams that fit the nature of the experience to a good extent. Keeping this fact in mind we should not be surprised to see studies reporting observations of hippocampal sequences of place cells before the animal has ever been exposed to that environment (Gupta et al., 2010; Dragoi and Tonegawa, 2013a,b). In another study Ólafsdóttir et al. 2015 reported that viewing the delivery of food to an un-visited part of an environment was necessary and sufficient for pre-activation of place cell sequences corresponding to that region of space (Ólafsdóttir et al., 2015). This result points at motivational drive affecting the incidence of pre-plays possibly for better comprehension of things about to happen in immediate future.

1.6 *Scientific Goals of this Thesis*

Hippocampal neurons burst in a highly coordinated fashion during sleep and immobility in association with hippocampal sharp waves (Buzsáki et al., 1983; Csicsvari et al., 1999). These population burst are thought to play a key role in both memory consolidation and memory recollection processes (Buzsáki, 1989; Jadhav et al., 2012; van de Ven et al., 2016). It has been shown that the content of these events relate to sequences of place cells, which can be interpreted as running trajectories in an environment (Nádasdy et al., 1999; Lee and Wilson, 2002). The sequences are observed to replay the trajectories in forward, backward, or mixed directions (Diba and Buzsáki, 2007; Foster and Wilson, 2006; Davidson et al., 2009). The rate of occurrence and content of any of these types of events are correlated with specific stages of the experiment. Sequences during sharp waves were classically thought to reflect the experiences an animal made during previous episodes of running on a maze (Lee and Wilson, 2002; Diba and Buzsáki, 2007). On the other hand, replay events during bursts

can also express preplay of trajectories that the animal is about to follow in the future in a familiar environment (Diba and Buzsáki, 2007; Pfeiffer and Foster, 2013). Other studies reported sequences that reflect future trajectories in yet unknown environments (Dragoi and Tonegawa, 2011; Grosmark and Buzsáki, 2016). This made the interpretation of sequences as a substrate for memory consolidation less straightforward, although the relation between sequences during sharp waves and memory remained intact. Correlations between sequences and future behavior could reflect preexisting task-specific schemata that facilitate the formation of novel memory traces (Dragoi and Tonegawa, 2013b). In this interpretation, the schemata are employed to code correlated parts of experience rather than creating such neuronal assemblies instantaneously upon experience. In this way hippocampus can memorize experiences with higher efficiency.

A classical way to study the role of sequences in relation to a memory system is to compare them to patterns of activity that occur during locomotion induced theta-oscillations (Vanderwolf, 1969; Buzsáki et al., 1983). While running, an animal traverses several place fields and sequences of place cells are also activated within one theta cycle (Figure 1.9). The sequential order of activation at the theta time scale thereby defines a theta sequence (Feng et al., 2015). According to some models (Tsodyks et al., 1996; Dragoi and Buzsáki, 2006) theta sequences and sequence replay during sharp waves both result from the same recurrent hippocampal connectivity. A second class of models (Skaggs and McNaughton, 1996; Melamed et al., 2004; Byrnes et al., 2011) predicts that replay is a result of synaptic plasticity triggered by intact theta sequences via spike-timing dependent plasticity (Levy and Steward, 1983; Blum and Abbott, 1996; Markram et al., 1997; Bi and Poo, 1999).

One way to distinguish between the two classes of models is to study the expression of sequence replay in animals with disrupted theta scale correlations. It has previously been shown that spike timing during theta states is strongly disrupted in rats with bilateral medial entorhinal cortex (MEC) lesions (Schlesiger et al., 2015). The MEC directly projects to the hippocampus and is one major source of information supporting spatial memory (Witter et al., 1989). Nevertheless place fields in MEC-lesioned rats are retained, although they are less abundant, less stable and less precise than in controls (Hales et al., 2014). The models explaining replay as a result of spike-timing dependent plasticity predict that sequences do not emerge during behavior in MEC-lesioned rats. In contrast, models that predict that replay is a consequence of any preexisting connectivity would predict that schema-related replay components, already encoded in the synaptic connections before the lesion, should

remain unaffected. The analysis of replay and pattern activation in animals with MEC lesions thus opens a possibility to probe both of the current views on hippocampal replay.

1.7 *Animal Experimental Methods*

All the experimental procedures leading to the collection of hippocampal electric potential in freely moving rats have been performed in the laboratory of Professor Stefan Leutgeb at university of California, San Diego. Since these procedures are not part of my doctoral study but nonetheless are very essential for understanding the results, I will review these methods in this section.

1.7.1 *Animal model*

For these set of experiments we used 12 experimentally naïve, male Long-Evans rats (Figure 1.16). All subjects weigh between 300 and 350 grams at the starting time of each experiment. The animals were divided in two groups. One experimental group with nearly complete lesions of the MEC (LES; $n=7$), and a control group that only experienced similar surgical procedures but no toxins were injected into the brain (CON; $n=5$). The assignment of animals to one of these groups were done in a random manner. After recovery from the first surgery, all subjects had a second surgery during which they got a recording implant consist of fourteen tetrodes. Rats were on a reversed 12 h light/dark cycle and kept in individual housing during the course of experiment. All behavioral tests and electrophysiological recordings performed in the dark phase of the daily cycle. After one week recovery period from the implantation procedure, rats were food restricted and maintained at $\sim 90\%$ of their ad libitum weight.

1.7.2 *Surgeries & Implantation*

Anesthesia was induced and maintained throughout surgery with isoflurane gas (0.8% – 2.0% isoflurane delivered in O_2 at 1 L/min). We start the procedure by positioning the animal in a stereotaxic instrument (David Kopf Instruments, 7324 Elmo Street, Tujunga, CA 91042). Then we adjust the incisor bar in a way that bregma is leveled with lambda. At the target site a small hole is drilled and a needle is lowered to the targeted tissue (in this case MEC). After completion of each lesion the animal was allowed to recover from anesthesia on a



Figure 1.16: The Long-Evans rat is an outbred rat developed by Drs. Long and Evans in 1915 by crossing several Wistar females with a wild gray male.

active heat pad. The control group underwent the complete surgical procedure, but no lesions were made.

In the MEC lesion group, excitotoxic lesions were produced by NMDA dissolved in aCSF (Harvard Apparatus, 84 October Hill Road, Holliston, Massachusetts 01746, United States) providing a solution with 10 mg/ml concentration. NMDA was injected at a rate of $0.1\mu\text{l}/\text{min}$ using a $10\mu\text{l}$ Hamilton (Reno, NV) syringe mounted on a stereotaxic frame and held with a Kopf model 5000 micro-injector. There was a 1 minute pause between lowering the needle and beginning the injection. After the injection, there was another minute pause before retracting the needle in order to reduce the spread of drug up the needle tract. Overall, NMDA was injected into 8 sites (total volume $1.04\mu\text{l}$) on each hemisphere. The anterior-posterior (AP) coordinates was determined using the location of the anterior border of the transverse sinus. The needle was inserted at $\text{ML} \pm 4.6$ with an angle of 22 degrees moving from posterior to anterior at that location with DV values: $-5.2, -4.7, -4.2, -3.7, -3.2, -2.7, -2.2, -1.7\text{mm}$.

Following the same protocol in prepping the animals for injection, we inserted a bundle of tetrodes in the cortex area lying above the dorsal hippocampus. Tetrodes were constructed by twisting four $17\mu\text{m}$ polyimide coated Platinum-Iridium (90%/10%) wires. The tip of each electrode was coated with Platinum to reduce the impedances to $200 - 300\text{k}\Omega$ at frequency of 1kHz. The tetrode bundle was targeted to the hippocampus in the right hemisphere (AP: 4.0., ML: ± 2.6).

MEC Lesion Group				
Animal Name	MEC II		MEC III	
	Left	Right	Left	Right
405	100%	94%	70%	52%
434	100%	98%	92%	94%
3656	100%	100%	100%	99%
3754	90%	91%	83%	87%
3756	100%	96%	97%	92%
3837	94%	100%	90%	100%
3838	86%	87%	72%	56%
3903	96%	97%	92%	96%

See Figure 1.18 for comparison plots and exemplar histology slides.

Table 1.1: Quantification of lesion extent in different individuals in MEC lesioned group.

1.7.3 Behavior

APPARATUS Behavior was conducted in a linear track maze (150cm × 7cm) located in a room which animal was experiencing for the first time (novel room). The track was covered with black contact paper and was elevated 50cm above the floor. Chocolate sprinkles were used as rewards at the end of each of the extremes of the track. A camera was mounted above the center of the maze and recorded the entire behavior. The trajectory of the animal was later on extracted from these videos. We have positioned a number of constant, salient visual cues in the room. During the rest sessions the animals were placed in a Plexiglass holding chamber (30cm × 56cm) located in a familiar room.

BEHAVIORAL TASKS Prior to any behavior tests rats were given at least 4 weeks to recover. After recovery, animals were handled and familiarized with the room where they had their rest sessions. Rats were allowed to explore the Plexiglas holding chamber for at least 12 times before the experiment began. Each session took about an hour to assure a complete familiarization with the resting environment. Over the course of familiarization, tetrodes were slowly lowered to the CA1 region of the hippocampus. During tetrode advancement and recordings, the signals were pre-amplified with a unity gain head-stage and then recorded with a data acquisition system with 64 digitally programmable differential amplifiers (Neuralynx, Tucson, AZ, USA). Spike waveforms with a peak above 40 – 45 μ V threshold were time-stamped and digitized at 32 kHz for 1 ms. In order to track the rat's head position more accurately, a LED was installed on the head-stage. Local field potentials were acquired by recording one

channel of each tetrode with the filters set to the 1 – 450 Hz band. As demonstrated in previous studies (Hales et al., 2014), sharp wave ripples were not diminished by the MEC lesion and could therefore be used to guide electrode advancement into the cell layers in all rats.

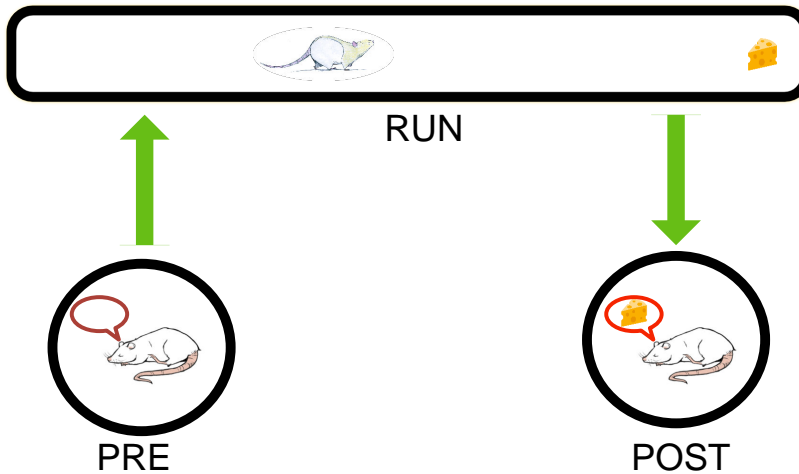


Figure 1.17: Scheme of behavioral paradigm. Rats running on a linear track for rewards at the end points (RUN). 1 hour rest sessions are recorded in a familiar environment prior (PRE) and post (POST) linear track session

Right after stably positioning the tetrode bundle in the CA1 cell layer, we have started with electrophysiology recordings while the animal is running back and forth along the linear track (RUN). Spikes and local field potentials were also recorded while the rat was resting in a transparent holding chamber in a familiar room for 1 hour prior (PRE) and 1 hour after (POST) the end of each recording day. The room was dimly illuminated using a single light source on a corner at approximately 2 meters from the sleep chamber. After the first sleep period, the animals were transported to a novel room to run back and forth on a linear track for food rewards (chocolate sprinkles). The behavior sessions were 30 min long. Immediately after, the rat was transported back to the familiar room and the second sleep period began. Each animal run 1 session per day (PRE, RUN, POST) for an average of 4 days. Each day the linear track was positioned in a different novel room with distinct visual cues. Data collection and analysis were not performed blind to the conditions of the experiment.

1.7.4 Histology

Rats were perfused transcardially after administration of an overdose of sodium pentobarbital. For perfusion, a phosphate buffered solution followed by 4% paraformaldehyde solution (in 0.1 M phosphate buffer) was used. Brain tissue was then removed from the skull and kept in a solution of 4% paraformaldehyde for 24 hours. After this, brains were transferred to a 30% sucrose solution where they stayed for an average of 48 hours. Sagittal sections (40 μm thick) were cut with a freezing microtome beginning just lateral to the hippocampus and continuing medially through the length of the hippocampal region for each hemisphere. Every section was mounted and stained with cresyl violet to track the hippocampal tetrode locations. Every fourth section was used to quantify the MEC lesion extent with the Cavalieri method. A sampling grid with unit area of $150\mu\text{m}^2$ was overlaid on all tissue images. For each slide, we counted the total number of grids in contact with each of the following anatomical regions: MEC layer II, MEC layer III, MEC deep (V/VI) layers, dorsal parasubiculum, ventral parasubiculum, and hippocampus. The total volume of tissue in each anatomical part is estimated as:

$$V^{\text{region}} = \tau f s \sum_{\text{All sections}} N_{\text{section}}^{\text{region}} \quad (1.1)$$

where τ and f are section thickness and sampling frequency of sections. $N_{\text{section}}^{\text{region}}$ is the number of selected grids counted per section and s is the unit area of the grid. In table 1.1 we report the damage to different parts in percentile which is estimated as:

$$\text{Damage percent} \approx \frac{V^{\text{region}}|_{\text{damage}}}{\langle V^{\text{region}} \rangle_{\text{control}}} \times 100 \quad (1.2)$$

$V^{\text{region}}|_{\text{damage}}$ is the volume of damaged tissue divided by the average volume of same tissue in the control rats and finally multiplied by 100 to get the percentile.

Confirming the previously described results in (Hales et al., 2014); Damage to the brain areas other than MEC was not substantial as indicated in table 1.1).

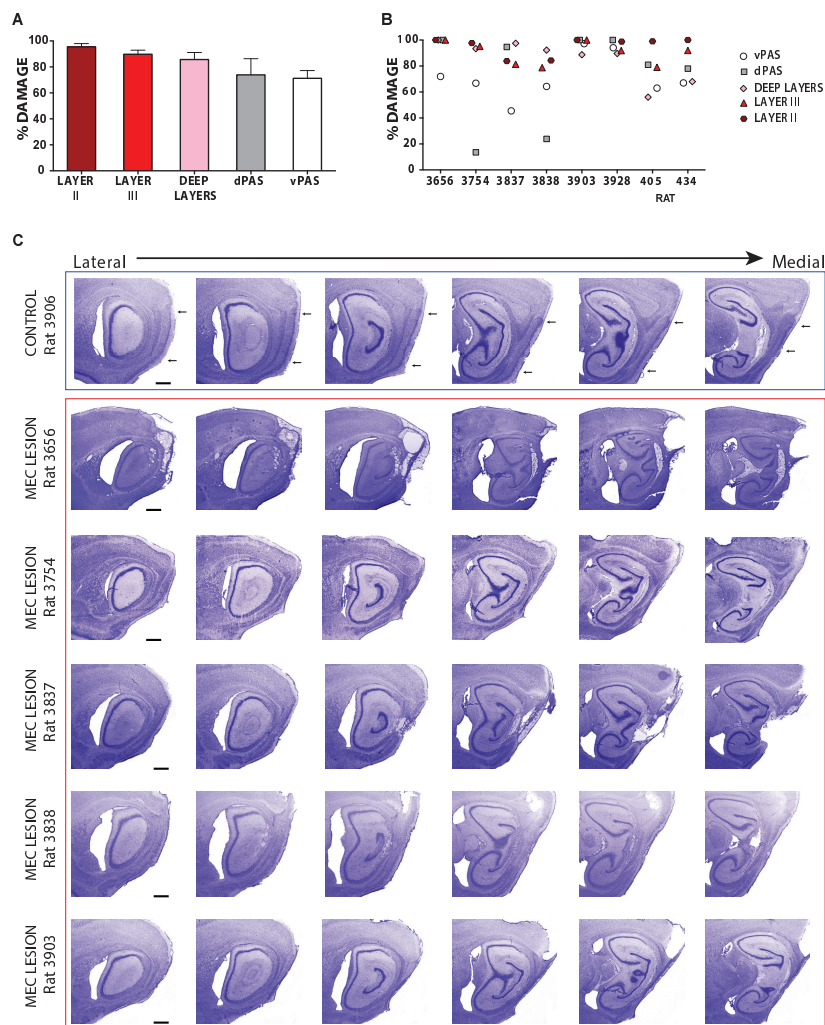


Figure 1.18: MEC lesions were nearly complete.

(A) Average lesion size ($n = 7$) Layer II, layer III, deep layers (V/VI), dorsal parasubiculum (dPAS), and ventral parasubiculum (vPAS) were quantified separately. Error bars represent SEM. (B) Percentage of lesioned tissue for each one of the rats included in the analysis. (C) Detailed illustration of complete series of sagittal sections. Scale bar=500 μm . First row correspond to a representative example of a control rat. The following 5 rows correspond to sagittal sections of 5 out of the 7 rats used for the analysis. Histology of rat 405 and 434 can be found in (Hales et al., 2014). Modified with permission from (Chenani et al.), submitted manuscript.

2

Materials and Methods

In this chapter a comprehensive review of the methods used to accomplish this study is given. I will explain about the analysis procedure that guided us to meaningful trends in the vast amount of data we have produced during this project. All behavioral experiments and electrophysiological recordings have been performed by Marta Sabariego, Magdalena Schlesiger and Emily Mankin in the laboratory of Professor Stefan Leutgeb at University of California San Diego. For the sake of continuity and comprehension of the work I have introduced all the parts done by my colleagues to the best of my knowledge in the previous chapter. For more detail on procedures prior to data acquisition please consult the section "Animal Experimental Methods" in the introduction.

2.1 Data Analysis

2.1.1 Rest Periods

As mentioned before rest periods took place in a familiar room (PRE and POST). I did not assess any behavioral measure to verify the state of sleep in animals. During this study I only considered long spans of time where animals were quite and immobile. Therefore I excluded all the time points where animals passed the speed threshold of $2 \frac{\text{cm}}{\text{s}}$. All immobile periods shorter than 10 seconds are also

excluded from the analysis.

2.1.2 Spike Sorting

In our recordings neuronal spike waveforms have been sampled with 32kHz, therefore each waveform is represented by an array of electrode voltages of size 32, over the 1ms time course of a spike (Figure 2.1). We can think of this array as a vector in a 32 dimensional orthogonal space. In these interpretation, each dimension x_i refers to voltage magnitude, i time steps after the beginning of the waveform. So x_0 would be the dimension that the first points in each waveform live in (v_0 in Figure 2.1) and x_{31} would be the dimension of last points (v_{31}). Ideally, if the relative position and orientation of a neuron and electrode are steady over the duration of the experiment, then by considering the fact that the change in the shape of neurons is negligible in time scales compared to experiment time, we can expect to observe stereotypic action potential traces from each neuron which is only depending on relative geometry between electrode and that particular neuron. This implies that vectors from different action potentials elicited from a single neuron should point towards the same point in the 32 dimensional hyperspace. Considering imperfections of the real world (or our models of the world), we expect action potential vectors of a particular neuron to form a cluster, confined in a region of space. Therefore distinguishing different clouds in space is equivalent of identification of different "neurons". We can never be sure that a single cloud contains spike wave-forms that are purely coming from a single neuron. That could be due to symmetry in neuron-electrode configuration and limited measurement accuracy of recording instruments. A way around this problem is by addition of more electrodes in slightly different locations in the recording site. That was the main motivation behind the invention of tetrodes (Figure 2.2).

Single action potentials would be recorded slightly differently by different electrodes. Having more electrodes means having a more complete picture and therefore more resolving power between different "neurons". In this study, we have used tetrodes. Single neurons are detectable on some or all 4 channels of 1 tetrode. This means for each action potential we have potentially 4 different vectors. Usually most of the dimensions are not very informative when it comes to discriminating between neurons. In each recording, the diversity is usually distributed among a limited number of dimensions. Therefore, I transformed all action potential vectors into another orthogonal space with the same number dimensions but with the property that in this new space dimensions (p_i) are sorted with respect to

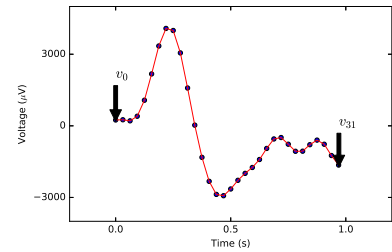


Figure 2.1: Spike waveform and sampling. The electric potential was sampled with 32 KHz, providing 32 sampling point per typical spike time of 1 ms.

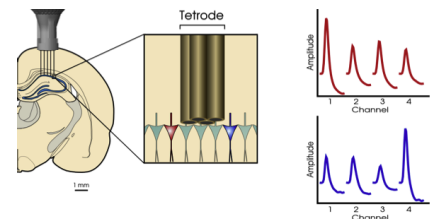


Figure 2.2: Tetrode and its usage in recording pyramidal layer of CA1. The right plots depict difference in shape of waveforms of red and blue neurons as seen by different channels on the tetrode. Source: [Wikipedia.org/wiki/Tetrode](https://en.wikipedia.org/wiki/Tetrode)

variability of vectors. This means that first component (p_0) of our vectors is the most diverse component followed by p_1 and so on. In this transformed space usually referred as principal components (PC) space, the first 3 dimensions [p_0, p_1, p_2] roughly contain 80% of the variability within data. I reduce the effective dimensionality of data by selecting only these components. Then I perform an unsupervised clustering on them using the masked EM algorithm implemented in the KlustaKwik software (Kadir et al., 2013). We visually evaluated the results of clustering using the MClust software (Figure 2.3). Low quality clusters and clusters suspected of not stemming from a biological sources were excluded from further analysis. Finally, the spike time stamps of accepted clusters were exported as individual spike trains.

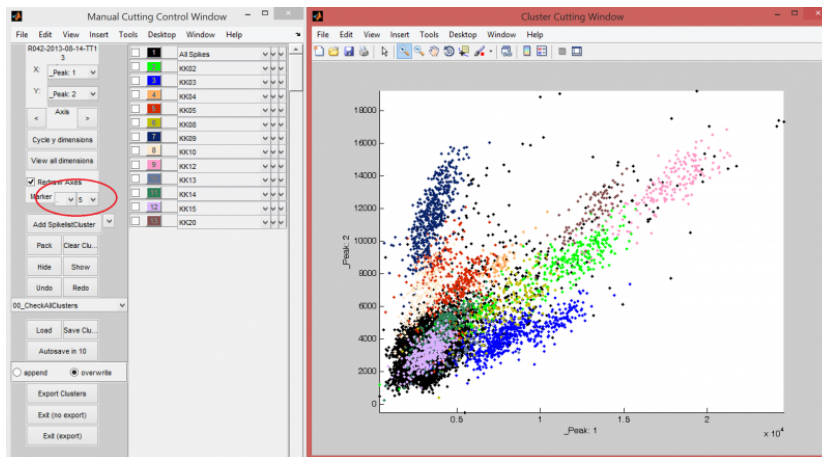


Figure 2.3: Spike Clusters Identification

Spike sorting GUI, MClust version 3.5, written by A. David Redish. The main window shows different clusters detected on one tetrad. Only well isolated clusters with biologically feasible properties were selected for further analysis.

2.1.3 Place Cell Identification

During the experiment we record the position of each animal with a behavior camera with 30 fps sampling rate. Then the position of the head is extracted from the video. This gives us an estimated trajectory for each animal. Trajectories are estimated for all experiment sessions (PRE, RUN, POST) and exported to files accordingly.

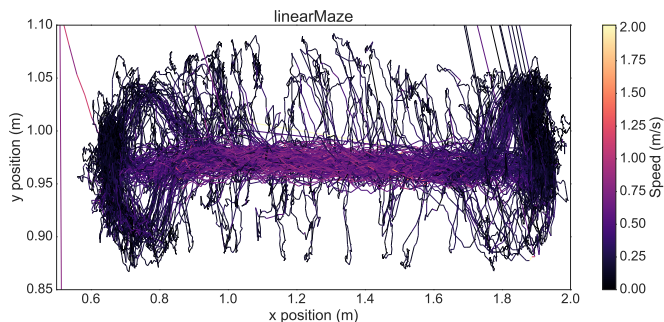


Figure 2.4: Recorded Trajectory of a Rat

Trace depicting the trajectory of animal in a RUN session. The heat map reflects the speed of animal. Bright region in the middle showing a stereotyped left-right running behavior.

During RUN, spike times of different units are used to infer the location of animals during each spike. Since the sampling of spikes was done on a much finer time scale, I linearly interpolated between trajectory data point whenever necessary in order to get an precise estimate of location at the time of spiking activity. Well trained animals show very stereotyped runs with an average of ~ 3 runs per minute (Figure 2.4). After estimating the end points of runs, I determine the direction and time span of each run. I calculated firing rates of different units with 5cm spatial resolution as the ratio of spike counts and time spent in that particular space. For firing unit i and position x_j we can write the firing rate as:

$$r_i[x_j] = \frac{N_i[x_j]}{N_{\text{points}}[x_j]\Delta t} \quad (2.1)$$

where $N_i[x_j]$ is the number of spikes in position x_j , $N_{\text{points}}[x_j]$ is number of trajectory points in positions x_j and Δt is the time difference between sampling trajectory points. At this point I put the firing rates along with direction of each run (leftward/rightward) under a two-way ANOVA test in order to find spatially modulated and directional selective units. From the set of spatially modulated units, I selected the candidates with a single peak (averaged over all runs) above 2 Hz for constructing place-templates. In order to construct templates, the average firing rate curves (solid lines in Figure 2.5) were convolved with Gaussian kernels ($\sigma = 3\text{cm}$), then I have extracted the location maximum rate of the convolved average

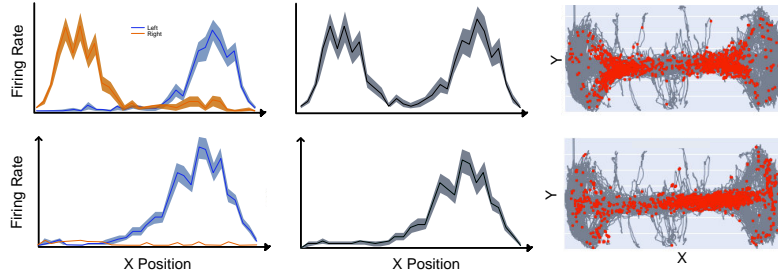


Figure 2.5: Activity of Two Representative uni and bi-directional Place Cells on a linear track maze.

Each row is showing a single firing unit during RUN. **Left:** Firing rates averaged for each running direction (blue, orange are leftward and rightward respectively). **Middle:** Average firing rate of same unit in all runs. **Right:** Individual spikes (red dots) overlaid on trajectory of animal (gray line).

firing rates for leftward and rightward runs separately and sorted cells with respect to these locations. In this way I get two sets of templates (one per running direction) to be used later in sequence analysis.

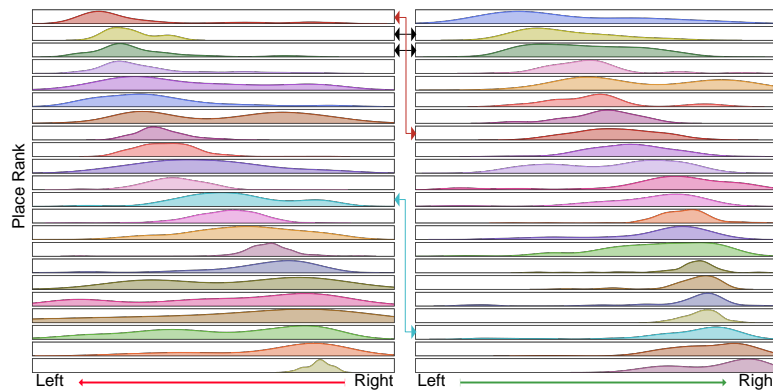


Figure 2.6: Place Cell Templates

Place cell templates of a representative RUN session. Same group of cells (color coded for the identity of neurons) usually appear in different order in two templates made for different directions of motion on a linear track. Some cells (black arrows) exhibit relatively similar place fields regardless of direction of motion while others (color arrows) completely change their fields in different directions.

2.1.4 Population rate & population bursts

The standard definition of population rate is the overall firing rate of all recorded firing units during the experiment. I have calculated the population rate as total number of spikes of all place fields per time bin of 1ms convolved with a Gaussian kernel ($\sigma = 30\text{ms}$).

Population bursts are defined as transient raise in firing activity of cells. In this project, population burst are defined as the time span while the population rate stayed at least 1 standard deviation (SD)

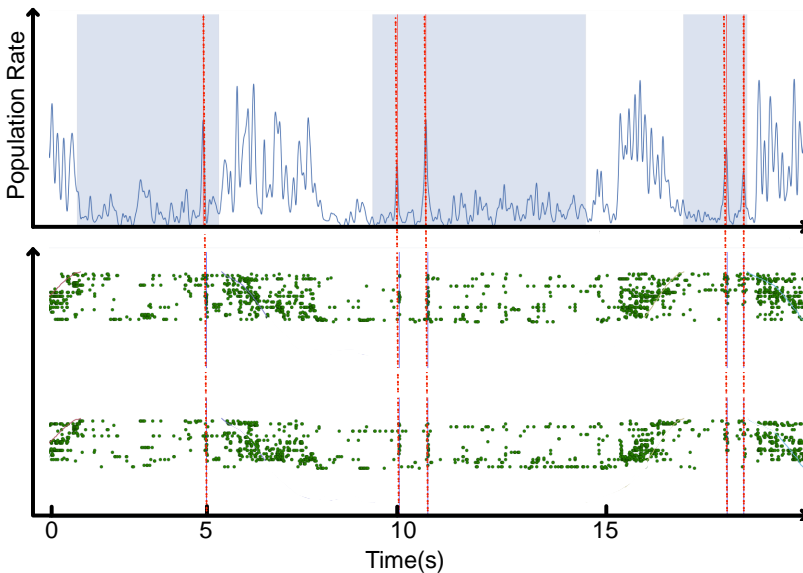


Figure 2.7: Detection of Population Bursts

Top: Population rate as a function of time during RUN. Dark boxes indicate immobile periods at the ends of linear track. **Bottom:** Raster plot of different firing units sorted with respect to left and rightward templates. Vertical lines indicate the time of detected bursts.

above its average during a period when the peak firing rate reached at least 3 SD above average. In order to avoid cases where such raise is dominated by a single or few bursting cells, I have only considered population burst with 5 or more active cells for the analysis. Burst rates were calculated as number of population bursts divided by immobility time in a sessions (PRE, RUN, POST). Sessions with 20 or less population bursts were excluded from further analysis.

2.1.5 Pattern activation analysis

This part of analysis included all firing units regardless of their type (interneuron vs. principal) and place modulation. The methodology of the analysis is mainly following (Peyrache et al., 2010). I start by estimating the firing rate of different units in time bins enforced by theta waves. In order to find appropriate time bins I transform the LFP signal of the whole recording session into frequency space using the fast Fourier transform algorithm. Then I back transform the 6 – 10 Hz part of spectrum to obtain the theta component of LFP. I define the time spans between two consecutive peaks in this filtered signal as theta cycles. Then by binning the spike times from individual units according to theta cycles and dividing by corresponding theta cycle, I estimate the firing rates in each cycle. For the j^{th} theta cycle we have:

$$r_i[\theta_j] = \left(\frac{N_{\text{spikes}}[\theta_j]}{\Delta t_{\theta_j}} \right). \quad (2.2)$$

In order to eliminate the effect of difference in average firing rate I subtract unit-wise mean and normalize these rates by unit-wise standard deviation (Z-score).

$$\bar{r}_i[\theta_j] = \frac{r_i[\theta_j] - \langle r_i[\theta_j] \rangle}{\sigma_{r_i}} \quad (2.3)$$

$\langle r_i[\theta_j] \rangle = \frac{1}{\Theta} \sum_{j=1}^{\Theta} r_i[\theta_j]$ and $\sigma_{r_i} = \sqrt{\frac{1}{\Theta} \sum_{j=1}^{\Theta} (r_i[\theta_j])^2 - \langle r_i[\theta_j] \rangle^2}$ are the average and standard deviation of firing rate for unit i respectively. Θ is the total number of bins (theta cycles) in each experiment session. In the next step I arrange these z-scored firing rates into population rate vectors $\vec{R}[\theta]$ as:

$$\vec{R}[\theta_j] = \begin{pmatrix} \bar{r}_1[\theta_j] \\ \bar{r}_2[\theta_j] \\ \vdots \\ \bar{r}_n[\theta_j] \end{pmatrix}.$$

These population vectors are defined for each experimental session (PRE, RUN, POST) over consecutive theta cycles. Using \vec{R} 's I calculate the covariance matrix in each RUN session as follows:

$$\mathcal{C} = \frac{1}{\Theta} \vec{R} \vec{R}^T = \frac{1}{\Theta} \sum_{\theta_j} \begin{pmatrix} \bar{r}_1[\theta_j] \\ \bar{r}_2[\theta_j] \\ \vdots \\ \bar{r}_n[\theta_j] \end{pmatrix} \begin{pmatrix} \bar{r}_1[\theta_j] & \bar{r}_2[\theta_j] & \cdots & \bar{r}_n[\theta_j] \end{pmatrix}. \quad (2.4)$$

In this form component \mathcal{C}_{ik} of the covariance matrix represents the pairwise correlations among units i and k .

Since \mathcal{C} is by definition a symmetric matrix, one can perform spectral decomposition (eigen-value decomposition) to rewrite the overall correlation matrix as sum of orthogonal patterns P_{λ_i} :

$$\mathcal{C} = \sum_{\lambda_i} \lambda_i P_{\lambda_i} \quad (2.5)$$

here λ_i are eigenvalues and $P_{\lambda} = V_{\lambda}^T V_{\lambda}$ is defined as outer product of the corresponding eigenvectors V_{λ} . In other words one can think of session wide correlations among observable neurons as weighted sum of orthogonal co-activation patterns whose importance is determined by the corresponding eigenvalue.

In order to identify persistent co-activation patterns which could potentially be linked to behavior I compare the eigenvalues of \mathcal{C} to eigenvalues of a random matrix. The null hypothesis in this case assumes that all co-activation in the data could be explained by random independent activity of different cells which in turn leads to a correlation matrix with special properties. Assuming we have N random independent variables each sampled Θ times ($\Theta > N$). Then

there is an upper bound on the eigenvalues of the correlation matrix among these variables as follows:

$$\lambda < \lambda_{\max} + N^{-\frac{2}{3}} \text{ with } \lambda_{\max} = \sigma^2 \left(1 + \sqrt{\frac{N}{\Theta}} \right)^2 \quad (2.6)$$

here σ is standard deviation of the normal distribution (Tracy and Widom, 1994; Marchenko and Pastur, 1967; Sengupta and Mitra, 1999). By using this limit I identify eigenvalues greater than $\lambda_{\max} + N^{-\frac{2}{3}}$ as significantly persistent (Peyrache et al., 2010). I repeat the same procedure to get the normalized firing rate and correlation matrices for the rest epochs (PRE/POST) as well. The session wide similarity of coactivation between RUN and rest could be written as:

$$S^{\text{RUN-P}} = \frac{1}{2} \sum_{i,j,i \neq j} C_{ij}^{\text{RUN}} C_{ij}^{\text{P}} \quad (2.7)$$

$$= \frac{1}{2\Theta_{\text{P}}} \sum_{\theta=1}^{\Theta_{\text{P}}} \sum_{i,j,i \neq j} \bar{r}_i^{\text{P}}[\theta] C_{ij}^{\text{RUN}} \bar{r}_j^{\text{P}}[\theta] \quad (2.8)$$

$$\equiv \frac{1}{2\Theta_{\text{P}}} \sum_{\theta=1}^{\Theta_{\text{P}}} R_0^{\text{RUN-P}}[\theta] \quad (2.9)$$

In these terms, $R_0[\theta]$ is basically a time dependent similarity measure between two epochs. By expanding C^{RUN} using equation 2.5 we can access the contribution of different patterns in overall similarity.

$$R_0^{\text{RUN-P}}[\theta] = \sum_{\ell} \lambda_{\ell} \sum_{i,j,i \neq j} \bar{r}_i^{\text{P}}[\theta] \left(\mathbf{P}_{ij}^{\ell} \right)^{\text{RUN}} \bar{r}_j^{\text{P}}[\theta] \quad (2.10)$$

$$= \sum_{\ell} \lambda_{\ell} R_{\ell}^{\text{RUN-P}}[\theta] \quad (2.11)$$

In following chapters, mean session wide activation strengths is referring to the time average of individual activation strengths of relevant patterns $R_{\ell}^{\text{RUN-P}}[\theta]$.

2.1.6 Sequence Analysis

Sequence analysis is another approach towards studying of neuronal population bursts. The idea of this type of analysis is to compare the time order of spiking activity in population bursts during some behavioral state to a specific order of firing deduced from firing activity in another behavioral state. In this case, after the identification of place cells, I order them by the location of their peak firing rate for each direction (leftwards/rightwards) separately (Figure 1.9 & 2.6). During population bursts, sequences are ordered based on the mean spike time of each neuron. I compute rank order correlation coefficients between the index sequence observed in a population

burst and either the template sequence derived from the place field centers (spatial similarity) or the sequence obtained from another population burst (motif similarity).

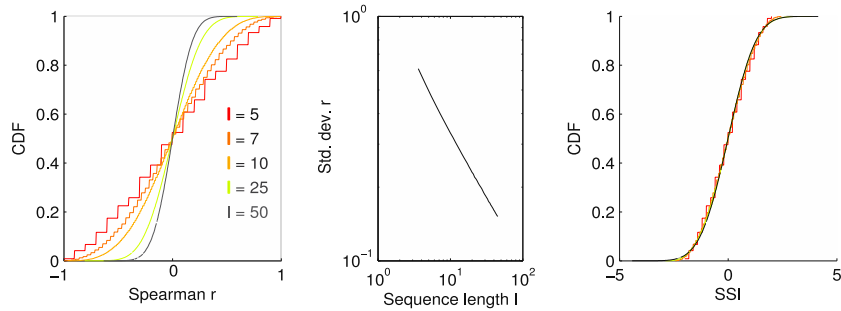


Figure 2.8: Rank-Order distribution of Random Sequences

Left: Cumulative distribution functions of rank order correlation coefficients for random sequences of length l . **Middle:** Standard deviations from distributions on the left as a function of l . **Right:** CDFs for SSIs and different sequence lengths l are almost identical (SSIs are rank order correlation coefficients scaled by the standard deviation from the middle graphs). Modified with permission from (Chenani et al.), submitted manuscript.

SIMILARITY INDICES (SSI/MSI). Since the distribution rank order correlation coefficients strongly depend on sequence length (Figure 2.8), the likelihood of observing a sequence with rank-order correlation c would also depend on the length of respective sequence. For example, while among sequences of length $l = 50$ it is virtually impossible to observe sequences which $|c| > 0.5$, there is a 50% chance of finding them among sequences of length $l = 5$. I needed to examine the likelihood of observation of a sequence by chance regardless of its length. Therefore I normalize rank-order correlation coefficients by the standard deviation of correlation coefficients obtained from random index permutations.

In this way we are able to pool all population bursts completely independent of the number of participating neurons. I use terms, spatial similarity index (SSI) and motif similarity index (MSI) for normalized rank-order correlation coefficients derived from place cell based templates and population burst-based templates, respectively. Finally, one should note that I excluded all experimental sessions with less than 20 population bursts from the analysis.

SIGNIFICANT SEQUENCES. A sequence is called significant if its SSI modulus is in the upper 5% quantile of the distribution of SSI moduli derived from random 10,000 shuffles of the cell indices. The shuffles were performed on the set of sequences from the respective session.

REPETITION INDEX In each session, I computed MSIs for all pairs of population bursts. For each population burst in a session I counted

how many MSI values were in the upper 5% quantile of an MSI distribution derived from random permutation of cell indices. This number k was divided by the standard deviation of k in the respective session to yield the repetition index.

PARTICIPATION INDEX. For each place cell I counted, how often it participated in a significant sequence in one session. The participation index is defined as the ratio of the counted number over total number of significant sequences. Sessions with less than 5 significant sequences were excluded from the analysis.

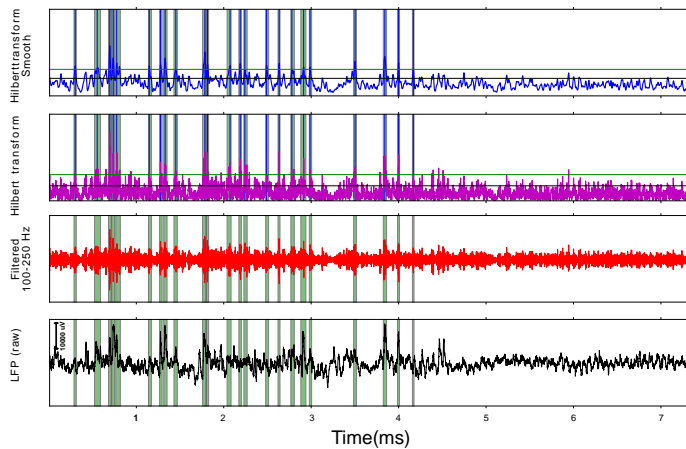


Figure 2.9: Detection of High Frequency Events (HFE)

2.1.7 Local field potential (LFP) analysis

All recording channels were visually inspected both in time and frequency domains. In each session the least noisy and most stable channels were selected for further analysis. Successively, the selected LFP signal were whitened using a second order autoregressive (AR,2) model (using python package statsmodels).

HFE IDENTIFICATION. Candidate events were detected using a threshold on the absolute value of the Hilbert transform (smoothed using a Gaussian kernel with $\sigma = 12$ ms) of the band-passed (100 – 250 Hz) LFP. Peaks reaching over 3σ (standard deviation) level were recorded as candidate events with event extent defined as times where the absolute value of the Hilbert transform rose above and went below the 1 SD level (Figure 2.9).

HFE CLUSTERING. After identification of HFE events, whitened signals of all events were transformed to frequency space using the

Control

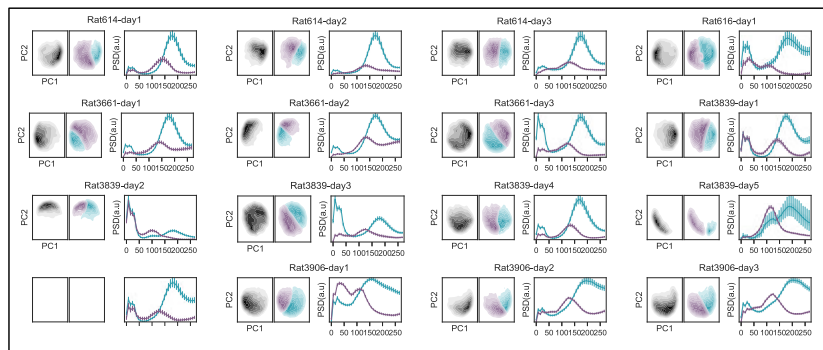
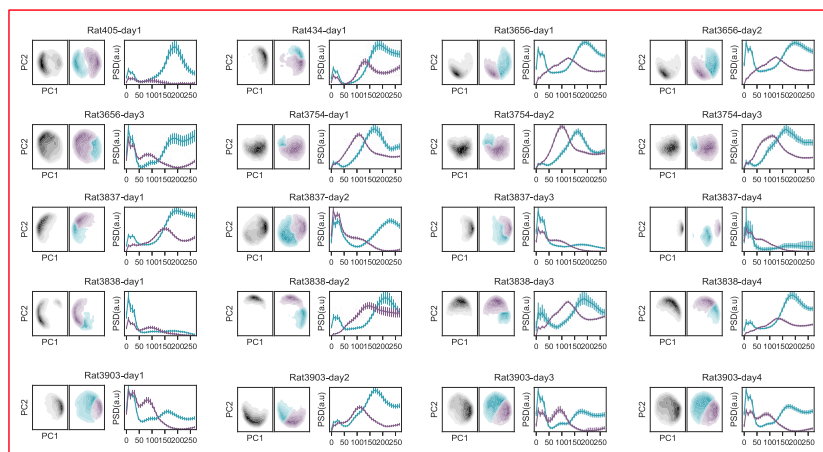


Figure 2.10: Clustering result of HFE's across all animals

MEC Lesioned



Top: The black box contain clustering result summarized in 3 plots per animal in control group. Two square plots on left of each panel show the density of HFE's in PC space. Right panel represents the average power spectrum in different clusters. **Bottom:** Same plots for lesion group. Note the low frequency component in power spectrums usually accompanied by SWRs. Modified with permission from (Chenani et al.), submitted manuscript.

multi-taper method (Thomson, 1982), resulting in power vectors on a frequency grid up to 300 Hz with resolution of ~ 10 Hz. Power vectors were projected to PC space and clustering was performed on the first two principal components using different clustering algorithms provided in python scikit-learn (Pedregosa and Varoquaux, 2011). Comparing the result of different algorithms (MiniBatchKMeans, Spectral Clustering, Ward, Birch) on each dataset I accepted the most stable partitioning of data across all clustering methods (Figure 2.10).

WAVELET ANALYSIS. I applied wavelet analysis on each 512 ms window around the peak of an HFE (Torrence and Compo, 1998) to ensure that HFEs were isolated in both time and frequency domains.

3

Results

In this chapter I will present the results I have obtained during my doctoral studies. These results are manifested in two submitted manuscripts. The majority of results represent a preliminary version of the submitted manuscript (Chenani et al.). Results of the last section in this chapter are also available in (Mankin et al., 2019).

3.1 Co-activation Patterns in Hippocampal Network with MEC Lesion

It has been reported that place fields are generally more scarce among hippocampal neurons in MEC lesioned rats (Hales et al., 2014). Therefore as a first approach, I analyzed co-activation patterns among all observed neurons, independent of having to define place fields during RUN. As previously explained in the last chapter, I generated a population rate vector for each theta cycle of the local field potential and computed the covariance matrix of these vectors after cell-wise normalization (Figure 3.1).

Subsequently the activity patterns were derived as the significant principal components (Figure 3.2 left, see Methods) of the population rate vectors obtained during RUN. Finally, the co-activation strengths $R_\ell[\theta]$ of these activity patterns during PRE and POST session were obtained as the projection of the population rate vectors during the relevant session (PRE/POST) to these principal components (Figure

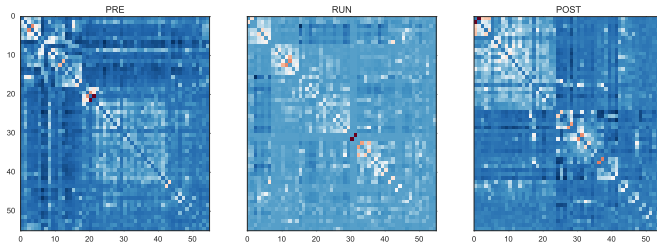


Figure 3.1: Epoch wide Correlation Matrices

Covariance matrix obtained from z-scored population rate vectors obtained during PRE, RUN and POST epochs. Each row (column) represent the average coactivity of a neuron with all the other neurons observed over the course of an experiment. Modified from (Chenani et al.), submitted manuscript.

3.1 & equation 1.13 in section 2.1.5).

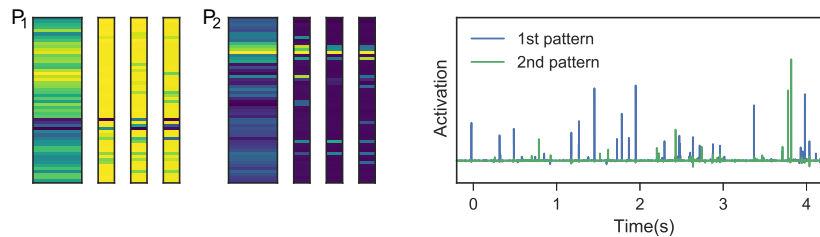


Figure 3.2: co-activation patterns persisted across epochs.

Left: Two examples of significant eigenvectors (wide columns, P_1 & P_2) from the covariance matrix in Figure 3.1 and three matching example pattern vectors from PRE or POST rest sessions. **Right:** Activation (scalar product between patterns and eigenvectors) as a function of time during POST. Modified from (Chenani et al.), submitted manuscript.

To our surprise, I observed significant time-averaged mean activation strengths in the PRE and POST sessions among MEC-lesioned animals as well as control group (one-sample t-test of activation values z-scored relative to surrogate; $p = 5.3 \times 10^{-6}$ for PRE control, $p = 8.4 \times 10^{-8}$ for POST control, $p = 2.4 \times 10^{-18}$ for PRE lesion, $p = 1.4 \times 10^{-10}$ for POST lesion); see Figure 3.3. Therefore I examine for correlation between mean activation strengths between PRE and POST. Again, both groups exhibit significant correlation between sessions (Control: Spearman's $r = 0.73$, $p = 7.3 \times 10^{-10}$; MEC-lesioned: $r = 0.77$, $p = 0$). These findings indicate that the RUN session had only limited effect on the presence of existing recurring patterns of coactive neurons during PRE that persisted in POST after the RUN session. This is in line with the idea of a stable pool of schemas in hippocampus that are recruited during novel experiences and also played out afterwards.

I went into more depth study of these correlations, in order to see whether they also exist on individual basis or they are solely emerging as a result of pooling data across different days and animals. For each recording, I fitted a line to PRE-POST mean activations of signif-

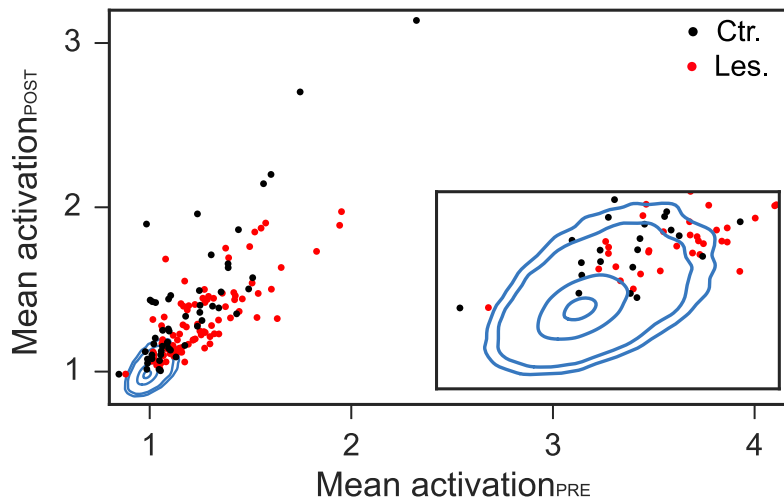


Figure 3.3: Average Reactivation of RUN patterns

Session wide mean POST activation vs. mean PRE activation for all significant eigenvectors from control animals (black, Ctr.) and MEC lesioned animals (red, Les.). The blue contours delineate the null distribution obtained by 50000 random permutations of cell indices. Modified from (Chenani et al.), submitted manuscript.

icant co-activation patterns during RUN. As depicted in Figure 3.4, both groups show significant regression slopes above 1 (signed rank test: control, $p = 2.4 \times 10^{-4}$; MEC-lesioned, $p = 7.1 \times 10^{-4}$). This is a hint that co-activation patterns are boosted by the RUN session. Accordingly, the relative change in activation $(\text{POST}-\text{PRE})/(\text{POST}+\text{PRE})$ was also significantly positive in both groups (signed rank tests; $p = 2.5 \times 10^{-9}$ for controls and $p = 2.4 \times 10^{-4}$ for MEC lesioned animals; see right panel in Figure 3.4). It is interesting that even MEC lesioned animals show such significant boost although it is less pronounced in comparison to the control group (comparison between regression slopes, ranksum test; $p = 5.4 \times 10^{-3}$, see left panel on Figure 3.4; relative change, ranksum test: $p = 5.8 \times 10^{-5}$; see right panel on Figure 3.4). Overall, co-activation study of hippocampal neuronal assemblies in MEC-Lesioned rats reveals that the boost of pattern activation by behavior is significantly reduced but not completely abolished by lesions.

3.2 Are place cell sequences replayed in MEC-lesioned animals?

Following the results of pattern activation analysis which indicate that RUN sessions affect POST pattern activation to a lesser extent in MEC-lesioned animals, I asked whether I can identify the activity features that are less extensively amplified during POST in MEC-

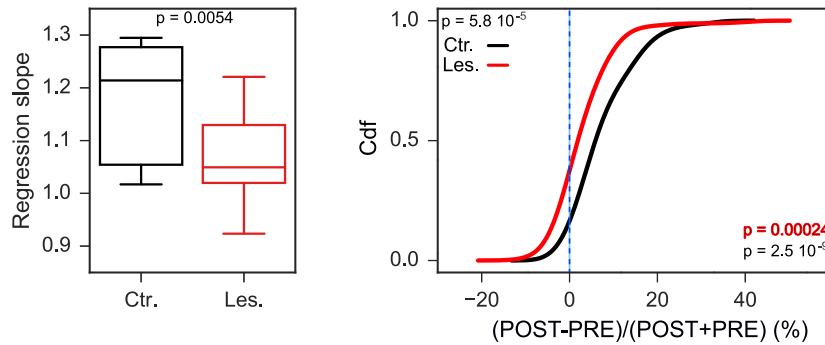


Figure 3.4: Average Reactivation of RUN patterns (Regression Slopes)

Left: Session wise linear regression slopes from data points in Figure 3.3. Linear regression is performed on an individual basis. The resulting slopes are compared in two experimental groups. **Right:** Cumulative histogram of relative change $(\text{POST-PRE})/(\text{POST+PRE})$. For the details on p-values please consult the text. Modified from (Chenani et al.), submitted manuscript.

lesioned animals. Mean activation strength stems from a compound signal that includes both the similarity to the RUN patterns and the rate of the co-activation events. One should also be aware that the previous analysis only considers co-activation of neurons in a timescale of $\sim 120\text{ms}$, therefore it is blind to phenomena happening on shorter time scales. Sequential activation of neurons maybe the most known of such phenomena. I studied the sequential activity only among units which showed clear place fields in at least one running direction on the linear track (total $n = 414$ in controls; $n = 247$ in lesioned animals). From these cells I constructed two template sequences, one for each running direction (Figure 3.5; see section 2.1.3).

I then extracted multi-unit population bursts in PRE, RUN and POST sessions (Figure 2.7; see section 2.1.3) and correlated the spike sequences during these population bursts with each template using rank order correlation coefficients (see section 2.1.4 & (Diba and Buzsáki, 2007)).

I introduce a spatial similarity index (SSI) as a measure of similarity between sequences during population bursts and place cell sequences. In essence SSI is the rank order correlation coefficient of cell indices normalized by the standard deviations of the sequence length distributions (see section 2.1.6; Figure 3.7). A z-score normalization takes care of the effect that the distributions of correlation coefficients in the surrogate data narrowed down around zero with increasing sequence length (Figure 2.8). Therefore, I was able to compare between sessions with different numbers of place cells, including those of MEC-lesioned animals. Since I use the modulus of

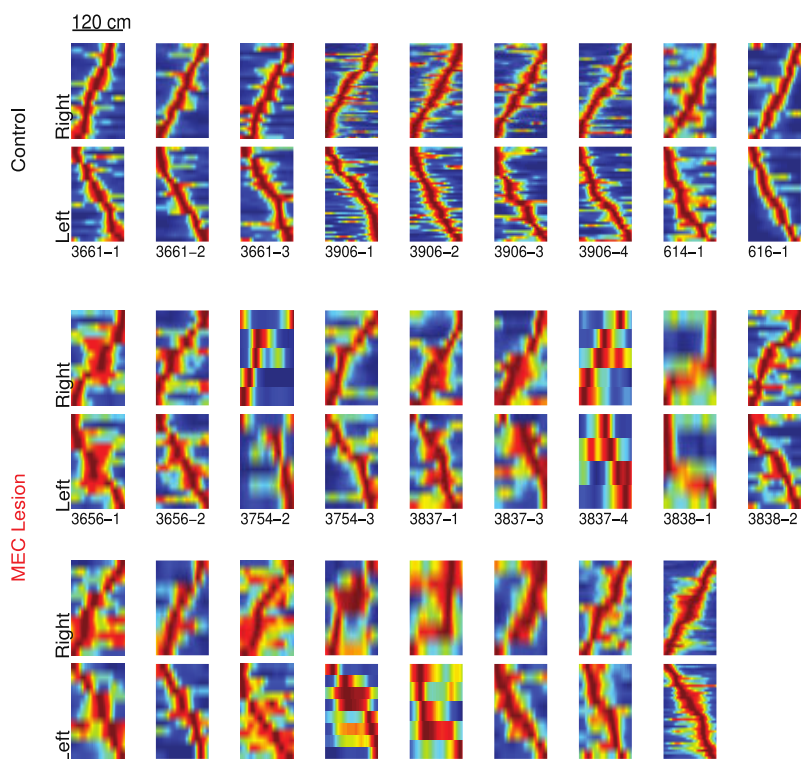


Figure 3.5: Place Cell Templates

Place fields for all sessions (labels below) separated into rightward and leftward runs (each line shows a place cell's firing rate along the linear track). Fields are ordered according to the position of the peak firing rate. Modified from (Chenani et al.), submitted manuscript.

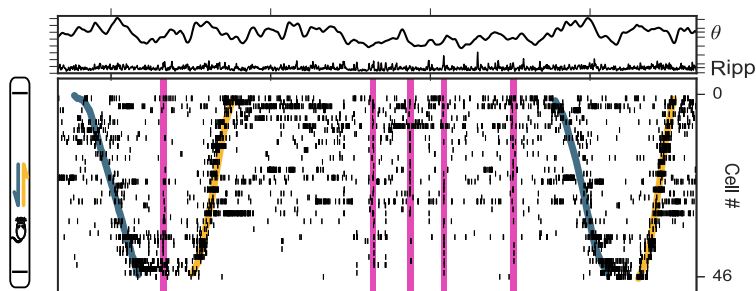


Figure 3.6: LFP and spiking activity during RUN

Example data from the RUN session of a control animal. **Top:** local field potential: theta and ripple power as indicated. (Bottom: Spike raster plot overlaid on run trajectories (colored curved lines). Cells are ordered according to their place field centers on right ward runs (yellow). Leftward runs are marked in blue. Magenta bars indicate the time span of different population bursts. Modified from (Chenani et al.), submitted manuscript.

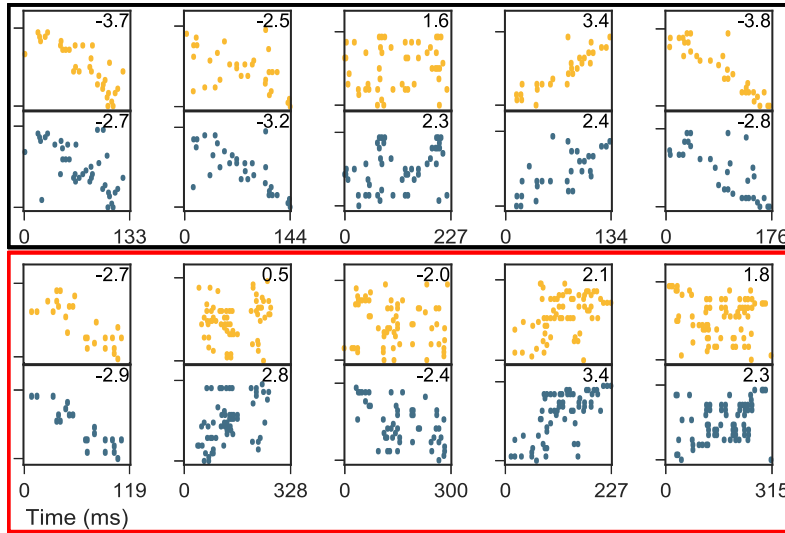


Figure 3.7: Sequence Rasters

Examples of zoomed in population bursts for rightward (top) and leftward (bottom) runs. Numbers are respective SSIs. Spikes are depicted in color according to color code in Figure 3.6. Black and red boxes contain sequences from control and lesioned group respectively. Modified from (Chenani et al.), submitted manuscript.

the normalized correlation coefficient for the statistical analysis I treat forward and backward in a similar way. The SSI thus represents a length-independent measure of how well an activity sequence from a population burst matches a template, independent of replay direction. After calculating SSIs for all recorded sequences I compared their distribution to those derived from 100,000 random permutations of the cell indices from the recorded sequences (CDF_0). The resulting cumulative excess probability (Δchance) of SSIs during all three conditions (PRE,RUN,POST) in both animal groups are shown in Figure 3.8. At the first glance it seems that Δchance in all cases exhibited a positive bias, indicating that sequences tend to be more similar to the spatial templates than chance.

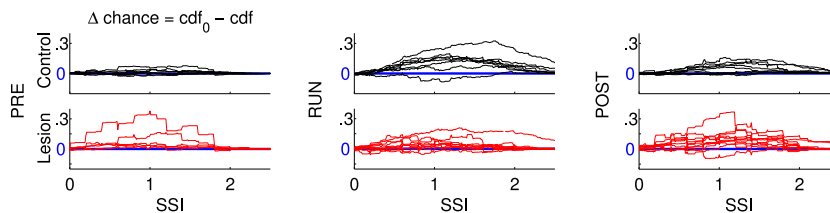


Figure 3.8: Spatial Similarity Index (SSI)

Excess cumulative probabilities for all sessions in control (black) and MEC-lesioned (red) animals under the three recording conditions (PRE,RUN,POST) as indicated. Modified from (Chenani et al.), submitted manuscript.

To assess the significance of this bias, I computed the fraction of replays exceeding the session-wise 95% quantile of the SSI distribution obtained from index permutations (Figure 3.8) and performed

a binomial test on whether the fractions of the significant sequences in all sessions exceeded the chance level of 5%. In control group, I observe consistent correlated (w.r.t the spatial templates) spike activity during population bursts. As demonstrated in Figure 3.9, fraction of significant sequences were significantly above chance in RUN and POST sessions (circles indicate 7 significant sessions out of 8 during RUN, and 7 significant sessions out of 9 during POST). The main observable feature in lesioned animals is variability in the data. This is already noticeable in the session-wise Δ chance plots in Figure 3.8 in accordance to the fact that p-value only reaches significance for the POST but not the RUN condition (Figure 3.9).

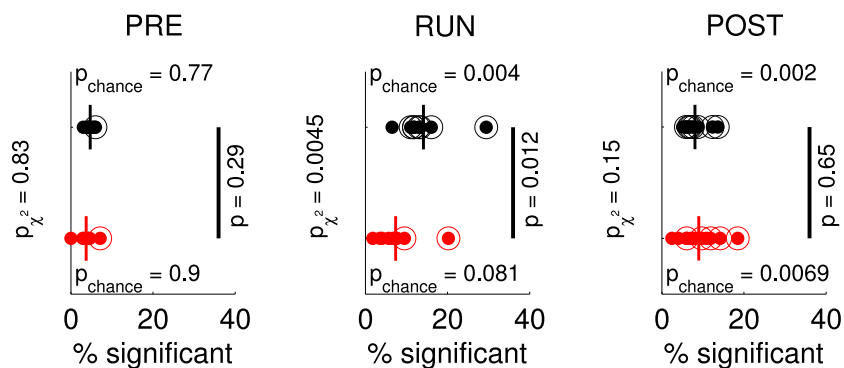


Figure 3.9: Comparison of significant sequence replays

Session-wise percentages of significant SSIs (p_{chance} : p-value of binomial test w.r.t the significance criterion of 5%, p : p-value of ranksum test comparing the medians of animal groups; p_{χ^2} : p value of χ^2 test comparing the categories "significant session" vs. "not significant session"). Modified from (Chenani et al.), submitted manuscript.

This is a sign of delayed establishment of replays across all sessions with lesioned animals. Looking at paired plots of significance proportions in Figure 3.11 one can observe a monotonic increase in significance ratios in MEC-lesioned group with POST having the highest percentages of significant sequences while in the control group the most significant replays happen during RUN. Moreover, for the lesioned animals the fractions of 2 out of 10 (RUN) and 5 out of 11 (POST) significant sessions are still significant considering a binomial test for the chance level of 5% (RUN $p = 0.01$; POST $p = 6 \times 10^{-6}$). For PRE sessions, SSIs are not significantly above chance for either group of animals (Figure 3.9), potentially owing to the limited numbers of place cells. However, I observe a clear trend towards positive Δ chance levels (Figure 3.8) consistent with the coactivation analysis and the lower fraction of replays of future behaviors reported for normal rats in (Grosmark and Buzsaki, 2016).

To compare the quality of replay between control and lesioned animals I first examined the differences of the fractions of signifi-

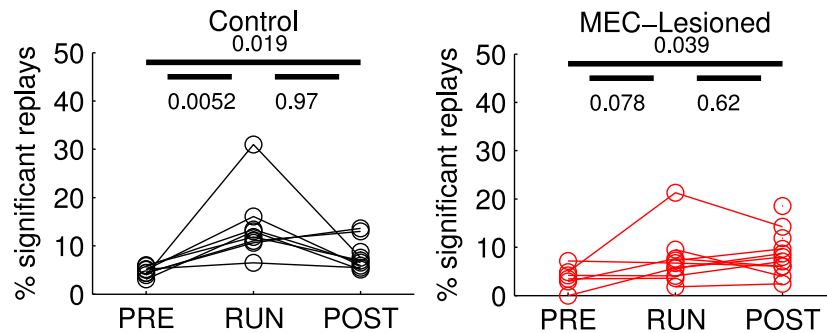


Figure 3.11: MEC lesions induce a delay in hippocampal replay.

Percentage of significant replays across sessions for control (left) and MEC-lesioned animals (right). P-values are derived from left-tailed paired t-tests. For control animals replay increases significantly during RUN, for animals with MEC lesions the increase of replay only reaches significance in the POST session. Note that the paired test (PRE vs. POST) in lesioned animals includes in only about half of the session (9 out of 17), since during many sessions in lesioned animals the criterion of having at least 20 bursts (allowing a reasonable estimate for the percentage of significant bursts) was not met. Modified from (Chenani et al.), submitted manuscript.

cant replay sequences using a ranksum test (Figure 3.9). I found a significantly larger percentage of significant sequences in control vs. lesioned animals only for RUN sessions. To assess the effects of the larger variability in the lesioned animals, I asked whether data from a single experimental session shows an above chance fraction of significant sequences (dots with circles in Figure 3.9). Then I put the answers as a categorical variable under a χ^2 test for homogeneity. During PRE, RUN and POST, the a χ^2 test results were consistent with the differences in medians. Thus MEC lesions seem to have a differential effect on the expression of sequence replay during the RUN and POST sessions. While during the RUN the fraction of significant replays is significantly reduced in the lesioned group, I did not find a significant difference to control animals over all POST sessions.

As mentioned in previous section, another factor that directly influences the co-activation strengths is the total rate of population bursts. I found that during RUN, POST and PRE, the rate of population bursts is consistently and significantly larger in control animals than in MEC lesioned animals (ranksum tests, p values as indicated in Figure 3.13).

Large burst rates, may not be necessary nor sufficient for high amount of sequence activation. Therefore I computed the rate of significant replays by multiplying the burst rate with the fraction of significant sequences. Comparing these rates of significant bursts between lesion and control group showed significantly larger rates in control animals during RUN and POST sessions (ranksum tests, p values shown in Figure 3.13). Thus, the reduced activation found in MEC-lesioned animals during the POST session by the co-activation analysis (Figure 3.4), is in agreement with reduced rates of significant

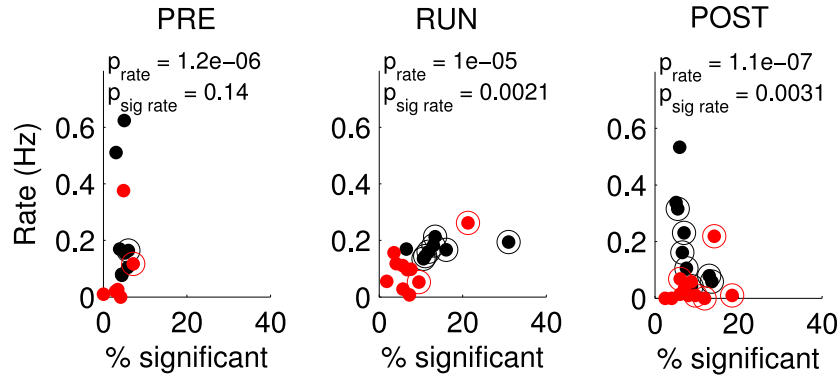


Figure 3.13: Burst rate and sequence replays

Rate of population bursts vs. percentage of significant SSIs (p_{rate} : p value of a ranksum tests of population burst rates, Control vs. Lesioned. $p_{\text{sig rate}}$: corresponding p value for rates of significant population bursts). Modified from (Chenani et al.), submitted manuscript.

replays.

3.3 Diversity in Spike Content of Population Bursts

So far, template-based analysis in the PRE session showed barely significant SSIs. The co-activation pattern analysis on the other hand, showed significant activation in PRE sessions for both control and MEC lesioned animals. The most probable scenario for this conflict could rise from recurring activity motifs that do not correspond to the spatial templates but may contribute to pattern activation. To identify such motifs, I repeated a similar analysis as for the spatial templates, but this time computed normalized rank order correlation coefficients between all pairs of sequences in a recording session. The correlation coefficients were again normalized to make them independent of sequence length and thereby transformed them into a motif similarity index (MSI). In contrast to SSIs, MSIs with negative sign (reverse replay) were not considered as similar motif. The ensuing analysis is summarized in Figure 3.14 and yielded that motifs were significantly detectable in all conditions except PRE sessions of MEC lesioned animals where the effect did not reach significance ($p = 0.079$, binomial test).

How much do the spatial sequences contribute to the motifs? To address this question, I counted the number of other observed sequences that were similar to each particular spatial sequence (MSI in the upper 5% quantile). Then I computed a repetition index for each sequence as number of similar partners normalized by the session-wise standard deviation in number of such partners for all spatial sequences. The cumulative distributions of repetition indices (Figure 3.16) show that significant spatial sequences were generally

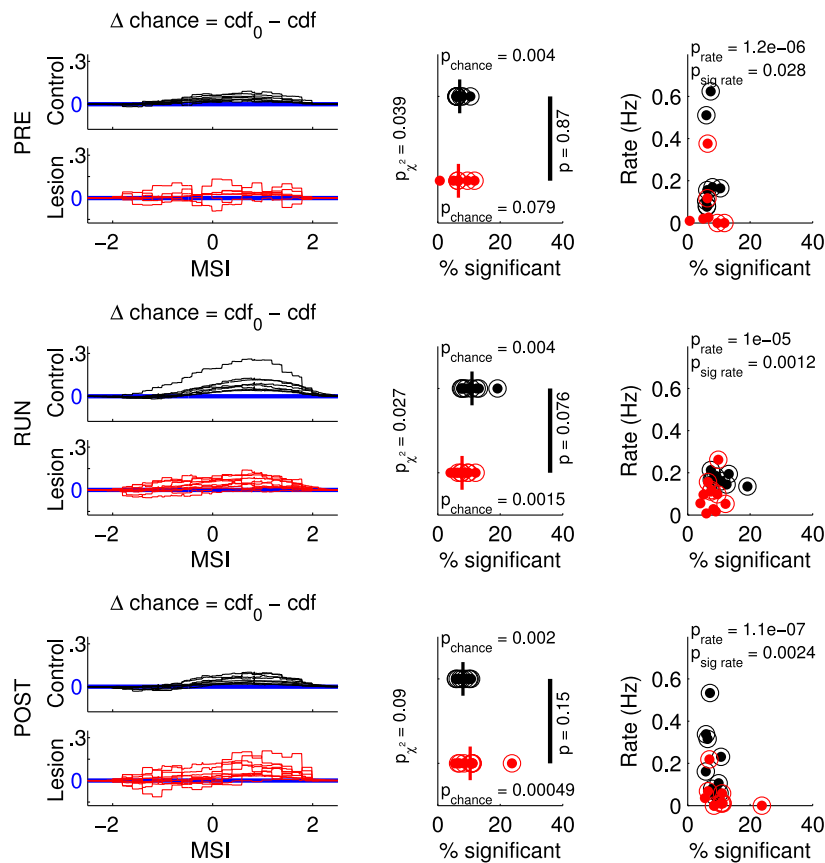


Figure 3.14: Motif similarity indices.

Excess cumulative probabilities for all sessions in control (black) and MEC-lesioned (red) animals under the three recording conditions (RUN, PRE, POST) as indicated. (Middle column) Session-wise percentages of significant MSIs (p_{chance} : p-value of binomial test regarding the chance level 5%, p : p value of ranksum test comparing the animal groups; p_{χ^2} : p value of χ^2 test comparing the categories "significant session" vs. "not significant session"). (Right column) Rate of population bursts vs. percentage of significant population bursts. Modified from (Chenani et al.), submitted manuscript.

repeated more often than other significant motifs.

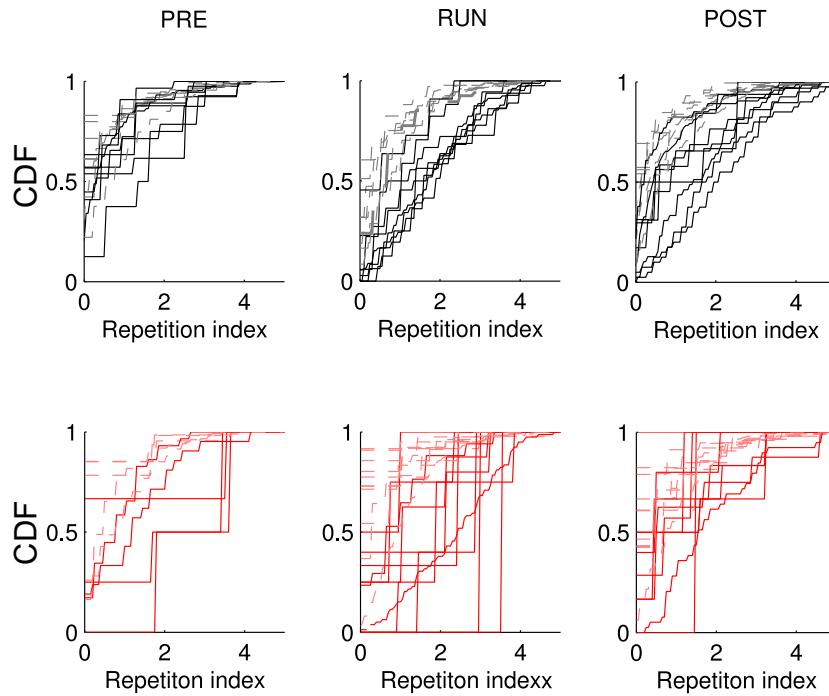


Figure 3.16: Reoccurring sequences.

Cumulative distributions of repetition indices for spatial (significant SSI, black) and non-spatial motifs (insignificant SSI, grey) in control animals for session types (RUN, PRE, POST) as indicated. Each CDF is derived from one session. Modified from (Chenani et al.), submitted manuscript.

This difference is significant (ranksum test, p values in Figure 3.16) except for sequences from the PRE sessions, which have only few significant replays in general (Figure 3.9). Moreover, spatial sequences seem amplified more strongly during POST sessions in lesioned animals than in control animals (Figure 3.18). Although sequences with high spatial similarity were generally replayed more frequently than those with less similarity, they only made up a small fraction of the overall number of population bursts (Figure 3.18). This fraction is larger in control animals than in lesioned animals only during RUN (ranksum test; p-values as indicated in Figure 3.18). Non-spatial sequences (low SSI) thus considerably contribute to burst activity and particularly during PRE sessions they show repetition indices indistinguishable to significant spatial sequences. The significant pattern activation in PRE sessions from Figure 1.10 therefore likely is also supported by those low SSI sequences.

3.4 Individual Contribution of Place Cells in Population Bursts

To see whether the expression of sequence replay in animals with MEC lesion during POST sessions is simply delayed (Figure 3.11) or

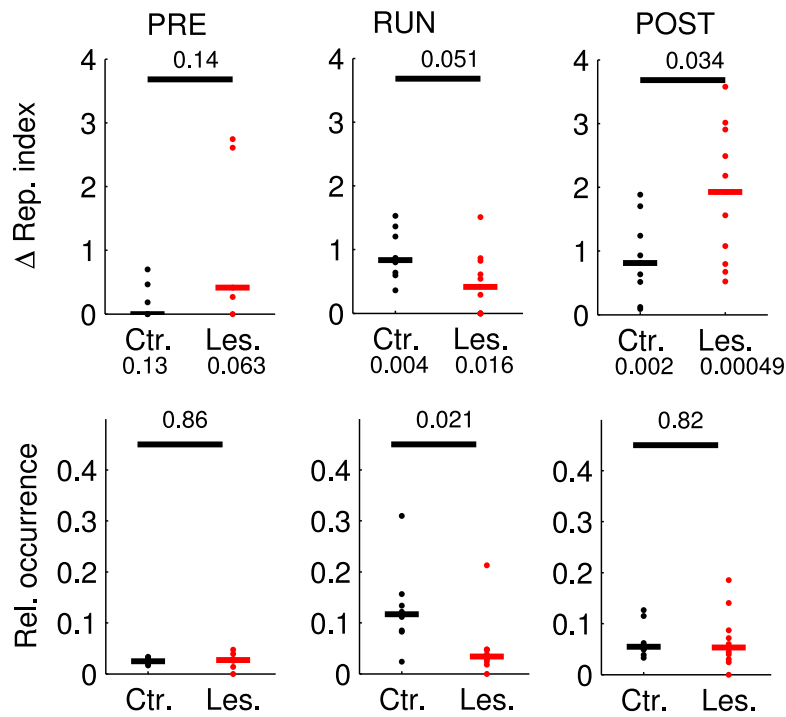


Figure 3.18: Spatial sequences recur more frequently.

Top: Difference of medians between spatial and non-spatial CDFs from Figure 3.16 (p-value above bar were obtained from ranksum test; p values below group labels were obtained from a one-sided signed rank test of o group median). **Bottom:** Relative occurrence computed as the fraction of spatially significant sequences among all population bursts (p-value obtained from ranksum test). Modified from (Chenani et al.), submitted manuscript.

whether it also shows qualitative differences to the replay in control animals, I examined the contribution of individual place cells by counting how often a single place cell was active in a significant spatial sequence. These activation numbers were then normalized by the total number of significant sequences in a session and is subsequently called participation index. For all conditions (PRE,RUN,POST) and both animals groups participation indices were significantly positively correlated with place field peak firing rates during RUN (Figure 3.20) and significantly negatively correlated with spatial information (Figure 3.20), providing evidence that sequence participation is a functionally relevant parameter.

Surprisingly, comparing participation indices between PRE and POST sessions showed a striking difference between data from control and MEC-lesioned animals (Figure 3.19A). The participation of single place cells in significant sequences increased from PRE to POST in both control and lesioned animals where the increase was moderately stronger among the lesioned animals (Figure 3.19B). This difference between the two animal groups, however, seemed to be expressed during the POST session (Figure 3.19), since only comparing changes in participation from RUN to POST exhibited this group difference, while comparing between PRE and RUN showed no significant difference in participation between control and lesioned animals (Figure 3.19). Consistently, I did not observe an increase of participation at all from RUN to POST in control animals (Figure 3.19). This finding corroborates our previous interpretation (Figure 2) that, contrary to control animals, significant spatial replay in lesioned animals is mostly established during POST sessions. Finally, I asked how much of the change in participation is predicted by place field properties and found that peak firing rates of place fields were un-predictive (Figure 3.20), while spatial information was significantly positively correlated with change in participation (Figure 3.20). This indicates that, both in lesioned and control animals, it is rather the small and crisp place fields that are plastically added to and removed from sequences, whereas the larger place fields tend to stay stable. Since spatial information is lower in lesioned animals (Hales et al., 2014) and I find an even stronger increase of participation in lesioned animals (Figure 3.19), I argue that the delayed expression of replay in lesioned animals seems not be a secondary effect of different place field properties.

3.5 *Distinct Types of High Frequency Events in Hippocampal LFP*

Sharp wave ripple events (SWRs) are known as the main host of population bursts in hippocampal formation. Despite the high cor-

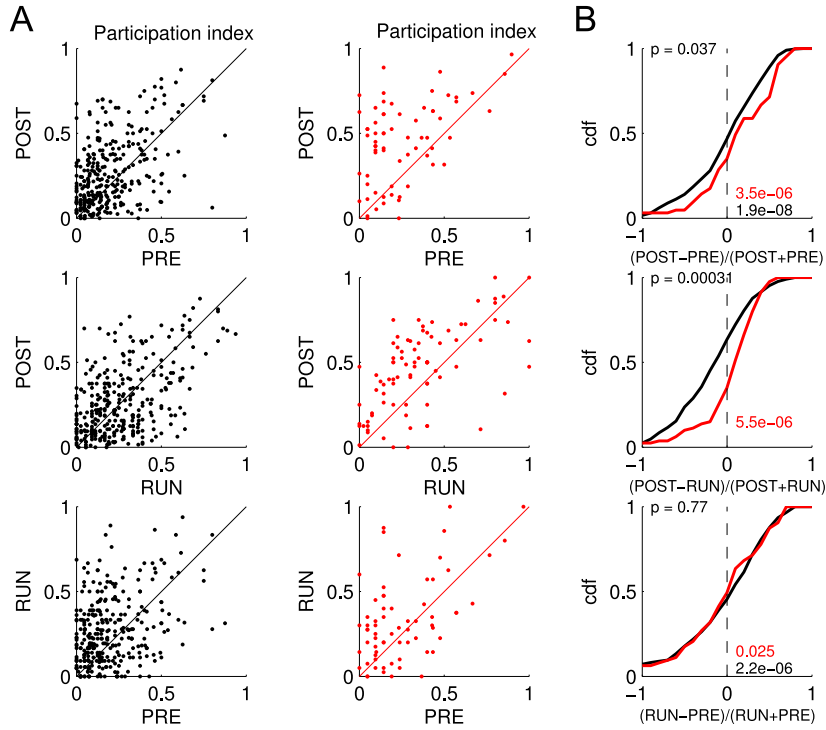


Figure 3.19: Place cell participation in spatial sequences.

Correlation of cell-wise participation in significant spatial sequences between two sessions. Each dot indicates the participation of a place cell in significant spatial sequences in the two sessions indicated on the axes. Left: control animals; right MEC-lesioned animals (Black: Control; Red: MEC lesion). (B) CDFs of the relative changes (as indicated at the x axis) from the data in A. The p values were from ranksum tests of identical group medians. Modified from (Chenani et al.), submitted manuscript.

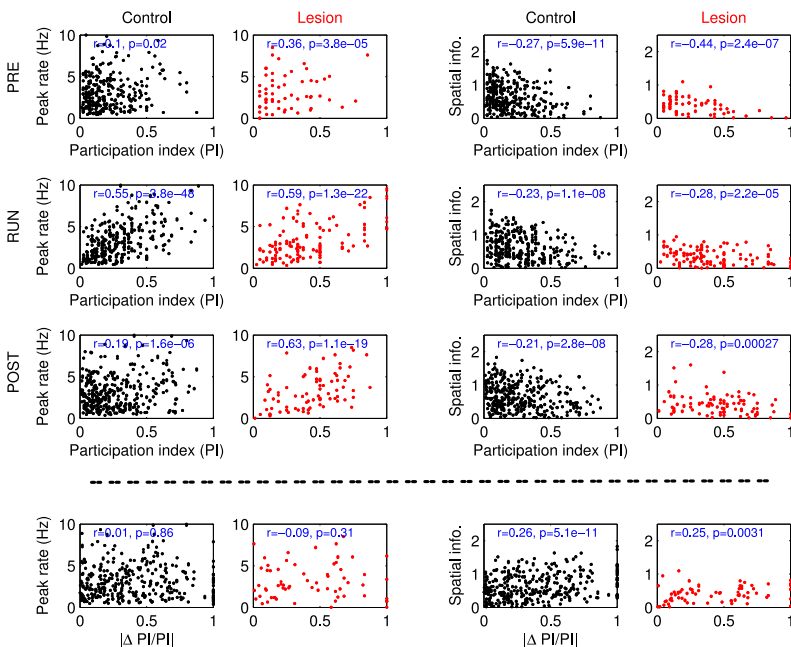


Figure 3.20: Participation indices correlate with place field properties.

Top: During all types of session arranged in rows (PRE; RUN, POST), peak firing rates of place fields (left) and spatial information (right) are significantly negatively correlated (Pearson's r) with participation indices introduced in Figure 3.19. Bottom: The modulus of the relative change of the participation index is independent of peak firing rate (left) but significantly positively correlated with spatial information.

relation, not all population bursts are accompanied with SWRs (Lee and Wilson, 2002). Based on substantial variations I have observed among SSI's, I looked into the relation between SSIs and SWRs in more details. To this end, I was performing a spectral analysis of field recordings (LFP) to identify SWRs. Peaks in the ripple band (100-250 Hz) were selected as candidates for high frequency events (HFE). I checked if all selected candidates are localized in both time and frequency space by visual inspection of wavelet transforms of detected HFE's (Figure 3.21).

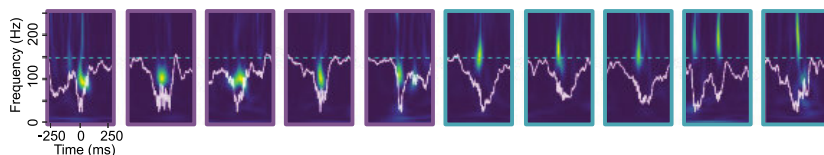


Figure 3.21: LFP high frequency events

Ten example traces (white) and corresponding power spectrograms of HFEs. Dashed cyan line indicates 150 Hz, roughly separating SWRs and FGBs. Modified from (Chenani et al.), submitted manuscript.

For each event I calculated power spectra vectors and subject them to principal component analysis. The first two principal components (PCs) allowed us to generally identify two clusters of high frequency

events (HFEs), one with a clear high-frequency peak at 150 to 200 Hz, called SWR in the following, and another one with a spectral peak between 100 and 150 Hz, which I called fast gamma burst (FGB) (Figure 3.22). I could consistently observe both clusters in all animals (Figure 2.10).

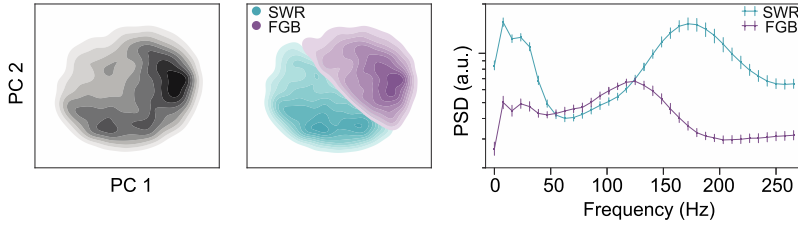


Figure 3.22: Clustering of high frequency events

Clustering sharp waves into SWR and FGBs for all sessions (as labeled). Principal component (PC) coordinates and power spectra. Note that the PCs are different between sessions and therefore the clustering appears different. Modified from (Chenani et al.), submitted manuscript.

As a first test, I looked at the ratio of SWRs to FGBs. In control animals, SWRs are taking over FGBs in POST sessions (ranksum test, $p = 0.0013$), while I could not spot such trend among MEC-lesioned animals ($p = 0.55$). This is indicative of distinct functional roles of the two types of HFEs in control animals, whereas in lesioned animals the balance between SWRs and FGBs seemed to not consistently vary between PRE and POST sessions.

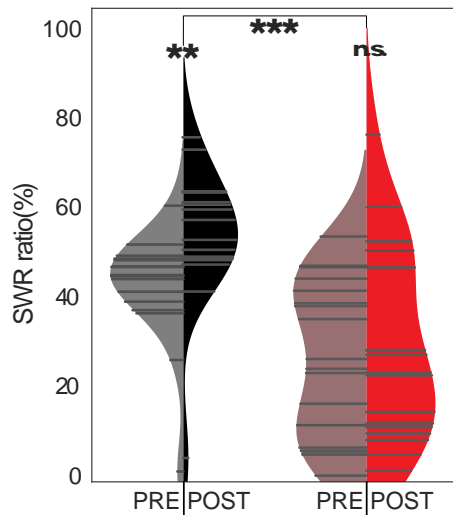


Figure 3.23: Overall contribution of SWRs and FGBs in LFP high frequency events

Share of SWRs in the PRE and POST, HFE counts (black: Control; red: MEC lesion). On top of having more share in general, SWRs show a consistent expansion in their share of HFEs in controls.

Does population activity differ under different subtypes of HFEs?

To answer this question I looked at multi-unit spiking activity triggered by the maximum power of each HFE (Figure 3.24). Multi-unit firing rates are generally enhanced in SWRs as compared to FGBs in both experimental groups. This is specially interesting considering that FGBs form the majority of HFEs in MEC-lesioned group (70% on average) but show half of firing activity of SWRs. Although the ratio of population rates during SWRs and FGBs seems to be preserved in MEC-lesioned group, HFEs in these animals are not accompanied by same amount of neuronal activity as in controls. The fact that both FGBs and SWRs in lesioned animals show similar reduction of neuronal activity and keep their relative activity ratio stands against the hypothesis that FGBs are just SWRs but with less number of participating neurons caused by overall reduction in population activity due to lesions. It seems that in the absence of MEC input, CA1 network loses its consistency in terms of both firing activity and HFEs proportions. Considering SWRs and FGBs as two distinct phenomena, MEC lesions seem to affect SWRs and leave the FGBs almost intact(Figure 3.23).

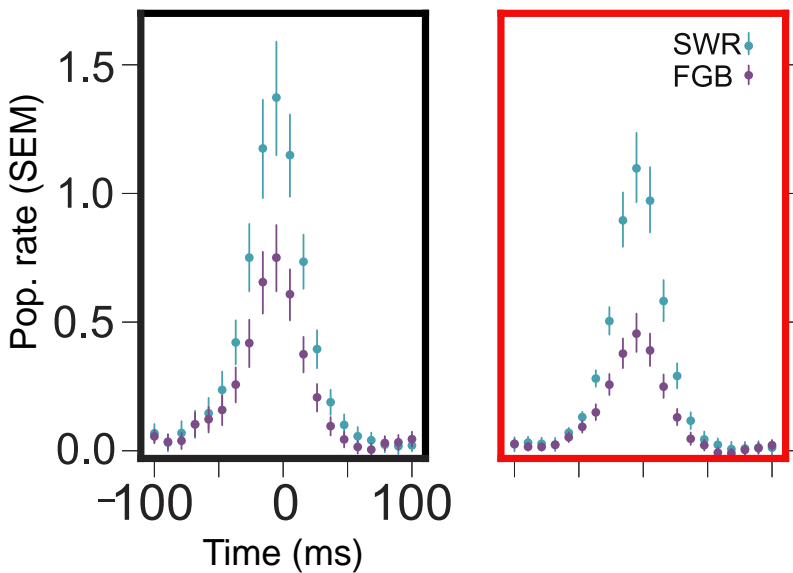


Figure 3.24: Neuronal activity during HFEs

Population rates (z-score) triggered by the peak of the HFE event. Error bars are 65%-percentiles. Modified from (Chenani et al.), submitted manuscript.

In terms of temporal cross correlation between HFEs and population burst, population bursts in control animals tend to raise their locking to SWRs during POST sessions(ranksum test, $p = 0.0013$). In lesioned animals this increase did not reach the significance level

(Figure 3.25).

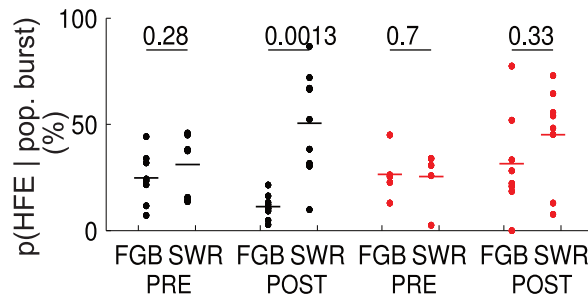


Figure 3.25: Population burst during HFEs

Percentages of population bursts that coincide with an HFE in a ± 150 ms window. P values above bars were obtained from ranksum tests. Modified from (Chenani et al.), submitted manuscript.

This is a hint towards the fact that SWRs might indeed correlate with sequence replay during population burst. Therefore I focused on population bursts with significant SSIs (Figure 3.26). As expected, spatial sequences were significantly more frequent during SWR in the POST session than in the PRE session (ranksum test, p-values indicated in Figure 3.26). Such a significant increase was neither found for FGBs nor for lesioned animals. The specific types of HFEs thus, at least in control animals, express distinct levels of plasticity in sequence replay.

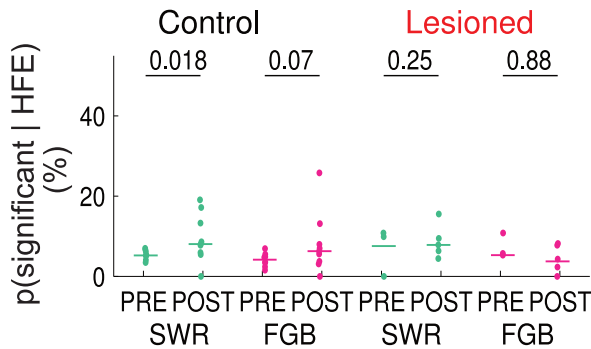


Figure 3.26: Spatial sequences during HFEs

Percentage of significant spatial sequences in control animals in a ± 150 ms second window close to an HFE. Modified from (Chenani et al.), submitted manuscript.

To see whether this distinctive role of HFEs also carries over to place field participation as introduced in section 3.4 (Figure 3.19), I separately computed participation indices for SWRs and FGBs in control and lesioned animals. In the control group, participation was significantly increased during SWR of the POST session (as compared to participation in all significant sequences of the PRE session) whereas during FGB participation was significantly decreased (Figure 3.28 top; signed rank tests; p values as indicated in colors) leading to a significantly larger participation during POST SWR than during

POST FGB (ranksum test on relative changes as indicated in Figure 3.28) In the lesioned group, I only observed increases in the participation index (Figure 3.28 bottom). The lack of decreased participation during FGBs in lesioned animals thus may contribute an important factor in the delayed establishment of sequence replay observed in Figures 3.11 and 3.19.

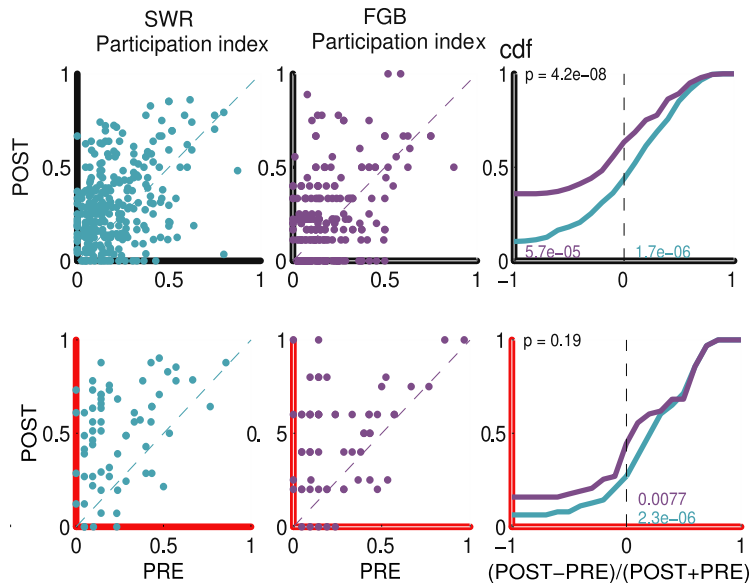


Figure 3.28: Spatial sequences during HFEs

Correlation of cell-wise participation in significant spatial sequences between PRE and POST sessions. Only significant replays are considered in a ± 150 ms window triggered by an SWR (left) or FGB (middle). Right: CDF of relative changes. P value (black) was obtained from a ranksum tests on the medians of the two groups. Colored p values were obtained from sign rank tests of the median being smaller than 0 (purple, FGB) or large than 0 (cyan, SWR). Modified from (Chenani et al.), submitted manuscript.

Finally, to connect these findings on the distinct roles of HFEs to pattern activation analysis from section 2.1.5, I computed how many pattern activation peaks coincided with an HFE. Consistent with our results on the spatial sequences, I found that also pattern activation peaks were only enhanced in the POST session, when they coincided with an SWR, and not an FGB, whereas activation in control animals was even slightly decreased during FGBs (Figure 3.30).

These results corroborate the differential role of the two types of HFEs in that SWRs are associated with an enhancement of activation, whereas FGBs signal a reduction of the activation. MEC-lesioned animals generally showed a lower fraction of SWR-associated pattern activations, even in the PRE session and no PRE - POST difference in activation was observable during FGBs. MEC lesions thus seem to reduce the facilitation of pattern activation during SWRs and the depression of place field participation during FGBs.

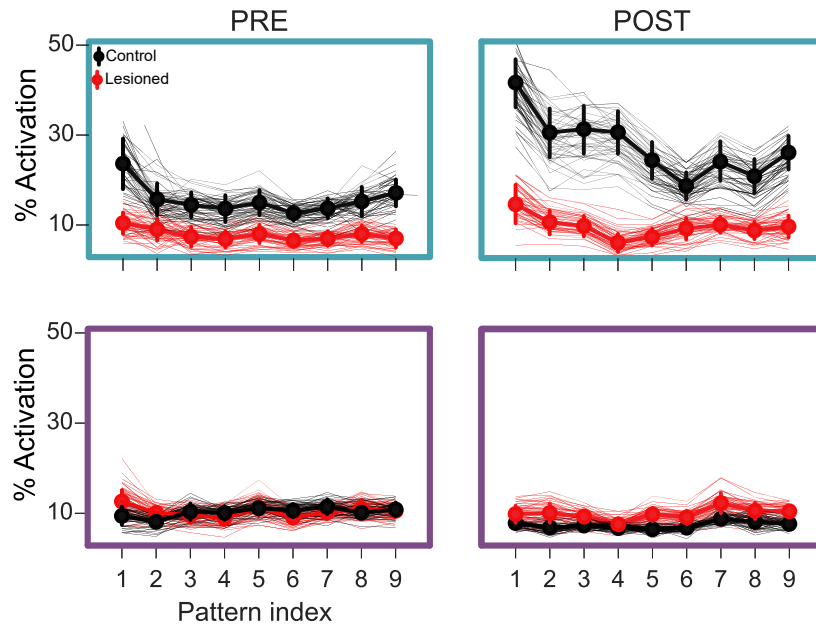


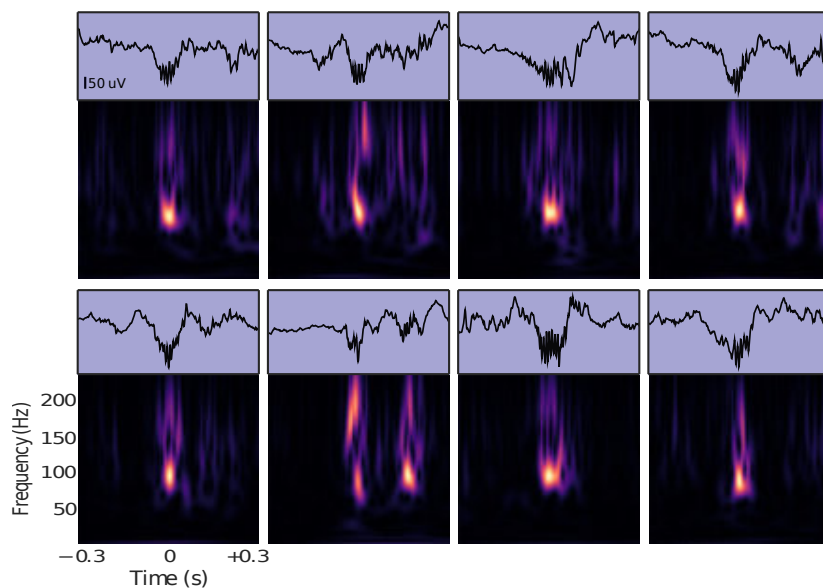
Figure 3.30: co-activation patterns during HFEs

Percentage of pattern activation peaks coinciding with an SWR event in a ± 50 ms window. Labels on the x-axis indicate the pattern (principal component) from the activation analysis. Modified from (Chenani et al.), submitted manuscript.

3.6 HFE classes are not exclusive to Rats

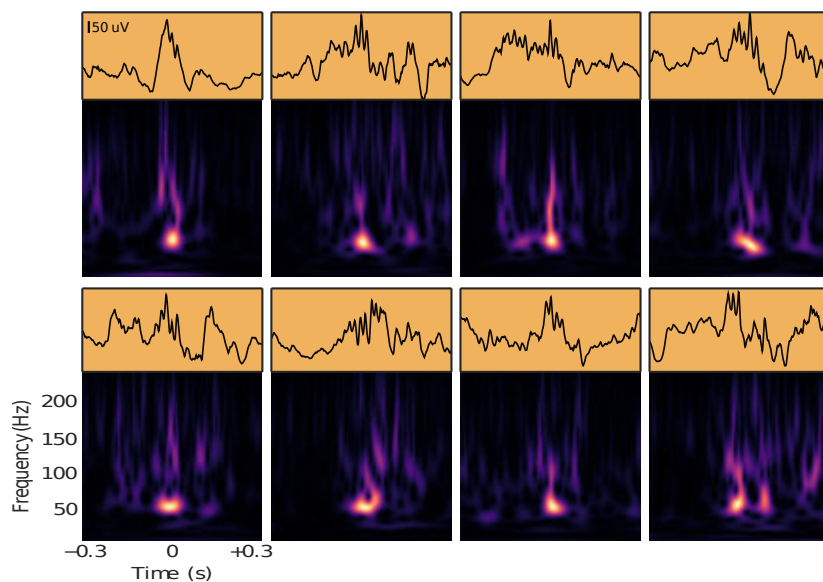
As a part of my studies on hippocampal population bursts in rodents, I have collaborated with a team of scientists in Munich and San Diego. In this project, I investigated the hippocampal code for space in Mongolian gerbils. The results are presented in a manuscript to be published in the journal *Hippocampus* (Mankin et al., 2019). I have studied the dynamics of high frequency events in this rodent using in vivo electrophysiology data in behaving animals. In this analysis, I have used the data from electrodes with largest power in the ripple band (150 – 200Hz). This indicates that the electrode was positioned close to pyramidal layer of CA1. Just like the study on rats I mainly focused on resting periods before and after a behavioral session during which gerbils usually engaged in a spatial navigation task. I used the same methods for detecting HFE's and searching for further clustering within detected events. After clustering I could identify the classic sharpwave ripple (Figure 3.31) events with the peak ripple frequency around 180Hz (Figure 3.33). Consistent with my finding in rats I could also identify a second class of HFE's with slightly less peak ripple frequency, namely the fast gamma bursts (Figure 3.32).

The envelopes of the low frequency components of the SWRs showed the expected bimodal shape where a negativity is followed



Raw LFP traces accompanied by spectrograms of several SWRs. Time span is a 600 ms window around the peak time of ripple oscillation. Modified with permission from (Mankin et al., 2019).

Figure 3.31: Sharp wave ripple examples observed in Mongolian gerbils.



Raw LFP traces accompanied by spectrograms of several FGBs. Time span is a 600 ms window around the peak time of ripple oscillation. Modified with permission from (Mankin et al., 2019).

Figure 3.32: Fast gamma burst examples observed in Mongolian gerbils.

by a positivity (Figure 3.31,3.33 right) (Buzsáki et al., 1992), whereas FGBs exhibited rather unimodal, mostly positive low frequency components envelopes (Figure 3.32,3.33 right).

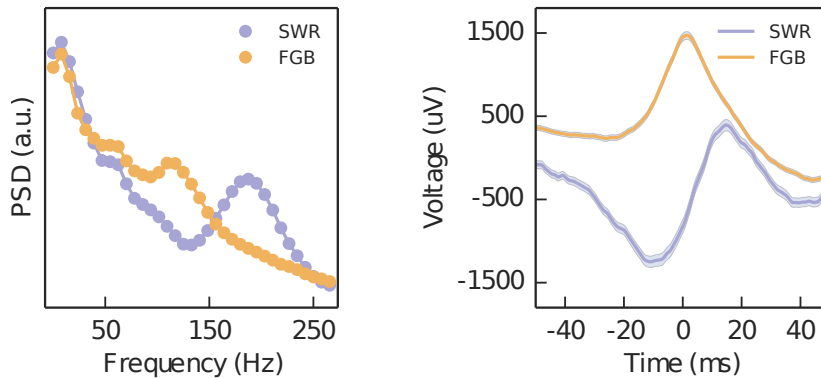


Figure 3.33: HFE's cluster in two distinct classes in Mongolian gerbils.

Subclasses of high frequency events in the LFP of Mongolian gerbils show distinguishable characteristics both in high frequency (left) and low frequency regime (right). Modified with permission from (Mankin et al., 2019)

Looking at the inter-event interval distribution (Figure 3.34 left), I observed that on average, FGBs occurred in a more burst-like fashion than SWRs, *i.e.*, at lower inter-event intervals (IEIs) than SWRs (ranksum test; $p = 3.4 \times 10^{-29}$ during non-theta sleep state). During resting states while theta oscillations were present, I found that the pattern of lower IEIs for FGBs compared to SWRs was retained ($p = 5.0 \times 10^{-126}$). In addition, durations of SWRs were slightly

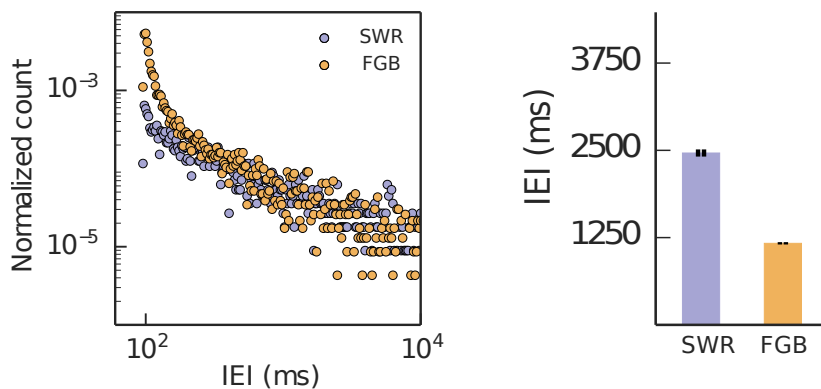


Figure 3.34: Inter-event intervals and duration of HFEs in Mongolian gerbils.

Modified with permission from (Mankin et al., 2019)

longer during resting theta state than non-theta sleep (ranksum test; $p = 2.8 \times 10^{-11}$), whereas FGBs were similar in theta and non-theta states ($p = 0.67$) (Figure 3.35 right). Both SWRs and FGBs are typically shorter than 200 ms and their median durations were not significantly different (ranksum test, $p = 0.67$, Figure 3.35). Only less than 1 percent of the high frequency events detected by our algorithm exhibits longer duration (Figure 3.35), assuring of a reasonably

good performing of my detection algorithm. Finally, I have analyzed

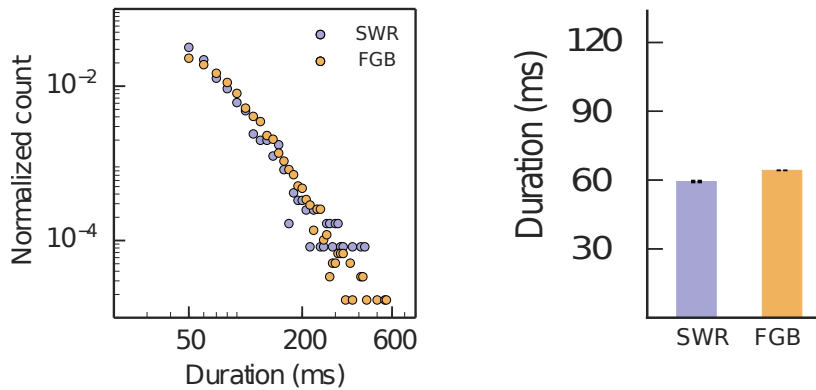


Figure 3.35: Inter-event intervals and duration of HFEs in Mongolian gerbils.

Modified with permission from (Mankin et al., 2019)

the increase in population activity during the two types of LFP events (Figure 3.36). During FGBs I observed only a moderate increase in population activity of less than one half of a standard deviation of the baseline activity, while during SWRs, unit activity was about four times larger (1.6 standard deviations above the average value or $\sim 1.6\sigma$), indicating that during SWRs, CA1 generates a much more prominent population output than during FGBs.

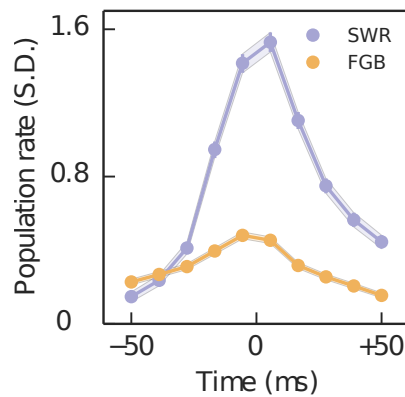


Figure 3.36: CA1 population activity during HFE's in Mongolian gerbils.

Modified with permission from (Mankin et al., 2019)

It is clear from this study, that gerbils exhibit CA1 SWRs of similar frequency content as rats, and in addition, show clear signs of a second type of CA1 populations bursts in the fast gamma range, similar to a phenomenon that has been observed in rats (Sullivan et al., 2011) and macaque monkeys (Ramirez-Villegas et al., 2015). In comparison to Figure 3.24, one can see a very good agreement between population rates in two species. SWRs manage to raise the population activity only up to $\sim 1.5\sigma$ in rats which is surprisingly similar to what they do in gerbil's hippocampus ($\sim 1.6\sigma$). This would

also suggest that there should be a functional correlate for these types of high frequency oscillations. Otherwise it would be quite a hard task to come up with an explanation of such similar artifact among different species.

4

Discussion

In this chapter I will review the results of our study in the context of the existing research. In our study, we examined the activity of neuronal populations in hippocampal CA1 regions in animals with extensive bilateral lesions of the medial entorhinal cortex. In almost total lack of hippocampal phase precession and strongly disrupted theta correlations (Schlesiger, 2016), we observed abundance of co-activation patterns and sequence replay during quiet wakefulness and rest in both experimental groups. Local field potential of MEC-lesioned animals also exhibit the main oscillations of hippocampal network, namely theta, gamma (slow and fast) and sharp wave ripples. Having these in mind we have made a number of interesting observations in these animals, shedding light on different aspects of hippocampal function during rest and immobility. The results of this work are mainly presented in numbered items and accompanied by further discussions and links to particular manuscripts when needed. Parts of the discussion are based on the submitted manuscript (Chenani et al.).

4.1 MEC-lesioned Rats Exhibit Coordinated Activity Among their CA1 Neurons

Analysis of the co-firing activity of all recorded CA1 neurons (regardless of their response to location) yielded the following results:

1. Time averaged neuronal co-activation strengths are significantly above chance in both PRE and POST sessions, even in MEC-lesioned animals.
2. Mean co-activation is significantly correlated between PRE and POST sessions in both groups.
3. Correlated activity was boosted between PRE and POST sessions in both groups although lesioned animals exhibited such boost to a much lower extent.

These findings indicate that RUN session had only limited effect on the presence of existing recurring co-activation patterns. This finding is in agreement with the idea of preexisting activity schemas (Dragoi and Tonegawa, 2013b) to be utilized during novel experiences (the first class of models we considered in this thesis).

4.2 MEC Lesions Disturb the Activity of CA1 Network

Generally, we found the network dynamics of MEC lesioned rats to be less consistent. This relative inconsistency is previously reported in properties of place cells in these animals (Schlesiger, 2016). In this study we observe traces of similar trend, both in population activity and local field potential.

4. In the lesion group, the distribution of regression slopes in Figure (3.4, left) is more spread with the mean value close to one, indicating less coordinated activity among these animals in comparison to controls.
5. The expression of spatial sequence replay was inconsistent across animals with MEC lesions. This is true for all experimental sessions (Figure 3.8 & 3.9).
6. The fraction of significant sequences from control animals are significantly above chance in RUN and POST sessions.
7. The MEC-lesioned data shows more variability in the number of animals showing significant replays (2 out of 10 (RUN) and 4 out of 11 (POST) in sessions).
8. LFP studies also revealed a high degree of heterogeneity in the ratio of SWRs to FGBs in these animals. Although SWRs usually have lower share in total number of HFEs in these animals, the variability in this ratio is much higher compared to controls (Figure 3.23).

4.3 *Reduction in Hippocampal Replay*

9. We observe a larger percentage of significant sequences in control compared to lesioned animals only for RUN sessions.
10. We found that during rest periods of RUN, POST and PRE sessions, the rate of population bursts was consistently and significantly larger in control compared to MEC-lesioned animals.

The overall reduction in the incidence rate of replays in lesioned animals (Figure 3.13) could be due to the fact that transitions from down to up states in the entorhinal cortex are a major trigger of hippocampal sharp waves (Sirota et al., 2003; Isomura et al., 2007; Clemens et al., 2011; Sullivan et al., 2011) and thus this lack of MEC input partly results in the general reduction of hippocampal population activity. In accordance to this result, we observed a strong decline in the number of HFEs in our MEC-lesioned animals. The remaining events may either be initiated by down to up transitions in the lateral entorhinal cortex (Tahvildari et al., 2007) or be intrinsically generated inside the hippocampus (Maier et al., 2011).

4.4 *Replay Quality in Absence of MEC Input*

The effect of MEC lesions on hippocampal replay is not only in the quantity of those events. It seems that MEC lesions also affect the quality of replays in hippocampus.

11. Significant spatial sequences were generally repeated more often than other significant motifs. This difference is significant except for sequences from the PRE sessions, which have only few significant replays in general.
12. Spatial sequences are amplified more strongly during RUN sessions in control animals vs. MEC-lesioned animals, while during POST sessions MEC-lesioned animals show stronger amplification as compared to controls.
13. Despite the fact that sequences with high spatial similarity are replayed more often than those with less similarity, they only contribute to a small fraction of the overall number of population bursts. This fraction was larger in control animals than in MEC-lesioned animals only during RUN.
14. There is always a positive correlation between participation index of place cells in significant sequence replays and place cells peak firing rate. This seems to be regardless of experimental group or experiment session (PRE, RUN, POST).

15. Development of participation indices show a striking difference between two groups. This difference is most prominent between RUN and POST sessions where place cells in lesioned animals show a greater increase of participation in significant sequences replayed in POST session.

These effects are not only confined to changes in the relative occurrence of behaviorally related activity patterns, but more importantly they reduce plasticity of significant spatial sequences. We have shown that participation of established place cells during POST sessions is strongly increased in lesioned animals. This is definitely not the case for control animals where participation of individual place cells exhibited cell specific increase and decrease (Figure 3.19). Observation of less plastic sequences during the POST session in some of the MEC-lesioned animals, might link to schemas (Dragoi and Tonegawa, 2013a) that have been acquired prior to the lesion and that still recur in the hippocampus. The schemas are most probably conceived by normal operation of the hippocampal formation prior to the lesion when place cell correlations were still intact (Schlesiger et al., 2015; Schlesiger, 2016). An alternative mechanism for sequence replay was suggested by Stark et al., 2015. They reported high rank-order correlations between replays and place field templates even for optogenetically induced artificial population bursts. According to their idea heterogeneous cellular excitability would result in consistent sequences of neuronal discharges (Stark et al., 2015). With this background, the plasticity reflected as changes in participation indices would represent modulations of excitability. This is consistent with our finding about participation indices changing the most for cells with small place fields and thus putatively lower excitability (Figure 3.20). In this context, the lack of decreased participation indices after MEC lesions is a very interesting observation pointing towards that lesions prohibit a reduction of cellular excitability, possibly counteracting the deafferentation of the strong MEC input pathway.

4.5 *Specific Decrease in Relative Rate of Sharp Wave Ripples*

By analyzing the hippocampal LFP we checked for differences in behavior of high frequency events (HFE) among two groups. We could consistently identify two types of such events with different frequency content. The first group which we refer to as sharp-wave ripples (SWR) have a clear peak in frequency range 150 – 200Hz while the second type, fast gamma bursts (FGB) have their peak frequency in the range of 100 – 150Hz. Considering these two types of HFEs we observed these notable facts:

16. The ratio of SWRs to FGBs in control animals was significantly increased in POST sessions in contrast to MEC-lesioned animals, where no such increase was identified.
17. Multi-unit spiking activity is generally enhanced in SWRs compared to FGBs. This observation is valid for both MEC-lesioned and control animals. Although among MEC-lesioned group such increase was weaker.
18. The same sub-groups (SWR and FGB) of HFEs are identified in the hippocampal LFP of Mongolian gerbils.
19. In a great degree of agreement, multi-unit activity in gerbils is also enhanced during SWRs as compared to FGBs.
20. Population bursts including replays with significant spatial similarity index are significantly more frequent during SWRs in the POST session than in the PRE session only in control group. Such increase was neither found for FGBs nor for MEC-lesioned animals.
21. The degree of participation of place cells in replays was significantly increased during SWRs of the POST session. On contrary in replays accommodated by FGBs, participation was significantly decreased. Therefore we observe larger participation during POST SWRs than during POST FGBs.
22. The increase in the participation index during SWRs is also observable in MEC-lesioned group, but not the decrease of participation during FGBs.
23. Finally, we observed that pattern activation peaks were enhanced in the POST session, only in coincidence of SWRs.

There are evidences indicating that isolated hippocampus is capable of generating sharp waves ripples (Bragin et al., 1995b,a). They have reported an overall increase in number of sharp wave ripples after animals recovered from bilateral MEC lesions. On contrary, our observations of rest periods activity does not support such increase in frequency of population bursts in lesioned animals. Generally we observe a decrease in the incidence rate of population burst, potentially due to different methods used to perform the lesions. On the other hand, our finding supports a recent study by Yamamoto & Tonegawa reporting from acute optogenetic inactivations of MEC layer III during quiet wakefulness, which found reduced incidence rates of sharp wave ripple bursts (Yamamoto and Tonegawa, 2017).

Hippocampal high frequency events have often been shown to correlate with pattern reactivation (e.g. (Lee and Wilson, 2002)

; (O'Neill et al., 2008); (van de Ven et al., 2016); see (Buzsaki, 2015) for review). Our data provides a more detailed picture of these events. First we were able to distinguish between two types of these events, Sharp Wave Ripples (SWR) & Fast Gamma Bursts (FGB). We observed that SWRs selectively (as compared to FGBs) boost pattern activation and the playing out of spatial sequences. Another interesting fact shows that HFEs are more decoupled from pattern activation events in PRE sessions as opposed to POST. This effect is more pronounced in MEC-lesioned animals compared to controls. This becomes visible by looking at the fraction of activation peaks during sharp waves which is strongly reduced as compared to POST sessions from control animals (Figure 3.30). At the same time, the total percentage of HFEs is still similar to control levels (Figure 3.25). This decoupling suggests that the less plastic, putatively schema-related, sequences in PRE sessions (and also in POST sessions of MEC-lesioned animals) are less linked to HFEs whereas particularly the patterns and sequences that underwent plastic changes (mostly in POST sessions of control animals) tend to be over proportionally accompanied by SWRs and FGBs. SWRs specifically involve activation of parvalbumin positive basket cells (Schlingloff et al., 2014; Forro et al., 2015; Polepalli et al., 2017) and somatostatine positive bistratified cells (Katona et al., 2014), and thus the distinct local inhibitory circuitry seem to facilitate the activation of patterns and sequences that were recently altered during RUN associated network dynamics (Zarnadze et al., 2016).

While the causal mechanistic link between HFEs and participation dynamics of place cells is still matter of speculation. The differential effect of SWRs and FGBs on place cell participation reveals an interesting functional correlate of LFP signals. On the one hand, it is plausible to think of distinct plasticity induced participation rates in the population bursts resulting in different field potential shapes. This is possible through differential activity dependent recruitment of interneuronal circuits. On the other hand the distinct types of HFEs might be provoked by prong pathways that then recruit different subsets of place cells leading to distinct participation rates. Since no obvious differences have been found by Sullivan et al. 2011 concerning the anatomical pathways triggering of SWRs and FGBs, we currently assume that both types of HFEs may be evoked inside hippocampus in quiet similar fashion. One candidate for such process would be via ramping activity in CA2 region (Oliva et al., 2016). Such assumption would suggest two types of HFEs as a result of a differential intrinsic recruitment of cells within hippocampus.

4.6 *Decline in Plasticity Over the Course of Reconsolidation*

It is well known in the field of memory reconsolidation that the recall of a memory trace renders it unstable and allows for its modification by new experiences (Alberini et al., 2006; Besnard et al., 2012; Nader, 2015). In 2002, Milekic and Alberini showed that while the memory is hippocampus dependent, protein synthesis blockade would remove an existing fear memory only if the memory was recalled shortly before or after the blockade. This is a significant indication of synaptic plasticity affecting recently acquired memories on recall. Similarly, Moncada and Viola (2007) could translate memories from short term into long term memories by exposing the animal to a novel environment in temporal proximity of the acquisition of the short-term memory. Our observation on the plastic nature of participation degree among place cells in control animals (Figure 3.19) points towards a similar direction. In animals with MEC lesions, synaptic plasticity in hippocampus is on a putative decline; as suggested by lower rate of replay events (Figure 3.13) and virtual lack of cells with declined participation indices (Figure 3.19 & Figure 3.28). Therefore we expect memory traces in MEC-lesioned rats not to be extensively affected over the course of memory recollection. Observation of recurring pattern activation (Figures 3.3 and 3.4), even in PRE sessions (Hirase et al., 2001), is a perfect fit into this reconsolidation hypothesis, since the observed increase of mean pattern activation in POST sessions (particularly of control animals) together with the strong correlation between PRE and POST activation (Figures 3.2 & 3.3) would be anticipated, in case of modification of antecedent patterns during RUN. The strong reduction of POST activation as a result of MEC lesions (Figure 3.4, right panel), once again, suggests that in these animals the antecedent memory traces are less vulnerable, either because of relative scarcity of population bursts in comparison to controls or due to the fact that spike-timing correlations are corrupted. Further studies will shed light on extent of efficacy of these possible scenarios.

Acknowledgments

First and foremost, I thank my supervisor Prof. Dr. Christian Leibold for accepting me as a PhD student in his lab and giving me the opportunity of exploring the realm of neuroscience. I thank Christian for his guidance and support over the years, for giving me much free rein in my research, for his patience when I got lost into details, and for disentangling my ideas numerous times, teaching me how to transform them into actual science.

I thank all the people I had the honor to collaborate with and without them this project would never become a reality.

- Prof. Dr. Stefan Leutgeb for his supervision and insight, specially in behavioral science where I had virtually no skills prior to this project.
- Dr. Kay Thurley, consistent support and helpful consultation over the last few years specially at the beginig of the project and providing me with basis of what later on developed to my analysis software.
- Dr. Magdalena Schlesiger, for performing the behavior and electrophysiological experiments and providing the data sets which have started the project.
- Dr. Marta Sabariego, for performing majority of experimental work including lesion surgeries, electrophysiology and behavior.

I would also like to thank Simon Lehnert, Dinu Patirniche, Mauro Monsalve Mercado and Johannes Nagele for their company and inspiring discussions.

I thank the current and former members of the computational neuroscience labs at the LMU Biozentrum, as well as the members of Bernstein center for computational neuroscience in Munich, for inspiring discussions and fun meetings.

Last, but certainly not least, I would like to express my deepest gratitude to Azadeh. I simply could not have made it without her support.

Eidesstattliche Versicherung/Affidavit

Hiermit versichere ich an Eides statt, dass ich die vorliegende Dissertation 'Influence of Medial Entorhinal Cortex on CA₁ Population Bursts' selbstständig angefertigt habe, mich ausser der angegebenen keiner weiteren Hilfsmittel bedient und alle Erkenntnisse, die aus dem Schrifttum ganz oder annähernd übernommen sind, als solche kenntlich gemacht und nach ihrer Herkunft unter Bezeichnung der Fundstelle einzeln nachgewiesen habe.

I hereby confirm that the dissertation 'Influence of Medial Entorhinal Cortex on CA₁ Population Bursts' is the result of my own work and that I have only used sources or materials listed and specified in the dissertation.

Alireza Chenani
22.01.2019

Bibliography

- M. Abeles, H. Bergman, E. Margalit, and E. Vaadia. Spatiotemporal Firing Patterns in the Frontal-Cortex of Behaving Monkeys. *Journal Of Neurophysiology*, 70(4):1629–1638, 1993. ISSN 00223077.
- L. Acharya, Z. M. Aghajan, C. Vuong, J. J. Moore, and M. R. Mehta. Causal Influence of Visual Cues on Hippocampal Directional Selectivity. *Cell*, 164(1-2):197–207, 2016. ISSN 10974172.
- C. M. Alberini, M. H. Milekic, and S. Tronel. Mechanisms of memory stabilization and de-stabilization. *Cellular and Molecular Life Sciences*, 63(9):999–1008, 2006. ISSN 1420682X. DOI: 10.1007/s00018-006-6025-7.
- D. G. Amaral and P. Lavenex. The Dentate Gyrus: A Comprehensive Guide to Structure, Function, and Clinical Implications. In *Progress in Brain Research*, pages 3–790. 2007. ISBN 9780444530158.
- M. Bartos, I. Vida, and P. Jonas. Synaptic mechanisms of synchronized gamma oscillations in inhibitory interneuron networks. *Nature Reviews Neuroscience*, 8(1):45–56, 2007. ISSN 1471-003X.
- H. Belchior, V. Lopes dos Santos, A. B. L. Tort, and S. Ribeiro. Increase in hippocampal theta oscillations during spatial decision making. *Hippocampus*, 24(6):693–702, 2014. ISSN 10981063.
- M. A. Belluscio, K. Mizuseki, R. Schmidt, R. Kempster, and G. Buzsáki. Cross-frequency phase-phase coupling between θ and γ oscillations in the hippocampus. *The Journal of neuroscience*, 32(2):423–35, 2012. ISSN 1529-2401.
- R. W. Berg, D. Whitmer, and D. Kleinfeld. Exploratory Whisking by Rat Is Not Phase Locked to the Hippocampal Theta Rhythm. *The Journal of neuroscience*, 26(24):6518–6522, 2006. ISSN 0270-6474.
- S. D. Berry and R. F. Thompson. Prediction of learning rate from the hippocampal electroencephalogram. *Science*, 200(4347):1298–300, 1978. ISSN 0036-8075.

- A. Besnard, J. Caboche, and S. Laroche. Reconsolidation of memory: A decade of debate, 2012. ISSN 03010082.
- G. Bi and M. Poo. Distributed synaptic modification in neural networks induced by patterned stimulation. *Nature*, 401(6755): 792–796, 1999. ISSN 00280836.
- K. W. Bieri, K. N. Bobbitt, and L. L. Colgin. Slow and Fast Gamma Rhythms Coordinate Different Spatial Coding Modes in Hippocampal Place Cells. *Neuron*, 82(3):670–681, 2014. ISSN 10974199. DOI: 10.1016/j.neuron.2014.03.013.
- V. P. Bingman, C. Salas, and F. Rodriguez. Evolution of the Hippocampus. In Marc D Binder, Nobutaka Hirokawa, and Uwe Windhorst, editors, *Encyclopedia of Neuroscience*, pages 1356–1360. Springer Berlin Heidelberg, Berlin, Heidelberg, 2009. ISBN 978-3-540-29678-2.
- V. P. Bingman, F. Rodríguez, and C. Salas. The Hippocampus of Nonmammalian Vertebrates. In Jon H Kaas, editor, *Evolution of Nervous Systems*, pages 479–489. Academic Press, Oxford, second edition, 2017. ISBN 9780128040966.
- K. I. Blum and L. F. Abbott. A Model of Spatial Map Formation in the Hippocampus of the Rat. *Neural Computation*, 8(1):85–93, 1996. ISSN 0899-7667.
- C. N. Boccara, F. Sargolini, V. H. Thoresen, T. Solstad, M. P. Witter, E. I. Moser, and M. B. Moser. Grid cells in pre- and parasubiculum. *Nature Neuroscience*, 13(8):987–994, 2010. ISSN 1097-6256.
- A. Bragin, G Jandó, Z. Nádasdy, J. Hetke, K. Wise, and G. Buzsáki. Gamma (40-100 Hz) oscillation in the hippocampus of the behaving rat. *The Journal of neuroscience*, 15(1):47–60, 1995a. ISSN 0270-6474.
- A. Bragin, G. Jando, Z. Nádasdy, M. van Landeghem, and G. Buzsáki. Dentate EEG spikes and associated interneuronal population bursts in the hippocampal hilar region of the rat. *Journal of neurophysiology*, 73(4):1691–705, 1995b. ISSN 0022-3077.
- M. P. Brandon, J. Koenig, J. K. Leutgeb, and S. Leutgeb. New and Distinct Hippocampal Place Codes Are Generated in a New Environment during Septal Inactivation. *Neuron*, 82(4):789–796, 2014. ISSN 10974199. DOI: 10.1016/j.neuron.2014.04.013.
- N. Burgess, E. A. Maguire, and J. O’Keefe. The human hippocampus and spatial and episodic memory, 2002. ISSN 08966273.
- R. D. Burrwell. The Parahippocampal Region: Corticocortical Connectivity. *Annals of the New York Academy of Sciences*, 911(1):25–42, 2006. ISSN 00778923. DOI: 10.1111/j.1749-6632.2000.tb06717.x.

- G. Buzsáki. Hippocampal sharp waves: Their origin and significance. *Brain Research*, 398(2):242–252, 1986. ISSN 0006-8993. DOI: 10.1016/0006-8993(86)91483-6.
- G. Buzsáki. Two-stage model of memory trace formation: A role for "noisy" brain states. *Neuroscience*, (3):551–570, 1989. ISSN 03064522.
- G. Buzsáki. The hippocampo-neocortical dialogue, 1996. ISSN 10473211.
- G. Buzsáki. Hippocampal sharp wave-ripple: A cognitive biomarker for episodic memory and planning. *Hippocampus*, 1188(973):n/a–n/a, 2015. ISSN 10509631. DOI: 10.1002/hipo.22488.
- G. Buzsáki, L. S. Leung, and C. H. Vanderwolf. Cellular bases of hippocampal EEG in the behaving rat. *Brain Research Reviews*, 6(2): 139–171, 1983. ISSN 01650173.
- G. Buzsáki, F. H. Gage, L. Kellényi, and A. Björklund. Behavioral dependence of the electrical activity of intracerebrally transplanted fetal hippocampus. *Brain Research*, 400(2):321–333, 1987. ISSN 00068993. DOI: 10.1016/0006-8993(87)90631-7.
- G. Buzsáki, Z. Horvath, R. Urioste, J. Hetke, and K. Wise. High-frequency network oscillation in the hippocampus. *Science*, 256 (5059):1025–1027, 1992. ISSN 0036-8075.
- S. Byrnes, A. N. Burkitt, D. B. Grayden, and H. Meffin. Learning a Sparse Code for Temporal Sequences Using STDP and Sequence Compression. *Neural computation*, 23:2567–2598, 2011. ISSN 0899-7667.
- P. M. B. Cahusac, E. T. Rolls, Y. Miyashita, and H. Niki. Modification of the responses of hippocampal neurons in the monkey during the learning of a conditional spatial response task. *Hippocampus*, 3(1): 29–42, 1993. ISSN 10981063.
- A. Chenani, M. Sabariego, M. I. Schlesiger, J. K. Leutgeb, S. Leutgeb, and C. Leibold. Hippocampal CA1 replay persists and becomes more rigid without inputs from medial entorhinal cortex. *Submitted manuscript*.
- S. Cheng and L. M. Frank. New Experiences Enhance Coordinated Neural Activity in the Hippocampus. *Neuron*, 57(2):303–313, 2008. ISSN 08966273.
- J. J. Chrobak and G. Buzsáki. Selective activation of deep layer (V-VI) retrohippocampal cortical neurons during hippocampal sharp waves in the behaving rat. *The Journal of neuroscience*, 14(10): 6160–6170, 1994.

- Z. Clemens, M. Mölle, L. Eross, R. Jakus, G. Rásonyi, P. Halász, and J. Born. Fine-tuned coupling between human parahippocampal ripples and sleep spindles. *European Journal of Neuroscience*, 33(3):511–520, 2011. ISSN 0953816X. DOI: 10.1111/j.1460-9568.2010.07505.x.
- L. L. Colgin. Mechanisms and Functions of Theta Rhythms. *Annual Review of Neuroscience*, 36(1):295–312, 2013. ISSN 0147-006X.
- L. L. Colgin. Rhythms of the hippocampal network. *Nature Reviews Neuroscience*, 17(4):239–249, 2016. ISSN 1471-003X. DOI: 10.1038/nrn.2016.21.
- L. L. Colgin and E. I. Moser. Gamma Oscillations in the Hippocampus. *Physiology*, 25(5):319–329, 2010. ISSN 1548-9213.
- L. L. Colgin, D. Kubota, Y. Jia, C. S. Rex, and G. Lynch. Long-term potentiation is impaired in rat hippocampal slices that produce spontaneous sharp waves. *The Journal of Physiology*, 558(3):953–961, 2004. ISSN 00223751. DOI: 10.1113/jphysiol.2004.068080.
- L. L. Colgin, T. Denninger, M. Fyhn, T. Hafting, T. Bonnevie, O. Jensen, M. B. Moser, and E. I. Moser. Frequency of gamma oscillations routes flow of information in the hippocampus. *Nature*, 462(7271):353–357, 2009. ISSN 0028-0836.
- J. Crane and B. Milner. What went where? Impaired object-location learning in patients with right hippocampal lesions. *Hippocampus*, 15(2):216–231, 2005. ISSN 10509631. DOI: 10.1002/hipo.20043.
- J. Csicsvari, H. Hirase, and A. Czurko. Fast network oscillations in the hippocampal CA1 region of the behaving rat. *The Journal of neuroscience*, 1999.
- J. Csicsvari, B. Jamieson, K. D. Wise, and G. Buzsáki. Mechanisms of gamma oscillations in the hippocampus of the behaving rat. *Neuron*, 37(2):311–322, 2003. ISSN 08966273. DOI: 10.1016/S0896-6273(02)01169-8.
- J. Csicsvari, J. O’Neill, K. Allen, and T. Senior. Place-selective firing contributes to the reverse-order reactivation of CA1 pyramidal cells during sharp waves in open-field exploration. *European Journal of Neuroscience*, 26(3):704–716, 2007. ISSN 0953816X. DOI: 10.1111/j.1460-9568.2007.05684.x.
- T. J. Davidson, F. Kloosterman, and M. A. Wilson. Hippocampal replay of extended experience. *Neuron*, 27(63):497–50., August 2009.
- M. Day, R. Langston, and R. G. M. Morris. Glutamate-receptor-mediated encoding and retrieval of paired-associate learning. *Nature*, 424(6945):205–209, 2003. ISSN 00280836. DOI: 10.1038/nature01769.

- L. de Hoz, J. Knox, and R. G. M. Morris. Longitudinal axis of the hippocampus: Both septal and temporal poles of the hippocampus support water maze spatial learning depending on the training protocol, 2003. ISSN 10509631.
- J. de la Rocha, B. Doiron, E. Shea-Brown, K. Josić, and A. Reyes. Correlation between neural spike trains increases with firing rate. *Nature*, 448(7155):802–806, 2007. ISSN 0028-0836. DOI: 10.1038/nature06028.
- K. Diba and G. Buzsáki. Forward and reverse hippocampal place-cell sequences during ripples. *Nature Neuroscience*, 10(10):1241–1242, oct 2007. ISSN 1097-6256. DOI: 10.1038/nn1961.
- G. Dragoi and G. Buzsáki. Temporal Encoding of Place Sequences by Hippocampal Cell Assemblies. *Neuron*, 50:145–157, April 2006.
- G. Dragoi and S. Tonegawa. Preplay of future place cell sequences by hippocampal cellular assemblies. *Nature*, 469(7330):397–401, jan 2011. ISSN 0028-0836.
- G. Dragoi and S. Tonegawa. Development of schemas revealed by prior experience and NMDA receptor knock-out. *eLife*, 2013(2), 2013a. ISSN 2050084X. DOI: 10.7554/eLife.01326.001.
- G. Dragoi and S. Tonegawa. Distinct preplay of multiple novel spatial experiences in the rat. *Proc. Natl. Acad. Sci.*, 110(22):9100–9105, 2013b. ISSN 0027-8424. DOI: 10.1073/pnas.1306031110.
- D. Dupret, J. O’Neill, B. Pleydell-Bouverie, and J. Csicsvari. The reorganization and reactivation of hippocampal maps predict spatial memory performance. *Nature neuroscience*, 13(8):995–1002, aug 2010. ISSN 1546-1726. DOI: 10.1038/nn.2599.
- V. Ego-Stengel and M. A. Wilson. Disruption of ripple-associated hippocampal activity during rest impairs spatial learning in the rat. *Hippocampus*, 20(1):1–10, 2010. ISSN 10509631. DOI: 10.1002/hipo.20707.
- A. D. Ekstrom, J. B. Caplan, E. Ho, K. Shattuck, I. Fried, and M. J. Kahana. Human hippocampal theta activity during virtual navigation. *Hippocampus*, 15(7):881–889, 2005. ISSN 10509631. DOI: 10.1002/hipo.20109.
- R. Epstein and N. Kanwisher. A cortical representation of the local visual environment. *Nature*, 392(6676):598–601, 1998. ISSN 0028-0836. DOI: 10.1038/33402.
- T. Evans, A. Bicanski, D. Bush, and N. Burgess. How environment and self-motion combine in neural representations of space. *The*

- Journal of Physiology*, 594(22):6535–6546, 2016. ISSN 00223751. DOI: 10.1113/JP270666.
- L. A. Ewell and M. V. Jones. Frequency-Tuned Distribution of Inhibition in the Dentate Gyrus. *The Journal of neuroscience*, 30(38):12597–12607, 2010. ISSN 0270-6474. DOI: 10.1523/JNEUROSCI.1854-10.2010.
- T. Feng, D. Silva, and D. J. Foster. Dissociation between the Experience-Dependent Development of Hippocampal Theta Sequences and Single-Trial Phase Precession. *The Journal of neuroscience*, 35(12):4890–4902, 2015. ISSN 0270-6474. DOI: 10.1523/JNEUROSCI.2614-14.2015.
- J. Ferbinteanu, R. M.D. Holsinger, and R. J. McDonald. Lesions of the medial or lateral perforant path have different effects on hippocampal contributions to place learning and on fear conditioning to context. *Behavioural Brain Research*, 101(1):65–84, 1999. ISSN 01664328. DOI: 10.1016/S0166-4328(98)00144-2.
- T. Forro, O. Valenti, B. Lasztocki, and T. Klausberger. Temporal organization of GABAergic interneurons in the intermediate CA1 hippocampus during network oscillations. *Cerebral Cortex*, 25(5):1228–1240, 2015. ISSN 14602199. DOI: 10.1093/cercor/bht316.
- D. J. Foster and M. A. Wilson. Reverse replay of behavioural sequences in hippocampal place cells during the awake state. *Nature*, 440(7084):680–683, mar 2006. ISSN 0028-0836. DOI: 10.1038/nature04587.
- D. J. Foster and M. A. Wilson. Hippocampal theta sequences. *Hippocampus*, 17(11):1093–1099, 2007. ISSN 10509631. DOI: 10.1002/hipo.20345.
- L. M. Frank, G. B. Stanley, and E.N. Brown. Hippocampal Plasticity across Multiple Days of Exposure to Novel Environments. *The Journal of neuroscience*, 24(35):7681–7689, 2004. ISSN 0270-6474. DOI: 10.1523/JNEUROSCI.1958-04.2004.
- F. R. Freeman, J. J. McNew, and W. R. Adey. Sleep of unrestrained chimpanzee: Cortical and subcortical recordings. *Experimental Neurology*, 25(1):129–137, 1969. ISSN 00144886. DOI: 10.1016/0014-4886(69)90076-4.
- M. Fyhn, S. Molden, M. P. Witter, E. I. Moser, and M. B. Moser. Spatial representation in the entorhinal cortex. *Science*, 305(5688):1258–64, 2004. ISSN 1095-9203. DOI: 10.1126/science.1099901.
- D. Gaffan. Scene-Specific Memory for Objects: A Model of Episodic Memory Impairment in Monkeys with Fornix Transection. *Journal*

- of Cognitive Neuroscience*, 6(4):305–320, 1994. ISSN 0898-929X. DOI: 10.1162/jocn.1994.6.4.305.
- D. Gaffan and R. C. Saunders. Running recognition of configural stimuli by fornixtransected monkeys. *The Quarterly Journal of Experimental Psychology Section B*, 37(1):61–71, 1985. ISSN 14641321. DOI: 10.1080/14640748508402087.
- P. R. Gill, S. J.Y. Mizumori, and D. M. Smith. Hippocampal episode fields develop with learning. *Hippocampus*, 21(11):1240–1249, jul 2011.
- G. Girardeau, K. Benchenane, S. I. Wiener, G. Buzsáki, and M. B. Zugaro. Selective suppression of hippocampal ripples impairs spatial memory. *Nature Neuroscience*, 12(10):1222–1223, 2009. ISSN 10976256. DOI: 10.1038/nn.2384.
- K. M Gothard, W. E Skaggs, and B. L. McNaughton. Dynamics of Mismatch Correction in the Hippocampal Ensemble Code for Space: Interaction between Path Integration and Environmental Cues. *The Journal of neuroscience*, 16(24):8027–8040, 1996. ISSN 0270-6474.
- E. Grastyán, K. Lissák, I. Madarász, and H. Donhoffer. Hippocampal electrical activity during the development of conditioned reflexes. *Electroencephalography and Clinical Neurophysiology*, 11(3):409–430, 1959. ISSN 00134694. DOI: 10.1016/0013-4694(59)90040-9.
- J. Green and A. Arduini. Hippocampal Electrical Activity in Arousal. *Journal of Neuro*, 17(6):533–57, 1954. ISSN 03043940. DOI: 10.1016/0304-3940(96)12650-1.
- A. L Griffin, Y. Asaka, R. D Darling, and S. D Berry. Theta-contingent trial presentation accelerates learning rate and enhances hippocampal plasticity during trace eyeblink conditioning. *Behavioral neuroscience*, 118(2):403–411, 2004. ISSN 0735-7044. DOI: 10.1037/0735-7044.118.2.403.
- A. D. Grosmark and G. Buzsáki. Diversity in neural firing dynamics supports both rigid and learned hippocampal sequences. *Science*, 351(6280), June 2016.
- A. S. Gupta, M. A. Van Der Meer, D. S. Touretzky, and D. A. Reish. Hippocampal Replay Is Not a Simple Function of Experience. *Neuron*, 65(5):695–705, 2010. ISSN 08966273. DOI: 10.1016/j.neuron.2010.01.034.
- O. V Haas. *Input-dependent neuronal representations of virtual environments in the hippocampus*. PhD thesis, LMU, 2017.

- T. Hafting, M. Fyhn, S. Molden, M. B. Moser, and E. I. Moser. Microstructure of a spatial map in the entorhinal cortex. *Nature*, 436(7052):801–806, 2005. ISSN 0028-0836. DOI: 10.1038/nature03721.
- J. B. B. Hales, M. I. Schlesiger, J. K. Leutgeb, L. R. Squire, S. Leutgeb, and R. E. Clark. Medial entorhinal cortex lesions only partially disrupt hippocampal place cells and hippocampus-dependent place memory. *Cell Reports*, 9(3):893–901, oct 2014. ISSN 22111247. DOI: 10.1016/j.celrep.2014.10.009.
- H. Hirase, X. Leinekugel, A. Czurko, J. Csicsvari, and G. Buzsáki. Firing rates of hippocampal neurons are preserved during subsequent sleep episodes and modified by novel awake experience. *Proceedings of the National Academy of Sciences*, 98(16):9386–9390, 2001. ISSN 0027-8424. DOI: 10.1073/pnas.161274398.
- J. M Hyman, B. P. Wyble, V. Goyal, C. A Rossi, and M. E Hasselmo. Stimulation in hippocampal region CA1 in behaving rats yields long-term potentiation when delivered to the peak of theta and long-term depression when delivered to the trough. *The Journal of neuroscience*, 23(37):11725–31, 2003. ISSN 1529-2401.
- K. M. Igarashi, H. T. Ito, E. I. Moser, and M. B. Moser. Functional diversity along the transverse axis of hippocampal area CA1. *FEBS Lett.*, 588(15):1–7, jun 2014. ISSN 1873-3468. DOI: 10.1016/j.febslet.2014.06.004.
- Y. Isomura, A. Sirota, S. Ozen, S. M. Montgomery, K. Mizuseki, D. A. Henze, and G. Buzsáki. Integration and Segregation of Activity in Entorhinal-Hippocampal Subregions by Neocortical Slow Oscillations. *Neuron*, 528(5):871–72, January 2007.
- J. Jacobs and M. J. Kahana. Direct brain recordings fuel advances in cognitive electrophysiology, 2010. ISSN 13646613.
- S. P. Jadhav, C. Kemere, P. W. German, and L. M. Frank. Awake Hippocampal Sharp-Wave Ripples Support Spatial Memory. *Science*, 336(6087):1454–1458, 2012. ISSN 0036-8075. DOI: 10.1126/science.1217230.
- D. Ji and M. A. Wilson. Coordinated memory replay in the visual cortex and hippocampus during sleep. *Nature Neuroscience*, 10(1):100–107, 2007. ISSN 1097-6256. DOI: 10.1038/nn1825.
- M. Jouviet and F. Michel. Electromyographic correlations of sleep in the chronic decorticate & mesencephalic cat. *Comptes rendus des seances de la Societe de biologie et de ses filiales*, 153(3):422–5, 1959. ISSN 0037-9026. DOI: 10.1016/j.neuroimage.2005.04.014.

- M. W. Jung, S. I. Wiener, and B. L. McNaughton. Comparison of spatial firing characteristics of units in dorsal and ventral hippocampus of the rat. *The Journal of neuroscience*, 14(12):7347–7356, 1994.
- R. Jung and A. E. Kornmüller. Eine Methodik der Ableitung lokalisierter Potentialschwankungen aus subcorticalen Hirngebieten. *Archiv für Psychiatrie und Nervenkrankheiten*, 109(1):1–30, 1938. ISSN 00039373. DOI: 10.1007/BF02157817.
- M. J. Jutras, P. Fries, and E. A. Buffalo. Oscillatory activity in the monkey hippocampus during visual exploration and memory formation. *Proceedings of the National Academy of Sciences of the United States of America*, 110(32):13144–9, 2013. ISSN 1091-6490. DOI: 10.1073/pnas.1302351110.
- S. N. Kadir, D. F. M. Goodman, and K. D. Harris. High-Dimensional Cluster Analysis with the Masked EM Algorithm. *Neural Computation*, 2394(11):10, sep 2013. ISSN 0899-7667. DOI: 10.1162/NECO.
- L. Katona, D. Lapray, T. J. Viney, A. Oulhaj, Z. Borhegyi, B. R. Micklem, T. Klausberger, and P. Somogyi. Sleep and Movement Differentiates Actions of Two Types of Somatostatin-Expressing GABAergic Interneuron in Rat Hippocampus. *Neuron*, 82(4):872–886, may 2014. ISSN 0896-6273. DOI: 10.1016/J.NEURON.2014.04.007.
- C. Kemere, M. F. Carr, M. P. Karlsson, and L. M. Frank. Rapid and Continuous Modulation of Hippocampal Network State during Exploration of New Places. *PLoS ONE*, 8(9):e73114, 2013. ISSN 1932-6203. DOI: 10.1371/journal.pone.0073114.
- A. Kepecs, N. Uchida, and Z. F. Mainen. Rapid and Precise Control of Sniffing During Olfactory Discrimination in Rats. *Journal of Neurophysiology*, 98(1):205–213, 2007. ISSN 0022-3077. DOI: 10.1152/jn.00071.2007.
- R. P. Kesner, M. R. Hunsaker, and M. W. Warthen. The CA3 subregion of the hippocampus is critical for episodic memory processing by means of relational encoding in rats. *Behavioral Neuroscience*, 122(6):1217–1225, 2008. ISSN 1939-0084. DOI: 10.1037/a0013592.
- K. B. Kjelstrup, T. Solstad, V. H. Brun, T. Hafting, S. Leutgeb, M. P. Witter, E. I. Moser, and M. B. Moser. Finite Scale of Spatial Representation in the Hippocampus. *Science*, 321(5885):140–143, 2008. ISSN 0036-8075. DOI: 10.1126/science.1157086.
- T. Klausberger, P. J. Magill, L. F. Márton, J.D B. Roberts, P. M. Cobden, G. Buzsáki, and P. Somogyi. Corrigendum: Brain-state- and cell-type-specific firing of hippocampal interneurons in vivo. *Nature*, 441(7095):902–902, 2006. ISSN 0028-0836. DOI: 10.1038/nature04910.

- J. J. Knierim and J. P. Neunuebel. Tracking the flow of hippocampal computation: Pattern separation, pattern completion, and attractor dynamics, 2016. ISSN 10959564.
- J. J. Knierim, I. Lee, and E. L. Hargreaves. Hippocampal place cells: Parallel input streams, subregional processing, and implications for episodic memory. *Hippocampus*, 16(9):755–764, 2006. ISSN 10509631. DOI: 10.1002/hipo.20203.
- B. R Komisaruk. Synchrony between limbic system theta activity and rhythmical behavior in rats. *Journal of comparative and physiological psychology*, 70(3):482–492, 1970. ISSN 0021-9940. DOI: 10.1037/h0028709.
- D. Kubota, L. L. Colgin, M. Casale, F. A Brucher, and G. Lynch. Endogenous waves in hippocampal slices. *J Neurophysiol*, 89(1):81–89, 2003. ISSN 0022-3077. DOI: 10.1152/jn.00542.2002.
- P. W Landfield, J. L McLaugh, and R. J Tusa. Theta rhythm: a temporal correlate of memory storage processes in the rat. *Science*, 175(4017):87–9, 1972. ISSN 0036-8075. DOI: 10.1126/science.175.4017.87.
- R. F Langston and E. R. Wood. Arbitrary associations in animals: what can paired associate recall in rats tell us about the neural basis of episodic memory? Theoretical comment on Kesner, Hunsaker, & Warthen (2008). *Behavioral neuroscience*, 122(6):1391–1396, 2008. ISSN 0735-7044. DOI: 10.1037/a0013966.
- A. K. Lee and M. A. Wilson. Memory of sequential experience in the hippocampus during slow wave sleep. *Neuron*, 36(6):1183–1194, dec 2002. ISSN 08966273. DOI: 10.1016/S0896-6273(02)01096-6.
- J. K. Leutgeb, S. Leutgeb, M. B. Moser, and E. I. Moser. Pattern Separation in the Dentate Gyrus and CA3 of the Hippocampus. *Science*, 315(5814):961–966, 2007. ISSN 0036-8075. DOI: 10.1126/science.1135801.
- S. Leutgeb, J. K. Leutgeb, A. Treves, M. B. Moser, and E. I. Moser. Distinct Ensemble Codes in Hippocampal Areas CA3 and CA1. *Science*, 305(5688):1295–1298, 2004. ISSN 0036-8075. DOI: 10.1126/science.1100265.
- C. Lever, R. Kaplan, N. Burgess, D. Derdikman, and J. J. Knierim. *Space, Time and Memory in the Hippocampal Formation*. 2014. ISBN 978-3-7091-1291-5. DOI: 10.1007/978-3-7091-1292-2.
- W. B. Levy and O. Steward. Temporal contiguity requirements for long-term associative potentiation/depression in the hippocampus. *Neuroscience*, 8(4):791–797, 1983. ISSN 03064522. DOI: 10.1016/0306-4522(83)90010-6.

- J. E. Lisman. Role of the dual entorhinal inputs to hippocampus: a hypothesis based on cue/action (non-self/self) couplets, 2007. ISSN 00796123.
- F Macrides, H B Eichenbaum, and W B Forbes. Temporal relationship between sniffing and the limbic theta rhythm during odor discrimination reversal learning. *The Journal of neuroscience*, 2(12):1705–1717, 1982. ISSN 0270-6474.
- N. Maier, V. Nimmrich, and A Draguhn. Cellular and Network Mechanisms Underlying Spontaneous Sharp Wave-Ripple Complexes in Mouse Hippocampal Slices. *The Journal of Physiology*, 550(3):873–887, 2003. ISSN 00223751. DOI: 10.1113/jphysiol.2003.044602.
- N. Maier, A. Tejero-Cantero, A. L. Dornn, J. Winterer, P. S. Beed, G. Morris, R. Kempter, J. F A Poulet, C. Leibold, and D. Schmitz. Coherent Phasic Excitation during Hippocampal Ripples. *Neuron*, 72(1), 2011.
- E. A. Mankin, F. T. Sparks, B. Slayyeh, R. J. Sutherland, S. Leutgeb, and J. K. Leutgeb. Neuronal code for extended time in the hippocampus. *Proceedings of the National Academy of Sciences*, 109(47):19462–19467, 2012. ISSN 0027-8424. DOI: 10.1073/pnas.1214107109.
- E. A. Mankin, G. W. Diehl, F. T. Sparks, S. Leutgeb, and J. K. Leutgeb. Hippocampal CA2 Activity Patterns Change over Time to a Larger Extent than between Spatial Contexts. *Neuron*, 85(1):190–202, 2015. ISSN 10974199. DOI: 10.1016/j.neuron.2014.12.001.
- E. A. Mankin, K. Thurley, A. Chenani, O. V. Haas, L. Debs, J. Henke, M. Galinato, J. K. Leutgeb, S. Leutgeb, and C. Leibold. The hippocampal code for space in Mongolian gerbils. *Hippocampus*, 30, 2019.
- J. R. Manns and H. Eichenbaum. Evolution of declarative memory, 2006. ISSN 10509631.
- V A Marchenko and L A Pastur. Distribution of Eigenvalues for Some Sets of Random Matrices. *Mathematics of the USSR-Sbornik*, 1(4):457–483, 1967. ISSN 0025-5734. DOI: 10.1070/SM1967v001n04ABEH001994.
- H. Markram, J. Lübke, M. Frotscher, and B. Sakmann. Regulation of Synaptic Efficacy by Coincidence of Postsynaptic APs and EPSPs. *Science*, 275(5297):213–215, 1997. ISSN 0036-8075, 1095-9203. DOI: 10.1126/science.275.5297.213.

- D. Marr. Simple Memory: A Theory for Archicortex. *Philosophical Transactions of the Royal Society B: Biological Sciences*, 262(841):23–81, 1971. ISSN 0962-8436. DOI: 10.1098/rstb.1971.0078.
- D. Marr. A Theory of Cerebellar Cortex. *Physiology*, 135(3):422–435, 2008. ISSN 08966273. DOI: 10.1038/nrn2055.
- J L McClelland, B. L. McNaughton, and R C O'Reilly. Why there are complementary learning systems in the hippocampus and neortex: Insights from the successes and failures of connectionist models of learning and memory. *Psychological review*, 102(3):419–57, 1995. ISSN 0033-295X. DOI: 10.1037/0033-295X.102.3.419.
- S. McKenzie, N. T. M. Robinson, L. Herrera, J. C. Churchill, and H. Eichenbaum. Learning Causes Reorganization of Neuronal Firing Patterns to Represent Related Experiences within a Hippocampal Schema. *The Journal of neuroscience*, 33(25):10243–10256, 2013. ISSN 0270-6474. DOI: 10.1523/JNEUROSCI.0879-13.2013.
- B. L. McNaughton, F. P. Battaglia, O. Jensen, E. I. Moser, and M. B. Moser. Path integration and the neural basis of the 'cognitive map'. *Nat Rev Neurosci*, 7(8):663–78, 2006. ISSN 1471-003X (Print). DOI: 10.1038/nrn1932.
- O. Melamed, W. Gerstner, W. Maass, M. Tsodyks, H. Markram, M. R. Mehta, A. K. Lee, and M. A. Wilson. Coding and learning of behavioral sequences, 2004. ISSN 01662236.
- J. F. Miller, M. Neufang, A. Solway, A. Brandt, M. Trippel, I. Mader, S. Hefft, M. Merkow, S. M. Polyn, J. Jacobs, M. J. Kahana, and A. Schulze-Bonhage. Neural activity in human hippocampal formation reveals the spatial context of retrieved memories. *Science*, 342(6162):1111–4, 2013. ISSN 1095-9203. DOI: 10.1126/science.1244056.
- Y. Miyashita, E. T. Rolls, P. M. Cahusac, H. Niki, and J. D. Feigenbaum. Activity of hippocampal formation neurons in the monkey related to a conditional spatial response task. *Journal of neurophysiology*, 61(3):669–78, 1989. ISSN 0022-3077.
- S. J Y Mizumori, G. M. Perez, M. C. Alvarado, C. A. Barnes, and B. L. McNaughton. Reversible inactivation of the medial septum differentially affects two forms of learning in rats. *Brain Research*, 528(1):12–20, 1990. ISSN 00068993. DOI: 10.1016/0006-8993(90)90188-H.
- M. M. Monsalve-Mercado and C. Leibold. Hippocampal Spike-Timing Correlations Lead to Hexagonal Grid Fields. *Physical Review Letters*, 119(3), 2017. ISSN 10797114. DOI: 10.1103/PhysRevLett.119.038101.

- M. B. Moser and E. I. Moser. Functional differentiation in the hippocampus, 1998. ISSN 10509631.
- Z. Nádasdy, H. Hirase, A. Czurkó, J. Csicsvari, and G. Buzsáki. Replay and Time Compression of Recurring Spike Sequences in the Hippocampus. *The Journal of neuroscience*, 19(21):9497–9507, 1999. ISSN 1529-2401.
- K. Nader. Reconsolidation and the dynamic nature of memory. In *Novel Mechanisms of Memory*, pages 1–20. 2015. ISBN 9783319243641. DOI: 10.1007/978-3-319-24364-11.
- K. Nakazawa, M. C. Quirk, R. A. Chitwood, M. Watanabe, M. F. Yeckel, L. D. Sun, A. Kato, C. A. Carr, D. Johnston, M. A. Wilson, and S. Tonegawa. Requirement for hippocampal CA3 NMDA receptors in associative memory recall. *Science*, 297(5579):211–218, 2002. ISSN 1095-9203.
- K. Nakazawa, T. J. McHugh, M. A. Wilson, and S. Tonegawa. NMDA receptors, place cells and hippocampal spatial memory. *Nature Reviews Neuroscience*, 5(5):361–372, 2004. ISSN 1471-003X.
- E. L. Newman, S. N. Gillet, J. R. Climer, and M. E. Hasselmo. Cholinergic Blockade Reduces Theta-Gamma Phase Amplitude Coupling and Speed Modulation of Theta Frequency Consistent with Behavioral Effects on Encoding. *The Journal of neuroscience*, 33(50):19635–19646, 2013. ISSN 0270-6474. DOI: 10.1523/JNEUROSCI.2586-13.2013.
- J. O’Keefe. Place units in the hippocampus of the freely moving rat. *Experimental Neurology*, 51(1):78–109, apr 1976. ISSN 10902430. DOI: 10.1016/0014-4886(76)90055-8.
- J. O’Keefe and J Dostrovsky. The hippocampus as a spatial map. Preliminary evidence from unit activity in the freely-moving rat. *Brain Research*, pages 171–175, 1971.
- H. F. Olafsdottir, C. Barry, A. Saleem, D. Hassabis, and H. Spiers. Hippocampal place cells construct reward-related sequences through unexplored space. *eLife*, (1):1–5, 2015. ISSN 2050-084X. DOI: 10.1007/s13398-014-0173-7.2.
- A. Oliva, A. Fernandez-Ruiz, G. Buzsáki, and A. Berenyi. Role of Hippocampal CA2 Region in Triggering Sharp-Wave Ripples. *Neuron*, 91(6):1342–1355, sep 2016. ISSN 08966273. DOI: 10.1016/j.neuron.2016.08.008.
- J. O’Neill, T. J Senior, K. Allen, J. R Huxter, and J. Csicsvari. Reactivation of experience-dependent cell assembly patterns in the hippocampus.

Nature Neuroscience, 11(2):209–215, 2008. ISSN 1097-6256. DOI: 10.1038/nn2037.

- G. Orr, G. Rao, F. P. Houston, B. L. McNaughton, and C. A. Barnes. Hippocampal synaptic plasticity is modulated by theta rhythm in the fascia dentata of adult and aged freely behaving rats. *Hippocampus*, 11(6):647–654, 2001. ISSN 10509631. DOI: 10.1002/hipo.1079.
- C. Papatheodoropoulos and E. Koniaris. α 5GABAA receptors regulate hippocampal sharp wave-ripple activity in vitro. *Neuropharmacology*, 60(4):662–673, 2011. ISSN 00283908. DOI: 10.1016/j.neuropharm.2010.11.022.
- J K Parkinson, E A Murray, and M Mishkin. A selective mnemonic role for the hippocampus in monkeys: memory for the location of objects. *The Journal of neuroscience*, 8(11):4159–4167, 1988. ISSN 0270-6474.
- C Pavlides and J. Winson. Influences of hippocampal place cell firing in the awake state on the activity of these cells during subsequent sleep episodes. *The Journal of neuroscience*, 9(8):2907–2918, 1989.
- F. Pedregosa and G Varoquaux. *Scikit-learn: Machine learning in Python*, volume 12. 2011. ISBN 9781783281930. DOI: 10.1007/s13398-014-0173-7.2.
- A. J. Pernia-Andrade and P. Jonas. Theta-Gamma-Modulated Synaptic Currents in Hippocampal Granule Cells InVivo Define a Mechanism for Network Oscillations. *Neuron*, 81(1):140–152, 2014. ISSN 08966273. DOI: 10.1016/j.neuron.2013.09.046.
- A. Peyrache, M. Khamassi, K. Benchenane, S. I. Wiener, and F. P. Battaglia. Replay of rule-learning related neural patterns in the prefrontal cortex during sleep. *Nature neuroscience*, 12(7):919–926, 2009. ISSN 1097-6256. DOI: 10.1038/nn.2337.
- A. Peyrache, K. Benchenane, M. Khamassi, S. I. Wiener, and F. P. Battaglia. Principal component analysis of ensemble recordings reveals cell assemblies at high temporal resolution. *Journal of Computational Neuroscience*, 29(1-2):309–325, 2010. ISSN 09295313. DOI: 10.1007/s10827-009-0154-6.
- B. E. Pfeiffer and D. J. Foster. Hippocampal place-cell sequences depict future paths to remembered goals. *Nature*, 497(7447):74–9, may 2013. ISSN 1476-4687. DOI: 10.1038/nature12112.
- V. C. Piatti, L. A. Ewell, and J. K. Leutgeb. Neurogenesis in the dentate gyrus: Carrying the message or dictating the tone, 2013. ISSN 16624548.

- J. S. Polepalli, H. Wu, D. Goswami, C. H. Halpern, T. C. Südhof, and R. C. Malenka. Modulation of excitation on parvalbumin interneurons by neuroligin-3 regulates the hippocampal network. *Nature Neuroscience*, 20(2):219–229, 2017. ISSN 1097-6256. DOI: 10.1038/nn.4471.
- M. C. Quirk, R. U. Muller, and J. L. Kubie. The firing of hippocampal place cells in the dark depends on the rat's recent experience. *The Journal of neuroscience*, 10(6), 1990.
- J. F. Ramirez-Villegas, N. K. Logothetis, and M. Besserve. Diversity of sharp-wave–ripple LFP signatures reveals differentiated brain-wide dynamical events. *Proceedings of the National Academy of Sciences*, page 201518257, 2015. ISSN 0027-8424. DOI: 10.1073/pnas.1518257112.
- P. R. Rapp and M. Gallaqher. Preserved neuron number in the hippocampus of aged rats with spatial learning deficits. *Neurobiology*, 93: 9926–9930, 1996. ISSN 0027-8424. DOI: 10.1073/pnas.93.18.9926.
- E. T. Rolls. Spatial view cells and the representation of place in the primate hippocampus, 1999. ISSN 10509631.
- E. T. Rolls. Pattern separation, completion, and categorisation in the hippocampus and neocortex. *Neurobiology of Learning and Memory*, pages 4–28, 2016. ISSN 1074-7427.
- E. T. Rolls and S. M. Stringer. Spatial view cells in the hippocampus, and their idiothetic update based on place and head direction, 2005. ISSN 08936080.
- E. T. Rolls, Y. Miyashita, P. M. Cahusac, R. P. Kesner, H. Niki, J. D. Feigenbaum, and L. Bach. Hippocampal neurons in the monkey with activity related to the place in which a stimulus is shown. *The Journal of neuroscience*, 9(6):1835–1845, 1989. ISSN 0270-6474.
- E. T. Rolls, J. Xiang, and L. Franco. Object, space, and object-space representations in the primate hippocampus. *Journal of neurophysiology*, 94(1):833–34, 2005.
- S. Royer, A. Sirota, J. Patel, and G. Buzsáki. Distinct Representations and Theta Dynamics in Dorsal and Ventral Hippocampus. *The Journal of neuroscience*, 30(5):1777–1787, 2010. ISSN 0270-6474. DOI: 10.1523/JNEUROSCI.4681-09.2010.
- F. Sargolini, M. Fyhn, T. Hafting, B. L. McNaughton, M. P. Witter, M. B. Moser, and E. I. Moser. Conjunctive Representation of Position, Direction, and Velocity in Entorhinal Cortex. *Science*, 312(5774):758–762, 2006. ISSN 0036-8075. DOI: 10.1126/science.1125572.

- M. I. Schlesiger. *The role of the medial entorhinal cortex in hippocampal spatial and temporal coding*. PhD thesis, LMU, 2016.
- M. I. Schlesiger, C. C Cannova, B. L. Bublil, J. B Hales, E. Mankin, M. P Brandon, J. K. Leutgeb, C. Leibold, and S. Leutgeb. The medial entorhinal cortex is necessary for temporal organization of hippocampal neuronal activity. *Nature Neuroscience*, 18(Rat 587):4–12, 2015. ISSN 1097-6256. DOI: 10.1038/nn.4056.
- D. Schlingloff, S. Kali, T. F. Freund, N. Hajos, and A. I. Gulyas. Mechanisms of Sharp Wave Initiation and Ripple Generation. *The Journal of neuroscience*, 34(34):11385–11398, 2014. ISSN 0270-6474. DOI: 10.1523/JNEUROSCI.0867-14.2014.
- E. W. Schomburg, A. Fernández-Ruiz, K. Mizuseki, A. Berényi, C. A. Anastassiou, C. Koch, and G. Buzsáki. Theta Phase Segregation of Input-Specific Gamma Patterns in Entorhinal-Hippocampal Networks. *Neuron*, 84(2):470–485, 2014. ISSN 10974199. DOI: 10.1016/j.neuron.2014.08.051.
- W B Scoville and B Milner. Loss of recent memory after bilateral hippocampal lesions. *Journal of Neurology, Neurosurgery & Psychiatry*, 20(1):11–21, 1957. ISSN 0022-3050. DOI: 10.1136/jnnp.20.1.11.
- A M Sengupta and P P Mitra. Distributions of singular values for some random matrices. *Phys. Rev. E*, 60(3):3389–3392, 1999. ISSN 1063-651X. DOI: 10.1103/PhysRevE.60.3389.
- T. J. Senior, J. R. Huxter, K. Allen, J. O’Neill, and J. Csicsvari. Gamma Oscillatory Firing Reveals Distinct Populations of Pyramidal Cells in the CA1 Region of the Hippocampus. *The Journal of neuroscience*, 28(9):2274–2286, 2008. ISSN 0270-6474. DOI: 10.1523/JNEUROSCI.4669-07.2008.
- P. R. Shirvalkar, P. R. Rapp, and M. L. Shapiro. Bidirectional changes to hippocampal theta-gamma comodulation predict memory for recent spatial episodes. *Proceedings of the National Academy of Sciences*, 107(15):7054–7059, 2010. ISSN 0027-8424. DOI: 10.1073/pnas.0911184107.
- J. H. Siegle and M. A. Wilson. Enhancement of encoding and retrieval functions through theta phase-specific manipulation of hippocampus. *eLife*, 3:e03061, 2014. ISSN 2050084X. DOI: 10.7554/eLife.03061.
- A. Sirota, J. Csicsvari, D. Buhl, and G. Buzsáki. Communication between neocortex and hippocampus during sleep in rodents. *Proceedings of the National Academy of Sciences*, 100(4):2065–2069, 2003. ISSN 0027-8424. DOI: 10.1073/pnas.0437938100.

- W. E. Skaggs and B. L. McNaughton. Replay of Neuronal Firing Sequences in Rat Hippocampus During Sleep Following Spatial Experience. *Science*, 271(5257):1870–1873, 1996. ISSN 0036-8075. DOI: 10.1126/science.271.5257.1870.
- W. E. Skaggs, B. L. McNaughton, M. A. Wilson, and C. A. Barnes. Theta phase precession in hippocampal neuronal populations and the compression of temporal sequences. *Hippocampus*, 6(2):149–172, 1996. ISSN 10509631. DOI: 10.1002/(SICI)1098-1063(1996)6:2<149::AID-HIPO6>3.0.CO;2-K.
- M. L. Smith and B. Milner. The role of the right hippocampus in the recall of spatial location. *Neuropsychologia*, 19(6):781–793, 1981. ISSN 00283932. DOI: 10.1016/0028-3932(81)90090-7.
- I Soltesz and M Deschênes. Low- and high-frequency membrane potential oscillations during theta activity in CA1 and CA3 pyramidal neurons of the rat hippocampus under ketamine-xylazine anesthesia. *Journal of neurophysiology*, 70(1):97–116, 1993. ISSN 0022-3077. DOI: 10.1523/JNEUROSCI.4673-07.2008.
- L. R. Squire. The Neuropsychology of Human Memory. *Annual Review of Neuroscience*, 5(1):241–273, 1982. ISSN 0147-006X. DOI: 10.1146/annurev.ne.05.030182.001325.
- L. R. Squire and S. Zola-Morgan. The medial temporal lobe memory system. *Science*, 253(5026):1380–1386, 1991. ISSN 0036-8075. DOI: 10.1126/science.1896849.
- E. Stark, L. Roux, R. Eichler, and G. Buzsáki. Local generation of multineuronal spike sequences in the hippocampal CA1 region. *Proceedings of the National Academy of Sciences*, 112(33):10521–10526, 2015.
- B. A. Strange, M. P. Witter, E. S. Lein, and E. I. Moser. Functional organization of the hippocampal longitudinal axis. *Nature Reviews Neuroscience*, 15(10):655–669, sep 2014. ISSN 1471-003X. DOI: 10.1038/nrn3785.
- D Sullivan, J. Csicsvari, K. Mizuseki, S. Montgomery, K. Diba, and G. Buzsáki. Relationships between Hippocampal Sharp Waves, Ripples, and Fast Gamma Oscillation: Influence of Dentate and Entorhinal Cortical Activity. *The Journal of neuroscience*, 312(23):8605–8616, 2011.
- S. S. Suzuki and G. K. Smith. Spontaneous EEG spikes in the normal hippocampus. V. Effects of ether, urethane, pentobarbital, atropine, diazepam and bicuculline. *Electroencephalography and Clinical Neurophysiology*, 70(1):84–95, 1988. ISSN 00134694. DOI: 10.1016/0013-4694(88)90198-8.

- B. Tahvildari, E. Fransen, A. A. Alonso, and M. E. Hasselmo. Switching between "on" and "off" states of persistent activity in lateral entorhinal layer III neurons. *Hippocampus*, (4):257–263, 2007.
- J. S. Taube. Head direction cells recorded in the anterior thalamic nuclei of freely moving rats. *The Journal of neuroscience*, 15(1 Pt 1):70–86, 1995. ISSN 0270-6474.
- J. S. Taube, R. U. Muller, and J B Ranck. Head-direction cells recorded from the postsubiculum in freely moving rats. I. Description and quantitative analysis. *The Journal of neuroscience*, 10(2):420–35, 1990a. ISSN 0270-6474. DOI: 10.1212/01.wnl.0000299117.48935.2e.
- J. S. Taube, R. U. Muller, and J. B. Ranck. Head-direction cells recorded from the postsubiculum in freely moving rats. II. Effects of environmental manipulations. *The Journal of neuroscience*, 10(2):436–447, 1990b. ISSN 0270-6474. DOI: 10.1212/01.wnl.0000299117.48935.2e.
- J. S. Taube, J. P. Kesslak, and C. W. Cotman. Lesions of the rat postsubiculum impair performance on spatial tasks. *Behavioral and Neural Biology*, 57(2):131–143, 1992. ISSN 01631047. DOI: 10.1016/0163-1047(92)90629-I.
- D. J. Thomson. Spectrum estimation and harmonic analysis. *Proceedings of the IEEE*, pages 1055–1096, 1982.
- E.C. Tolman. Maps in your mind. *Psychological Review*, 55:189–208, 1948. ISSN 0033-295X. DOI: 10.1037/h0061626.
- C. Torrence and G. P. Compo. A Practical Guide to Wavelet Analysis. *Bulletin of the American Meteorological Society*, 79(1):61–78, 1998. ISSN 00030007. DOI: 10.1175/1520-0477(1998)079<0061:APGTWA>2.0.CO;2.
- C. A. Tracy and H. Widom. Level-spacing distributions and the Airy kernel. *Communications in Mathematical Physics*, 159(1):151–174, 1994.
- A. Treves and E. T. Rolls. Computational constraints suggest the need for two distinct input systems to the hippocampal CA3 network. *Hippocampus*, 2(2):189–199, 1992. ISSN 10981063. DOI: 10.1002/hipo.450020209.
- A. Treves and E. T. Rolls. Computational analysis of the role of the hippocampus in memory, 1994. ISSN 10509631.
- M V Tsodyks, W E Skaggs, T J Sejnowski, and B. L. McNaughton. Population dynamics and theta rhythm phase precession of hippocampal place cell firing: a spiking neuron model. *Hippocampus*, 6(3):271–280, 1996. ISSN 1050-9631. DOI: 10.1002/(SICI)1098-1063(1996)6:3.

- J. J. Tukker, P. Fuentealba, K. Hartwich, P. Somogyi, and T. Klausberger. Cell Type-Specific Tuning of Hippocampal Interneuron Firing during Gamma Oscillations In Vivo. *The Journal of neuroscience*, 27(31):8184–8189, 2007. ISSN 0270-6474. DOI: 10.1523/JNEUROSCI.1685-07.2007.
- N. Ulanovsky and C. F Moss. Hippocampal cellular and network activity in freely moving echolocating bats. *Nature Neuroscience*, 10(2):224–233, 2007. ISSN 1097-6256. DOI: 10.1038/nn1829.
- G. M. van de Ven, S. Trouche, C. G. McNamara, K. Allen, and D. Dupret. Hippocampal Offline Reactivation Consolidates Recently Formed Cell Assembly Patterns during Sharp Wave-Ripples. *Neuron*, 92(5):968–974, 2016. ISSN 10974199. DOI: 10.1016/j.neuron.2016.10.020.
- N. M. van Strien, N. L. M. Cappaert, and M. P. Witter. The anatomy of memory: an interactive overview of the parahippocampal–hippocampal network. *Nature Reviews Neuroscience*, 10(4):272–282, 2009. ISSN 1471-003X. DOI: 10.1038/nrn2614.
- C. H. Vanderwolf. Hippocampal electrical activity and voluntary movement in the rat. *Electroencephalography and Clinical Neurophysiology*, 26(4):407–418, 1969. ISSN 00134694. DOI: 10.1016/0013-4694(69)90092-3.
- Y. Wang, S. Romani, B. Lustig, A. Leonardo, and E. Pastalkova. Theta sequences are essential for internally generated hippocampal firing fields. *Nature Neuroscience*, 18(2):282–288, 2014. ISSN 1097-6256.
- A. M. Wikenheiser and D. A. Redish. Hippocampal theta sequences reflect current goals. *Nature Neuroscience*, 18(2):289–294, feb 2015. ISSN 1097-6256.
- M. A. Wilson and B. McNaughton. Dynamics of the hippocampal ensemble code for space. *Science*, 261(5124):1055–1058, 1993. ISSN 0036-8075. DOI: 10.1126/science.8351520.
- M. A. Wilson and B. L. Mcnaughton. Reactivation of hippocampal ensemble memories during sleep. *Science*, 265(5172):676–679, 1994.
- J. Winson. Loss of hippocampal theta rhythm results in spatial memory deficit in the rat. *Science*, 201(4351):160–163, 1978. ISSN 0036-8075. DOI: 10.1126/science.663646.
- M. P. Witter and D. G. Amaral. Hippocampal Formation. In *The Rat Nervous System*, pages 635–704. 2004. ISBN 9780080542614. DOI: 10.1016/B978-012547638-6/50022-5.
- M. P. Witter, D. G Amaral, and G W Van Hoesen. Topographical organization of the entorhinal projection to the dentate gyrus of the monkey. *Journal of Neuroscience*, 9(1):216–228, 1989. ISSN 0270-6474.

- E R Wood, P. Dudchenko, and H. Eichenbaum. The global record of memory in hippocampal neuronal activity. *Nature*, 397(6720):613–616, 1999. ISSN 0028-0836. DOI: 10.1038/17605.
- J. Yamamoto and S. Tonegawa. Direct Medial Entorhinal Cortex Input to Hippocampal CA1 Is Crucial for Extended Quiet Awake Replay. *Neuron*, 96(1):217–227, 2017. ISSN 10974199. DOI: 10.1016/j.neuron.2017.09.017.
- M. M. Yartsev and N. Ulanovsky. Representation of Three-Dimensional Space in the Hippocampus of Flying Bats. *Science*, 340(6130):367–372, 2013. ISSN 0036-8075. DOI: 10.1126/science.1235338.
- M. M. Yartsev, M. P. Witter, and N. Ulanovsky. Grid cells without theta oscillations in the entorhinal cortex of bats. *Nature*, 479(7371):103–107, 2011. ISSN 0028-0836. DOI: 10.1038/nature10583.
- A. Ylinen and G. Buzsáki. Sharp Wave-Associated High-Frequency Oscillation (200 Hz) in the Intact Hippocampus: Network and Intracellular Mechanisms. *The Journal of neuroscience*, 15(January):30–46, 1995.
- S. Zarnadze, P. Bäuerle, J. Santos-Torres, C. Böhm, D. Schmitz, J. R.P. Geiger, T. Dugladze, and T. Gloveli. Cell-specific synaptic plasticity induced by network oscillations. *eLife*, 5, May 2016. ISSN 2050084X. DOI: 10.7554/eLife.14912.
- C. Zheng, K. W. Bieri, S. G. Trettel, and L. L. Colgin. The relationship between gamma frequency and running speed differs for slow and fast gamma rhythms in freely behaving rats. *Hippocampus*, 25(8): 924–938, 2015. ISSN 10981063. DOI: 10.1002/hipo.22415.
- C. Zheng, K. W. Bieri, Y. T. Hsiao, and L. L. Colgin. Spatial Sequence Coding Differs during Slow and Fast Gamma Rhythms in the Hippocampus. *Neuron*, 89(2):398–402, 2016.